FLAVOR-DEPENDENT EFFECTS OF E-CIGARETTE LIQUIDS AND THEIR CHEMICAL CONSTITUENTS ON LUNG EPITHELIAL TOXICITY AND CELL Ca^{2+} SIGNALING

Temperance Rebecca Rowell

A dissertation submitted to the faculty at the University of North Carolina at Chapel Hill in partial fulfillment of the requirements for the degree of Doctor of Philosophy in the Department of Cell Biology and Physiology in the School of Medicine.

Chapel Hill
2018

Approved by:

Robert Tarran

Kathleen Caron

Keith Burridge

Ilona Jaspers

Mehmet Kesimer

ABSTRACT

Temperance Rebecca Rowell: Flavor-Dependent Effects of E-cigarette Liquids and their Chemical Constituents on Lung Epithelial Toxicity and Cell Ca^{2+} Signaling
(Under the direction of Robert Tarran)

E-cigarettes (e-cigs) are a cigarette alternative that do not contain tobacco or tar, and whose e-liquids are available in over 7,000 flavors. While marketed as a safer smoking alternative, the basic health effects of vaping commercially available e-liquids and their constituent components (i.e., propylene glycol (PG), vegetable glycerin (VG), nicotine, flavors) are not well understood. However, inhalation of diacetyl (butter flavor) has been shown to cause bronchiolitis obliterans ('Popcorn Lung'). In this dissertation, we sought to better understand the biological effects of flavored e-liquids and their chemical constituents on airway cells.

We first screened 13 flavored e-liquids, PG/VG, and nicotine for toxicity in a pulmonary epithelial cell line. We demonstrated that the responses were both dose- and flavor-dependent by exposing cells to either the unheated or heated (aerosolized) e-liquids. 4 of 13 flavored e-liquids had more pronounced toxicity effects than the PG/VG base or other flavors, and did not share a flavoring chemical between them that might be universally toxic. We then demonstrated that the toxic effects that we were measuring were either due to (1) direct cytotoxicity or (2) inhibiting cell proliferation. We further explored the ability of flavored e-liquids to inhibit cell proliferation by characterizing their effects on intracellular Ca^{2+} signaling, which can affect cell proliferation and apoptosis. Specifically, we demonstrated that a Banana Pudding-flavored e-liquid could stimulate phospholipase C-dependent inositol 1,4,5-triphosphate generation leading to ER Ca^{2+} depletion and elevations in cytosolic Ca^{2+}. Moreover, we screened 100 additional e-liquids and found 42 of 100 elicited cytosolic Ca^{2+} responses, suggesting many flavors can alter Ca^{2+} homeostasis. Analysis of their chemical constituents correlated

the presence of common flavorings (e.g., ethyl vanillin, vanillin, and ethyl maltol) with the cytosolic Ca^{2+} responses. Additional testing confirmed that those flavors caused dose-dependent Ca^{2+} signaling. Altered Ca^{2+} homeostasis can have profound effects on airway physiology and has been implicated in disease (i.e., cancer, autoimmune diseases, inflammation). Therefore, these products should be further assessed for their flavor-dependent effects on airway physiology (e.g., Ca^{2+} homeostasis) and potential consequences of long-term inhalation toxicity from chronic vaping.

ACKNOWLEDGEMENTS

I want to first and foremost thank my advisor, Dr. Rob Tarran, for the opportunity to work in his lab and specifically, on this project. Through it, I was afforded the independence to lay the scientific foundation for a new and important research focus in our laboratory that also resulted in timely publications informing consumer health and regulatory agency rulings. I would also like to thank each and every member of my dissertation committee (Drs. Kathleen Caron, Keith Burridge, Ilona Jaspers, and Mehmet Kesimer). My committee members offered sound and supportive guidance that I greatly appreciated and was instrumental in completing my degree. I also greatly appreciate their efforts to ensure that I was actively supported in my career development at the committee level.

I would also like to briefly thank all of the members of the Tarran lab, Marsico Lung Institute, SoM TCORS, and the Department of Cell Biology and Physiology. While they are too numerous to individually thank here, I appreciated all of the camaraderie and scientific support from a number of students, post-docs, faculty, and staff from all of these groups who were instrumental in me earning my degree. Specifically, I would like to thank Dr. Tongde Wu for her neverending scientific, professional, and personal encouragement. I really could not have done this without her!

During my time at UNC, I have changed my career focus and embraced my new passions in big part thanks to the TIBBS/BBSP office staff, a number of UNC administrators involved in professional development, and members of the 2017-2018 GPSF Cabinet and Executive Branch. As I look to transition away from the bench and into academic administration/STEM education, outreach, and student advocacy, I would not be as prepared or excited about my next career step without the awesome career mentorship of Drs. Beka Layton, Erin Hopper, and Shernita Lee. I also want to thank my amazing peer support system outside of the lab, especially Amanda Raimer and Andy Chan. Somehow we managed to

navigate the ups and downs of grad school together with biscuits from Neal's Deli, nights out dancing, love of zoos/aquariums, and our annual trips to the Outer Banks. Additionally, I want to acknowledge my long-distance partner-in-crime, Kelly Masuda. Our friendship has lasted for almost a decade already and even with 3,000+ miles between us, you are always one of my most constant and often my biggest advocate for anything in my life.

Lastly, I would like to thank the undying support, love, and patience of my family (Scott, Michelle, Stephanie, John, Amy, and Ian). Specifically, I want to thank my parents for continued patience in following and engaging in my academic pursuits. They have always been proud parents and excited to share my research and achievements with all of their friends and coworkers. I also want to thank my siblings for their years of support. I have been lucky to have a special relationship with each one of you that has only grown with time, and each of you inspires me to pursue my goals daily.

TABLE OF CONTENTS

LIST OF TABLES

LIST OF FIGURES

LIST OF ABBREVIATIONS

2-APB	2-aminoethoxydiphenyl borate
AFU	Arbitrary fluorescence units
AGC	Protein kinases A, G, and C
ATP	Adenosine triphosphate
BALF	Broncho-alveolar lavage fluid
BEGM	Bronchial epithelial growth medium
BP	Banana pudding
Ca^{2+}	Calcium
CAMKIV	Calcium/calmodulin-dependent protein kinase IV
cAMP	Cyclic adenosine monophosphate
CCCP	Carbonyl cyanide m-chlorophenyl hydrazine
Cd	Cadmium
CDC	Centers for disease control
CFTR	Cystic fibrosis transmembrane conductance regulator
CHRNA	Cholinergic receptor, nicotinic, alpha
CHRNB	Cholinergic receptor, nicotine, beta
Cr	Chromium
CREB	cAMP response element binding
COPD	Chronic obstructive pulmonary disease
DAG	Diacylglycerol
DAPI	4’6-diamidino-2-phenylindole
DMSO	Dimethyl sulfoxide
EC_{50}	Half maximal effective concentration
EDTA	Ethylenediaminetetraacetic acid

EGTA	Thylene glycol-bis(2-aminoethylether)-N,N,N’,N’-tetraacetic acid
ENDS	Electronic nicotine delivery systems
ER	Endoplasmic reticulum
FBS	Fetal bovine serum
FDA	Food and drug administration
GAPDH	Glycerldehyde 3-phosphate dehydrogenase
GC-MS	Gas chromatography-mass spectometry
GPCR	G protein-coupled receptor
GRAS	Generally recognized as safe
HASMC	Human airway smooth muscle cells
HBEC	Human bronchial epithelial culture
Hg	Mercury
IC_{50}	Half maximal inhibitory concentration
IL	Interleukin
InsP	Inositol phosphate
IP	Immunoprecipitation
IP_3	Inositol 1,4,5-triphosphate
IP_3R	Inositol ,1,4,5-triphosphate receptor
K^+	Potassium
LDH	Lactate dehydrogenase
MCP-1	Monocyte chemoattractant protein-1
MEM	Minimal essential media
MTT	3-(4,5-Dimenthylthiazol-2-yl)-2,5-diphenyltetrazolium bromide
Na^+	Sodium
NA	Numerical aperture
nAChR	Nicotinic acetylcholine receptor

ND	Not determined
NT	Not tested
NNK	Nicotine-derived nitrosamine ketone
NO	Nitric oxide
NS	Not significant
OX/ROS	Oxidants/reactive oxygen species
$P2Y_2R$	Purinergic receptor $P2Y_2$
PBS	Phosphate-buffered saline
PFA	Paraformaldehyde
PG	Propylene glycol
PKA	Protein kinase A
PKC	Protein kinase C
PIP_2	Phosphatidylinositol 4,5-bisphosphate
PLC	Phospholipase C
PREP	Potential to reduced exposure products
p-Tyr	Phosphorylated tyrosine
RTK	Receptor tyrosine kinase
RT-PCR	Real time polymerase chain reaction
SCC	Solitary chemosensory cells
SD	Standard deviation
SDS-PAGE	Sodium dodecyl sulfate polyacrylamide gel electrophoresis
SEM	Standard error of the mean
SERCA	Sarco/endoplasmic reticulum calcium transport ATPase
SPLUNC1	Short palate, lung, and nasal epithelium clone 1
SOCE	Store-operated Ca^{2+} entry
STIM1	Stromal interaction molecule 1

TAS1R/T1R	Taste 1 receptor member/sweet taste receptor
TAS2R/T2R	Taste 2 receptor member/bitter taste receptor
TRPA	Transient receptor potential ankyrin
TRPM	Transient receptor potential menthol
TRPV	Transient receptor potential vanilloid
UTP	Uridine triphosphate
VG	Vegetable glycerin
YFP	Yellow fluorescent protein

Chapter 1: Introduction - Will Chronic E-cigarette Use Cause Lung Disease?

1.1. Overview

Chronic tobacco smoking is a major cause of preventable morbidity and mortality worldwide. In the lung, tobacco smoking increases the risk of lung cancer, and also causes chronic obstructive pulmonary disease (COPD), which encompasses both emphysema and chronic bronchitis. E-cigarettes (e-cigs), or electronic nicotine delivery systems (ENDS), were developed over a decade ago and are designed to deliver nicotine without combusting tobacco. Although tobacco smoking has declined since the 1950s, e-cig usage has increased, attracting both former tobacco smokers and never smokers. E-cig liquids (e-liquids) contain nicotine in a glycerol/propylene glycol vehicle with flavorings, which are vaporized and inhaled. To date, neither e-cig devices, nor e-liquids, are regulated by the Food and Drug Administration (FDA). The FDA has proposed a deeming rule, which aims to initiate legislation to regulate e-cigs, but the timeline to take effect is uncertain. Proponents of e-cigs say that they are safe and should not be regulated. Opposition is varied, with some opponents proposing that e-cig usage will introduce a new generation to nicotine addiction, reversing the decline seen with tobacco smoking, or that e-cigs generally may not be safe and will trigger diseases like tobacco. In this review, we shall discuss what is known about the effects of e-cigs on the mammalian lung and isolated lung cells *in vitro*. We hope that collating this data will help illustrate gaps in the knowledge of this burgeoning field, directing researchers toward answering whether or not e-cigs are capable of causing disease.

---

[1]This chapter previously appear as an article published in American Journal of Physiology Lung Cell Molecular Physiology and is reprinted with permission with some modifications. The original citation is as follows: **Rowell TR, Tarran R.** Will chronic e-cigarette use cause lung disease?. *Am J Physiol Lung Cell Mol Physiol* 309: L1398-L1409, 2015.

1.1. Lung Anatomy & Physiology

The lung is a complex organ that is partitioned into two zones: the conducting zone and the respiratory zone. As air is inhaled, it passes down the trachea into a system of branching bronchi and bronchioles which comprise the conducting zone. It is also in the conducting zone that air is warmed, moistened, and passed through defenses to prevent infection. Air then flows into the respiratory zone at the end of the small airways where alveolar sacs (~480 million alveoli/lung) are enriched with their own blood supply (177). The lung's primary function is to exchange oxygen for carbon dioxide into the blood supply via alveolar capillary beds (262). It is also at the alveolar sacs that blood pH can be regulated with gas exchange. Specifically, carbon dioxide concentration can increase or decrease the blood pH and is regulated through ventilation rate.

The lung is one of the first lines of defense against inhaled allergens, environmental pollutants, and pathogens. Many different cell types comprise the lung and are important to providing defenses (i.e., physical barrier, local inflammatory responses, mucociliary clearance) (264). These cell types are summarized in Figure 1.3 and include the pulmonary epithelia that line the conducting zones and contain both ciliated and secretory (goblet) cells. Beneath the epithelia are layers of fibroblasts and connective tissue, as well as airway smooth muscle cells that are responsible for constricting and dilating the airways. Immune cells are present in the airways (e.g., resident macrophages) or are recruited by inflammatory signaling (e.g., neutrophils, dendritic cells). Lastly, the respiratory zone is rich in alveolar type 1 and 2 cells in the terminal sacs that exchange gas with the endothelial cells of the capillary beds nearby (193, 264). Prominent airway diseases such as COPD (emphysema and chronic bronchitis) or asthma involve the destruction and/or dysregulation of different lung cell types (i.e., bronchiolar alveoli and epithelia, airway smooth muscle cells), suggesting that they are all susceptible to chronic e-cig exposure.

1.2. E-cigarettes (E-cigs)

Electronic cigarettes or e-cigarettes (e-cigs), also known as ENDS, were designed to deliver aerosolized nicotine in a minimal liquid vehicle that was thought to be relatively safe compared with tobacco (Fig. 1.1). It has been proposed by e-cig manufacturers that, since these products do not burn

tobacco, they will not expose the lung to the same toxic chemicals as regular smoked tobacco and so will not cause the lung disease that is frequently associated with chronic tobacco inhalation, including lung cancer and COPD. E-cig users are a fast-growing subset of nicotine users who are described as vapers rather than smokers, since e-cigs heat and generate aerosols but do not burn e-liquids. There is considerable controversy regarding the disease risk and toxicity of e-cigs (178, 186, 209). However, because e-cigs do not currently fall under the auspices of the Food and Drug Administration (FDA), they have not undergone the typical toxicological evaluation, followed by human clinical trials that are required of other inhaled products (e.g., inhaled therapeutic agents), and, as such, no safety data exist from either humans or animals. Because of this, it is hard to predict whether these products will be benign when chronically inhaled, possibly over a lifetime, or whether they will induce tobacco-like disease or other types of lung disease such as bronchiolitis obliterans, a disease that has been caused by the inhalation of the buttery-tasting flavor diacetyl (124). The clinical evaluation of biomarkers of harm (e.g., inflammatory and cytotoxic markers) is required to inform the FDA and for ensuring safety and proper regulation. However, these studies are only just beginning in what can at best be described as "investigator-initiated trials" rather than formal clinical trials. A further confounder is that many e-cig users have switched after chronically smoking tobacco products, making it difficult to differentiate between the previous effects of tobacco vs. the effects of the e-cigs (58). To date, there are currently 1,273 e-cig articles on Pubmed, of which 135 are reviews and only 85 include the terms "e-cigarette" and "lung." In contrast, "tobacco" and "lung" yields 9,769 hits, indicating the lack of maturity of this field. In this review, we shall list and evaluate what is known about the effects of e-cig exposure on lungs/airways *in vivo* and *in vitro* (Fig. 1.3).

1.3. Health Effects of Nicotine and Tobacco Use

Nicotine is a highly addictive compound that, through nicotinic acetylcholine receptors (nAChR), exerts potent effects on the brain, including the saturation and desensitization of nAChRs (α4β2-subtype) leading to significant changes in the brain's physiology such as activation of the reward/pleasure regions of the cortex and reduced anxiety (24, 71, 210). Inhaling tobacco is a relatively simple and efficient way

of delivering nicotine into the bloodstream. Nicotine is a weak base that can be absorbed across the lung in its unionized form into the bloodstream (25). The effects of nicotine on the brain are complex and only just beginning to be understood. Importantly, its effects on the adolescent brain are markedly different compared with the adult brain and can affect neural development. For example, exposure to nicotine in adolescent rats led to an increased sensitivity to nicotine in these rats as adults, even if a smoking cessation period was introduced, suggesting that e-cig inhalation (i.e., vaping) by adolescents may have serious consequences later in life (59).

Nicotine craving causes a huge drive to continue smoking, and smokers maintain fairly constant plasma nicotine levels during waking hours, despite the significant risks: lung cancer (including both small cell and nonsmall cell) accounts for 27% of all diagnosed cancers and is the deadliest form of cancer, killing ~150,000 people in the United States of America (USA) per year (38, 221). It is thought that ~85% of all lung cancer is caused by smoking, and secondhand smoke exposure increases the chance of lung cancer by ~25% (38). COPD is also caused primarily by tobacco exposure in Western countries and kills a similar amount of people as lung cancer (~140,000/yr) (18, 87). COPD is also the third leading cause of death in the USA and worldwide (179), although tobacco exposure is a primary risk factor of COPD in first-world countries; smoke from biomass fuels is also a risk factor for COPD in second- and third-world countries (70). COPD often occurs with other comorbidities, and presentation with COPD is a major risk factor for the development of lung cancer (107, 165). The fact that tobacco exposure is a key factor in the development of both of these diseases was first denied by the tobacco industry and later accepted, following the Tobacco Master Settlement Agreement in 1998 (76, 116).

In the 1950s, ~50% of the adult population were regular tobacco smokers in the USA (224). Following the Surgeon General's 1954 report linking tobacco smoke with disease, a series of public health campaigns led to *1*) increased public awareness about the dangers of smoking, *2*) bans on tobacco advertising, *3*) age limits for purchasing tobacco, *4*) bans on tobacco products that allegedly target minors (e.g., flavored cigarettes), *5*) increased taxation on tobacco, and *6*) restrictions on where tobacco products can be smoked (e.g., bans on smoking in public places) (110, 191). Due to these pressures, tobacco

companies began developing “safe cigarettes.” In the 1980s, “low-tar” cigarettes were developed, which were purportedly safer than regular cigarettes because they exposed users to less of the tar phase from cigarettes. This premise was based on flawed science. In part, the reduced tar output was generated by putting holes at the base of the cigarette, which served to reduce airflow through the cigarette. However, these cigarettes were not safer than regular cigarettes. In fact, users learned to compensate by either covering up the holes with their fingers or taking larger puffs, thus negating the “low-tar effects” (96, 187). Furthermore, the gas phase of cigarette smoke is also highly toxic and was not addressed in “low-tar cigarettes” (176, 205). Additional types of safe cigarettes have been developed, including “heat not burn” types (e.g., the “Eclipse”), which heats a rod in the middle of the cigarette to give off tobacco smoke without burning it. This style of cigarette was not successful commercially (8), and there is no evidence that they are actually safer (101).

Despite these failed attempts at safe cigarettes, the Institute of Medicine issued a report in 2001 that outlined the feasibility of focusing efforts on harm reduction tobacco products, which were referred to as “Potential to Reduced Exposure Products” or “PREPs,” since they wanted to avoid implying “that any product currently known is safe” (238). At that time, there were no conclusive data that the current products on the market were reducing the individual users’ exposure to harmful tobacco substances. However, the committee did conclude that there was potential merit in “harm reduction” as a part of the national tobacco program that “emphasizes abstinence oriented prevention and treatment” (238). Thus, when e-cigs were brought to market, they appeared to be likely candidate PREPs, since they neither contain tobacco nor is the e-cig vapor produced by combustion. E-cigs were introduced into European markets in 2006 and in the USA in 2007 (206). The first generation of e-cigs were dubbed “cigalikes” due to their resemblance to conventional cigarettes, and they came in both rechargeable/refillable and disposable formats (206, 276). Subsequently, as their popularity grew, second- and third-generation e-cigs have been developed which, although they have ceased to resemble cigarettes, have significantly improved their ability to deliver nicotine through the lung and into the bloodstream (Fig. 1.1) (276). However, the health effects of long-term inhalation of e-cig aerosols are currently unknown.

1.4. Components of Neat and Heated Flavored E-liquids

Cigarette smoke is a complex and highly reactive mixture that includes metals (e.g., Cr, Cd, Hg), aldehydes (e.g., 4-aminobiphenyl, acrolein, formaldehyde), carbon monoxide, free radicals, and, of course, nicotine (82, 245). Adverse effects can be caused by adduct formation, especially of aldehydes, with DNA or proteins (183), or due to excessive oxidative stress (119). Aldehydes and heavy metals have been shown to have a number of cytotoxic effects on epithelia, including adduct formation to DNA (43, 237, 258). Additionally, tobacco smoke, as well as aldehydes, cadmium, and oxidative stress, also affect plasma membrane proteins such as the cystic fibrosis transmembrane conductance regulator (CFTR) (36, 49, 100, 230), which is required for fluid secretion in the lung (51, 87). In contrast, e-liquids (the flavored liquids that are heated to form the e-cig vapor) are thought to be much simpler and ostensibly contain nicotine (~6–18 mg/ml) in a liquid vehicle (typically propylene glycol and/or vegetable glycerin), along with sweeteners and flavorings (94).

To date, over 400 different brands of e-cigs have been produced (276). Unlike disposable e-cigs, second- and third-generation e-cigs contain a refillable tank to which the e-liquid is added, a battery-powered atomizer that generates the aerosol vapor from the e-liquid, and a mouthpiece that collects and delivers the aerosol (Fig. 1.1). This function is usually controlled by a microchip, which may activate a light-emitting diode at the tip of the e-cig during inhalation for aesthetics. The amount of aerosol that is generated is directly proportional to the power of the battery, which has led some users to modify their e-cig to increase battery power to get a greater nicotine "hit." This is not without risks, however, since there is a chance of battery explosion, which can lead to injury (34). Although the number of fires and explosions from e-cig devices has increased since inception, interestingly, many of these instances occurred while the device was being charged and are still considered rare (https://www.usfa.fema.gov/downloads/pdf/publications/electronic_cigarettes.pdf). An additional, behavioral modification that has developed among e-cig users is "dripping," which entails dripping e-liquid directly on the atomizer (i.e., the heating element) and inhaling the resultant vapor, which is supposed to give the largest amount of nicotine delivery possible with current e-cig devices (246).

Parameters of e-cig emission, such as aerosol size, mass output, and chemical composition, vary by device and e-liquid types and are predicted to impact the user's exposure to the e-cig aerosol. For example, aerosol size strongly affects how much of an aerosol is delivered to different regions of the lung and how much is retained in the oral cavity (23, 123).

There are currently over 7,000 different flavored e-liquids that are commercially available (276). Because these e-liquids are not FDA regulated, the vendors do not have to list their e-liquid ingredients, perform any safety testing before they reach the market, nor generate these products under Good Manufacturing Practice-type conditions. For example, the reported amount of nicotine has been found to vary by up to 20% from what is reported on the e-liquid label and has even been found in purportedly nicotine-free e-liquids (55, 56, 91). It is likely that many of the compounds used in e-liquids fall within the FDA's Generally Regarded as Safe (GRAS) list [http://www.accessdata.fda.gov/scripts/fdcc/?set_SCOGS]. The typical vehicle for e-liquids contains a mix of propylene glycol and glycerol, which are both GRAS products (34). To date, most GRAS testing/toxicology has been performed following oral ingestion rather than following aerosolization to the lung. For example, diacetyl is sometimes added to foods as a buttery flavor and is on the GRAS list, based on its oral toxicology (227). Due to the potential for adverse health effects from inhaling other chemicals, the Flavor and Extract Manufacturers' Association of the USA issued a statement warning that additives on the GRAS list apply to food only and should not be characterized as safe for use in e-cig products without further testing (https://www.femaflavor.org/safety-assessment-and-regulatory-authority-use-flavors-focus-e-cigarettes). Propylene glycol is used as a common e-liquid vehicle component in part because of its perceived low toxicity. However, both ocular and upper respiratory irritation were reported in nonasthmatic adults following a short controlled occupational exposure (265). Furthermore, diacetyl inhalation is known to cause bronchiolitis obliterans or "popcorn workers lung" (124). Bronchiolitis obliterans caused by the inhalation of diacetyl can cause a range of symptoms from mild reversible respiratory impairment to a more severe nonreversible lung obstruction from extensive scarring in the small airways (17). With no current consensus on e-cig user topography, it is possible that even

nonasthmatic users who vape frequently could experience, at the very least, respiratory irritation although to date no long-term data are available regarding chronic propylene glycol or flavorant exposure in humans.

1.5. E-liquid Thermal Decomposition (Pyrolysis)

E-cig aerosols are typically generated at temperatures of 100–250°C, which is predicted to cause pyrolysis of the e-liquid vehicle (274) and may also induce breakdown of other e-liquid constituents. Recently, formaldehyde has been detected in e-cig emissions (114). However, these data have been disputed (80). Part of the problem lies in deciding which temperature the e-liquid is heated to during the experiment vs. what occurs during actual vaping. For example, Jensen et al. found significant amounts of formaldehyde (~380 μg/10 puffs) in the emission from a tank-style e-cig device when the battery voltage was set at 5.0 V, with no formaldehyde being detected when a lower voltage (3.3 V) was used (114). Because the power consumption/electrical resistance of the coil was not quoted by Jensen et al., it will be hard to see how this observation transfers to other e-cig devices. That is, the power generated by the heating coil cannot be determined purely by the quoted voltage since it also depends on the current, and the temperature reached by the e-liquid is dependent on the power output of the heating element. Thus, for reproducibility, it may be useful for researchers to quote the power output of their e-cig device in addition to the puff profile used. Farsalinos et al. have reported that e-cig users do not use this higher voltage setting, and they also proposed that e-cigs only produce formaldehyde in "dry puff" conditions (80), where a dry puff refers to the scenario where there is little liquid on the atomizer coil and temperatures get higher than would be seen with sufficient liquid, leading to the potential for increased pyrolysis. However, acrolein and other carbonyls have also been found by other investigators both in neat e-liquids and in e-cig aerosols that were generated by unmodified e-cig devices (222), suggesting that the occurrence/production of these compounds may be more common than originally suspected. Interestingly, neat glycerin does not pyrolyze at 900°C. However, when diluted, significant amounts of acrolein were produced following pyrolysis of glycerol (39). Similarly, these aldehydes are known to be released from vegetable oil (of which glycerol is a major component) when it is heated during cooking,

even to 180°C, which is close to temperatures reported for e-cigs (130–350°C) (246). For example, the acrid smell that occurs when oil is burned on a stove is from acrolein (20, 40). Similarly, the chemical decomposition of sugars also causes the release of aldehydes, including acrolein (244).

It has been proposed that e-cig users tend to avoid the bitter taste that is associated with release of aldehydes during overheating/dry puffing and that, in actual e-cig users, aldehyde exposure never actually happens (80). However, during the aforementioned practice of dripping, where the e-liquids are placed directly on the coil, it is possible that significant pyrolysis occurs. Certainly, cigarettes can produce a harsh taste that is concomitant with the production of significant amounts of acrolein, formaldehyde, and other aldehydes, along with many other toxicants (244). However, this relatively unpleasant taste is soon overcome in new smokers due to the power of the nicotine drive (229) and due to cross-desensitization of transient receptor potential ankyrin subtype 1 (TRPA1) channels in sensory neurons (29). Therefore, it is also possible that e-cig users will "learn" to overcome any unpleasant taste due to increased aldehyde production if the nicotine drive is great enough. It is also worth pointing out at this point that many flavors are themselves aldehydes, including anisaldehyde (sweet), cinnamaldehyde (cinnamon), and isovaleraldehyde (nutty). The effects of these flavors on pulmonary surfaces are not known. However, their potential inclusion in e-liquids may increase overall aldehyde exposure to the lung. Indeed, cinnamaldehyde is present in some e-liquids (21) and activates TRPA1 (167), suggesting that they may exert effects on the lung. Similarly, activation of this ion channel in sensory neurons in the airways of rodents by unsaturated aldehydes has previously been shown to trigger neurogenic inflammation (9) and to inhibit the CFTR ion channel (4), suggesting that a higher aldehyde burden may indeed be toxic to the lung. However, the degree of adverse effects will likely depend on dose ranging and whether aldehydes are actually generated in sufficient quantities during real vaping conditions to trigger these responses.

In addition to aldehydes, Lerner et al. also found that e-cig aerosols generated from two separate devices produced oxidants and reactive oxygen species (OX/ROS) (137). Because the amount of OX/ROS changes with time as smoke matures, these data suggest that freshly produced e-cig aerosols may be more potent than "aged" e-cig aerosols, which has important implications for their study. Indeed,

with regular cigarette smoke, different biological effects are seen with freshly produced vs. aged smoke, with aged smoke often being less biologically potent, which has previously been attributed to the decline in OX/ROS over time (108). Furthermore, because OX/ROS are highly reactive, they may also react with other components in the e-cig aerosol, further changing its chemical composition. Indeed, Sussan et al. demonstrated that e-cigs contain 1011 free radicals/puff, which is about 100 times less than is seen in regular cigarettes (240), but still likely to exert significant biological effects (66).

1.6. E-cig Topography

When generating cigarette smoke through a smoke machine, there are several international standards. These standards are important since the rate and duration that air passes through a cigarette affects the burn temperature and the relative amount of chemicals that are subsequently produced (96, 150), and this is likely true for e-cigs. Also, smoking tobacco in a reproducible fashion facilitates cross-laboratory data comparisons. Smoking profiles are designed to mimic the inhalation topography seen in actual smokers. For example, the Federal Trade Commission/International Standard Organization protocol calls for 2 s/35 ml puff every 60 s, and this is likely the most common puff profile used in the laboratory. However, it has been suggested that this profile underestimates how much people actually inhale, and a second profile, called "Canadian Intense," which uses 2 s/55 ml puff every 30 s, has also been adopted, and it has recently been recommended that experiments be repeated with both profiles to study smoke generation over the range of exposures (96, 150). Similarly, for e-cigs, knowing user's puff topography characteristics will be important for setting smoke machine parameters in the laboratory and for studying appropriate e-cig emissions. To date, no consensus exists on how to set e-cig parameters, and nothing comparable to the Canadian Intense profile has been developed. However, Farsalinos et al. found that e-cig users took puffs of 4.2 s every 23 s, although they did not record the puff volume (78), whereas Lee et al. found the average puff duration to be 3.1 s (136). In contrast, Behar et al. found that the average puff duration was 2.75 s every 17 s, with an inhalation volume of 56 ml (22). These authors studied several different types of e-cig and found that parameters varied only slightly with the type of e-cig used. It may be that the users puff harder/more frequently on e-cig devices that are less efficient at

delivering nicotine to maintain sufficient plasma nicotine levels. Indeed, data suggested that users were able to maintain constant nicotine uptake, despite switching brands (22). Importantly, until a greater consensus is reached, these data suggest that a modified Canadian Intense profile may be a suitable parameter for studying e-cig aerosol generation.

1.7. Will Nicotine and Chemical Constituents in E-liquids/E-cigs Alter Airway Physiology?

Nicotine is a highly addictive substance that is a major component of both cigarette smoke and e-cig aerosols that can cause physiological changes to users through nAChRs expressed throughout the body (52). Traditionally, nAChRs were primarily studied as part of the acetylcholine neurotransmitter signaling system in the central and peripheral nervous system. However, nAChR expression has been characterized in the airways as well (52, 145, 155, 277). These ligand-gated ion channels are permeable to both Na^+ and divalent cations and are physiologically stimulated by acetylcholine. nAChRs contain five subunits of which different subtypes exist (e.g., α, β, γ and δ) (3, 166). For example, the $(\alpha4)_3$, $(\beta2)_2$ nAChR subunit configuration is the most common type in the brain while the $(\alpha7)_5$ or α3, α5, and β4 subunits are more common in the lung (247). Lee et al. found that inhaled nicotine from cigarette smoke caused airway irritation and a cough reflex via nAChRs expressed in pulmonary afferent neurons (132).

Interestingly, nAChRs regulate cell proliferation and inhibit apoptosis (69). For instance, Maouche et al. found that α7 nAChRs were enriched in basal lung epithelia and that, during development, α7 regulated basal cell proliferation (149), which is important for the maintenance of epithelial cell turnover and differentiation. It is well established that smoking is linked to lung cancer, and a hallmark of lung cancer is uncontrolled cell proliferation. West et al. reported that both nicotine and its metabolite (nicotine-derived nitrosamine ketone) stimulated Akt signal transduction downstream of nAChR activation, which altered cell proliferation and apoptosis in bronchial epithelia (263). Specifically, α3, α5, and β4 were identified as candidate genes for a potential role in lung cancer from genome-wide association studies (37, 109, 214, 235). Additionally, Lam et al. found different nAChR subunit gene expression profiles between nonsmokers and smokers with nonsmall cell lung cancer (128). In the same study, human bronchial epithelial cultures (HBECs) were exposed to nicotine, and expression was

compared before and after removal of nicotine. Interestingly, exposing HBECs briefly upregulated nAChR α1, α5, and α7 expression at 72 h that returned to baseline levels after removal of nicotine. While all classes of nAChRs are capable of desensitization through chronic agonist exposure, there are definite immediate effects of nicotine on nAChRs in a subunit-dependent manner. Although it is currently unknown whether chronic exposure of nAChR to nicotine via e-cigs can cause lung cancer, the role of nAChR α7 in contributing to nonsmall cell lung cancer by altering cell proliferation and apoptotic resistance has been reported (128, 180).

Many inflammatory cells contribute to COPD pathogenesis, including, but not limited to, dendritic cells, T and B lymphocytes, monocytes, macrophages, and neutrophils (18, 106). Of note, monocytes, macrophages, and neutrophils, which are impacted by inhaling cigarette smoke in the lungs, also express nAChRs. The effects of noncholinergic signaling in airway inflammatory cells have been described (93). Nicotine suppressed inflammation in human monocytes and in mouse macrophages (154, 272). Neutrophil influx occurs in COPD, and indeed neutrophils present in smokers have upregulated nAChR expression and display a reduced ability to undergo apoptosis (11, 54). Likely, these neutrophils are more sensitive to inhaled nicotine and have extended life spans, which may serve to prolong inflammation in the lungs. Taken together, these data indicate that nicotine has a proinflammatory effect on neutrophils. However, nicotine also has an anti-inflammatory effect on monocytes/macrophages, which may be negated in the case of cigarette smoke due to the inhalation of other proinflammatory products such as the tar phase. This dualism has curious implications for the chronic inhalation of nicotine from e-cig aerosols, since many of the cigarette tobacco and tar byproducts that contribute to inflammation are not present in e-cig aerosols. It is possible that the anti-inflammatory effects of nicotine, in the absence of proinflammatory constituents, could suppress the user's immune system. Certainly, it is reasonable to assume that high nicotine exposure from e-cigs will be a major pharmacological player following e-cig exposure in any organ where nAChR are expressed. Thus, e-cig use may affect inflammation in the airways that could alter a user's susceptibility to infection and/or increase the risk of developing COPD or lung cancer.

Despite nicotine's known addictive and airway irritant properties, it is also known to be bitter tasting. Because of this, e-cigs and their e-liquids present a novel mix of chemical constituents that not only contain nicotine but also flavors, sweeteners, and other chemicals, many of which have not been studied in the lung. Many of these chemicals are present to mask the bitter nicotine taste. Thus, while nicotine has been shown to alter many aspects of airway physiology, the potential exists for salty, sweet-, and bitter-flavored constituents from e-liquids to stimulate taste receptor signaling pathways that could alter airway physiology with chronic use. To date, however, there is no current literature on the effects of e-cigs and chronic vaping in pulmonary physiology of nAChRs or taste receptors. nAChRs are ligand-gated ion channels, similar to ion channels that regulate salty taste transduction (e.g., epithelial sodium channel) (103). However, sweet and bitter taste receptors are G protein-coupled receptors (GPCRs). GPCRs typically act through Gα proteins to activate phospholipase Cβ (PLCβ) that cleaves membrane-bound PIP_2 to generate inositol 1,4,5-triphosphate (IP_3) (64, 75, 233). IP_3 molecules act on ER IP_3 receptors (IP_3Rs), eliciting ER Ca^{2+} release. The ER transmembrane protein stromal interaction molecule 1 (STIM1) senses ER Ca^{2+} depletion and causes puncta formation to interact with the membrane Ca^{2+} channel Orai1 to initiate store-operated Ca^{2+} entry (SOCE) (Fig. 1.2*A*-*C*) (141, 189). Ca^{2+} continues to initiate signaling downstream by the phosphorylating proteins such as protein kinase Cα (PKCα) (65, 73). Of note, membrane receptor tyrosine kinases (RTKs) also have the ability to trigger a similar signaling mechanism, though RTKs are not known to detect tastants/odorants (161, 173).

Interestingly, the ability to taste bitter substances may contribute to smoking behavior and nicotine addiction (35, 72, 147). Bitter taste receptors (T2Rs) are ligand-activated GPCRs that use intracellular Ca^{2+} as a downstream signaling molecule. There are ~30 T2Rs expressed in humans. T2Rs are most abundant in the tongue, and T2R polymorphisms (e.g., T2R38) that impair the ability to taste bitter compounds have been correlated with populations that are more nicotine dependent and/or heavy smokers (118, 147). Furthermore, when tongue tissue was compared for T2R mRNA expression in smokers vs. nonsmokers, overall T2R gene expression was reduced in the smoking compared with the nonsmoking group (10). It is unknown whether the reduction of T2R gene expression was genetic or was

suppressed by a component of cigarette smoke. Yet, a correlation between T2R expression and age was present in the nonsmoker group and absent in the smoker group, suggesting that starting smoking earlier in life could suppress T2R gene expression and contribute to nicotine addiction.

Many T2Rs have been identified in the upper and lower airway epithelia as well as airway smooth muscle cells (50, 63, 223, 253). Interestingly, T2R38 polymorphisms have also been linked to increased susceptibility of upper respiratory infections (135). Although an endogenous ligand is still unknown, known bitter agonists activate these T2Rs and increase intracellular Ca^{2+}, stimulating ciliary beat frequency. Thus, they play a role in detecting noxious inhalants and expelling them from the airways due to increased rates of mucociliary clearance. Nasal mucosa have been reported to express both sweet receptors (T1Rs) as well as T2Rs in special nonciliated epithelial cells called solitary chemosensory cells (SCCs) (133). SCCs in the nasal epithelium harbor these receptors along with known components of the taste receptor signaling pathway and trigeminal nerve innervation. Tizzano et al. characterized the presence of SCCs with T2Rs and the T2Rs' ability to detect known bitter agonists and acyl-homoserine lactones (253), which are intercellular chemical signaling compounds secreted by Gram-negative bacteria, providing more evidence for T2R roles in innate immunity. Furthermore, Lee et al. found that T1Rs and T2Rs in nasal epithelium converge to arbitrate innate immunity (134), that is, when T1Rs are activated (e.g., hyperglycemia, chronic rhinosinusitis), they can block the antimicrobial effects of T2Rs, causing persistent airway infections. Together, these data suggest that taste reception in the airways is important to innate immunity.

Nonciliated SCCs are found throughout the lower airways, although T1Rs are not detected there (162, 163). Interestingly, Dehkordi et al. reported that intrapulmonary epithelial SCCs coexpress T2R38, its T2R signaling components, and many nAChR subunits in the same cells (60). Although it is unknown whether these two signaling pathways directly interact, it is possible that the coexpression of multiple chemosensation receptor types may increase the repertoire and sensitivity of airway cells to inhaled irritants, specifically nicotine. In this case, nicotine might be sensed by either receptor type, and an interaction might exist between downstream components of the T2R and nAChR signal transduction

pathways (e.g., Ca^{2+} as a common second messenger) that regulate cellular responses to nicotine. For example, triggering Ca^{2+} influx from the activation of one nAChR subunit can attenuate the response of a second subunit through desensitization of the stimuli or prolong increases in intracellular Ca^{2+} (86).

As mentioned previously, Ca^{2+} is a common second messenger that acts downstream of not only nAChRs but also transient receptor potential (TRP) membrane ion channels. TRP channels are non-selective cation channels that have the ability to increase cytosolic Ca^{2+} concentrations upon activation. Several subtypes have been discovered and some natural odorant molecules have been reported as targets (190). These TRP channel subtypes include TRP vanilloid (TRPV), TRP ankyrin (TRPA), and TRP melastatin (TRPM). For example, menthol is able to activate TRPM8 (160) and has been used in menthol cigarettes where the TRPM8 activation triggers a cooling sensation that suppresses the bitter nicotine flavor for smokers (182). Cinnamaldehyde is the common cinnamon flavoring used in food and now e-cig products and is capable of activating TRPA1 (16, 117). Lastly, vanillin is a common vanilla flavoring capable of activating TRPV1 and TRPV3 (143, 269).

1.8. Effects of E-liquids and E-cig Aerosols on Cultured Cells from the Lungs

Tobacco smoke is highly proinflammatory and has been shown to trigger the release of inflammatory cytokines from endothelia, epithelia, and leukocytes (30, 95, 131). These cytokines can then trigger additional changes, including goblet cell metaplasia and neutrophil influx (127). Inflammation may be beneficial in the short term, especially when resolving infection. However, chronic inflammation can act as a precursor to cancer, and continued influx of neutrophils, with the subsequent increase in free elastase levels, can lead to cell damage and denudation of the epithelia (32, 243). Tobacco exposure is also associated with cellular cytotoxicity, including increased apoptosis, autophagosome formation, membrane permeability, and mitochondrial damage (67, 115, 130, 213). Furthermore, micronuclei form when chromosomes or parts of chromosomes are excluded from daughter nuclei following cell division (81). As such, micronuclei formation is associated with a high risk of cancer and is a common assay that is used to screen for genotoxic substances, and increased micronuclei formation has been observed in cigarette smokers (61, 251). Tobacco smoke has also been shown to alter

gene expression and DNA methylation in both the whole lung and in airway epithelia (99, 184, 257), macrophages (68), and endothelia (273). Many of these assays have been established as outcome measures for tobacco smoke exposure, and they should be useful for probing the effects of e-cig exposure.

To date, many cell types have been exposed to e-liquids and/or e-cig aerosols. These cell types include lung epithelial cell lines (H292, A549), lung fibroblasts, human primary trachea-bronchial cells, and HaCaT keratinocytes (42, 137, 267). Whereas e-liquids are aerosolized, a common early approach has been to add e-liquids directly to cells at various dilutions. Although this protocol would not pick up any additional effects of pyrolysis due to heating the e-liquid, it is a useful first step to determine whether e-liquids themselves have inherent toxicity. Wu et al. exposed nondifferentiated tracheobronchial cultures to a tobacco-flavored e-liquid that contained either 18 mg/ml of nicotine (which equates to 111 mM) or was nicotine free for 24–48 h over the range (vol/vol) 0.01–0.3% (InnoVapor, Boise, ID) and found that exposures in this range did not increase lactate dehydrogenase (LDH) levels, suggesting that they were not cytotoxic (267). However, the upper levels of dosing caused significant increases in IL-6 and IL-8 levels, also increasing rhinovirus infection and rhinovirus-induced IL-6 secretion and decreasing mRNA levels of SPLUNC1, an innate defense molecule (248, 267). Whereas increases in IL-6 secretions have been detected after rhinovirus infections (195), the implication of this observation in the context of e-cig and/or tobacco exposure is not fully understood and needs additional testing. However, increased IL-6 responses to viral infection have been detected in COPD patients, suggesting that this may be a relevant assay for e-cig exposure (219). Lerner et al. found that e-liquids altered HFL-1 cell morphology (137). Bahl et al. tested the effects of e-liquids, directly added to murine pulmonary fibroblasts, human embryonic stem cells, and murine neural stem cells (15). Although effects of e-liquids were typically seen with ≥0.1% (vol/vol) addition, in general, the stem cells were more sensitive than the fibroblasts, suggesting that some cell types in the lung may be more vulnerable to e-cigs than others. Furthermore, of the 36 e-liquids tested, ~15 showed cytotoxicity, with cinnamon flavors being especially toxic. Of interest, the authors found significant variability in cytotoxicity from batch to batch, even for one flavor from one vendor, which suggests that poor quality control may exist in some cases.

In addition to directly studying the effects of e-liquids, they can be heated/aerosolized and then studied. Cervellati et al. exposed A549 (lung epithelial) and HaCaT (keratinocytes) cells to whole cigarette smoke or e-cig vapor from three combinations of e-cigs (nicotine; nicotine + flavor; no flavor, no nicotine) (42). After 50 min of smoke or aerosol exposure, cultures were then left for 24 h, and LDH release and cell viability were studied. No information was given regarding whether these cells were polarized or not. However, they found that, under these conditions, e-cigs with nicotine and/or flavor induced similar cytotoxicity (increased LDH release and decreased cell viability) as standard cigarettes while nicotine and flavor-free e-cigs did not have any effect. E-cig aerosols (generated using a 4 s/35 ml pulse) also caused an increase in IL-6 and IL-8 secretion, which in the case of one flavor (cinnamon roll) was greater than the IL-8 secretion seen with cigarette smoke extract addition (137).

The effects of e-cig exposure have also been studied on the lung's microvasculature. For example, Schweitzer et al. found that e-cigs decreased the electrical resistance of endothelial cells derived from mice, rats, and humans, and exerted significant effects on cell viability and 3-(4,5-dimethylthiazol-2-yl)-2,5-diphenyltetrazolium bromide production that were associated with changes in cell signaling (activation of p38 mitogen-activated protein kinase) (222). Interestingly, these changes were similar to those observed after exposure to cigarette smoke extract (222). They also detected increased phosphorylation of myosin light chain and Rho kinase following e-cig exposure, which may have been due to activation of sphingolipids (222). Changes in the permeability in the lung's microvasculature may induce edema and/or increase the number of leukocytes that can enter the lung, thus increasing inflammation, as described elsewhere (126).

1.9. Effects of E-cigs on the Murine Lung

Although little is known about the effects of e-cigs on humans, some studies have been performed in mice. E-cig exposure has been shown to elicit neuropharmacological effects, including upregulation of nAChR, in different areas of the brain and also caused signs of addiction and increased serum and cotinine levels, suggesting that comparable systemic nicotine levels can be obtained with e-cig exposure as are seen with tobacco exposure (2, 188). Lerner et al. exposed mice to e-cig aerosols for 5 h/day for 3

days and examined the mice 1 day later. They found that several cytokines were increased in the bronchoalveolar lavage of these mice, including IL-1α, IL-6, IL-13, and monocyte chemoattractant protein-1 (MCP-1) (2015). Of note, MCP-1 recruits macrophages to the lung, IL-6 is a proinflammatory cytokine, and IL-13 induces cellular remodeling and goblet cell hyperplasia. Schweitzer et al. found that an e-cig exposure regimen, which was equivalent in dose to exposure to smoke from two cigarettes, caused a significant increase in 8-oxo-2'-deoxyguanosine (8-oxo-dG) in both plasma and bronchoalveolar lavage (222). 8-oxo-dG is a marker of systemic oxidative stress and is indicative of DNA damage (169). They also detected increased nitrotyrosine levels in plasma. Nitrotyrosine can be formed following exposure to reactive nitrogen species such as peroxynitrite anion and nitrogen dioxide and is also a marker of cell stress/damage (204). A 2-wk exposure to e-cigs smoked under relatively standard conditions (2-s 35-ml puff) caused a significant increase in the number of macrophages in murine lungs and actually decreased IL-6 (222). The differences in IL-6 levels observed between the two experiments are most likely due to differences in smoking (vaping) regimens since one was acute and the other was chronic (137, 222). Mouse strain differences and/or differences in e-cig device/e-liquid may also have been factors.

After infection with *Streptococcus pneumonia*, e-cig-exposed mice were less able to clear this infection, suggesting that innate defense was impaired (240). They also found that H1N1 influenza virus infection also was poorly cleared. Although these data will need to be repeated by other groups, it is the first report that e-cig exposure leads to increased susceptibility to infection, which has important implications for the safety of e-cig users. Interestingly, increased susceptibility to pathogens is a hallmark of tobacco exposure and is seen following both viral and bacterial infections (84, 175, 197). In addition to these aerosol exposures, a 50-fold-diluted e-cig liquid has been shown to increase IL-4, IL-5, and IL-13 in allergen-sensitized mice when tracheally instilled (140), again suggesting that e-liquids can still have adverse effects even before they are vaporized.

The adverse effects of tobacco on both prenatal and postnatal development have been well described and include low birth weight, increased incidence of sudden infant death syndrome, and

development of lung disease later in life (e.g., asthma) (1, 90). Whereas most published studies to date have focused on adult mice, it has been demonstrated that e-cig exposure also adversely effects neonatal mice and leads to impaired development, including decreased weight gain and reduced cell proliferation in the lungs, suggesting that secondhand vaping may also potentially be a cause for concern and could adversely affect lung development (158).

1.10. Effects of E-cig Exposure in Humans

Currently, many adult e-cig users are former smokers and have a significant history of tobacco usage before using e-cigs and/or continue to be mixed tobacco/e-cig users (89, 192). This will make studying the chronic effects of e-cigs difficult since the airways/lung retain a significant memory of smoking history/exposure even after smoking cessation. For example, Rager et al. found significant evidence of DNA methylation in the nasal epithelia of ex-smokers (194). Thus, for any observed effects on e-cig smokers, the previous and/or current tobacco smoking history must be taken into account. That said, the largest and fastest-growing population of e-cig users who have never smoked tobacco is adolescents. For example, in North Carolina, 15% of high school students have vaped e-cigs, and 60% thought that e-cigs were safe. In contrast, among the same group, 24% had smoked cigarettes (7). This trend is reflected nationally (156).

It has been shown that short-term (e.g., 5 min) e-cig inhalation leads to comparable plasma cotinine levels as regular tobacco smoking and exerts rapid physiological effects on the cardiovascular system, including elevated heart rate (255). These data indicate that modern e-cigs are delivering significant amounts of nicotine to the bloodstream. Although to date no studies have been performed to look at the adverse effects of e-cigs on pulmonary health (e.g., inflammation, etc.), Vardavas et al. looked at the effects of 5 min e-cig exposure on pulmonary function using standard spirometry (256). Interestingly, they found that a 5-min e-cig exposure caused a significant increase in peripheral airway resistance, which is indicative of changes to the small airways. The authors noted that these changes were relatively small and likely not great enough to be of immediate clinical significance. However, the changes were observed after only 5 min of exposure, and they speculated that chronic exposure may lead

to greater changes in resistance. They also found that this 5-min exposure caused a significant decrease in exhaled nitric oxide (NO) levels. NO has a number of functions in the lung, and changes in NO levels can affect ciliary beating, transcription, inflammation, ion transport, and airway smooth muscle tone (31). NO is altered in many diseases, including asthma (increased), cystic fibrosis (decreased), primary ciliary dyskinesia (decreased), and COPD (may be suppressed or mildly increased) (275). Thus, it is possible that e-cig exposure could cause different lung disease to COPD.

1.11. Conclusions and Future Directions

There is a long history of deceptive marketing tactics used by the tobacco industry regarding the 'safety' of cigarettes (76). Thus, it is interesting to speculate whether the same will hold true for the nascent e-cig industry. Certainly, users want to believe that e-cig products are safe, but, unfortunately, no definitive data currently exist to prove or disprove this hypothesis. Studying e-cig exposure is very much like trying to hit a moving target, but one where researchers are not completely sure what the target looks like, since e-cig devices, the way that they are used, and the types/flavors of e-liquids available are constantly changing. However, some facts have been established: *1*) current e-cig devices deliver nicotine at comparable levels to cigarettes, and certainly at levels high enough to evoke physiological responses in humans and rodents (79, 158, 234), *2*) nicotine is highly addictive and, along with its metabolites, can cause cancer and affect neuronal development in adolescents irrespective of its source (71, 260), *3*) e-liquids have been shown to contain potentially toxic aldehydes and ROS (246), and *4*) some type of a biological response (e.g., change in cytokine levels) has been observed in the vast majority of murine in vivo and in vitro studies following e-cig vapor/e-liquid exposure (137, 222, 256). Although it seems certain that e-cig aerosols contain toxicants, it is fair to say that they likely contain less types of toxicants than cigarette smoke (i.e., e-cig aerosols likely have hundreds of chemicals in them while tobacco smoke has thousands of chemicals). The remaining question is then one of dose ranging, that is, are the toxicants in e-cigs present in sufficiently high concentrations to elicit lung disease over a similar time frame as tobacco smoking?

Given the paucity of information that is available regarding the effects, not only of e-cigs, but also of many of the chemical constituents of e-liquids on the lungs, we propose that all commercially available e-cig products be regulated in a similar fashion as any inhaled therapeutic agent, that is, thorough inhalation toxicology and safety-based clinical trials. Although this would be an undeniably expensive undertaking, the estimated value of the e-cig market is in the billion dollar range, indicating that tobacco and e-cig companies could likely foot this bill.

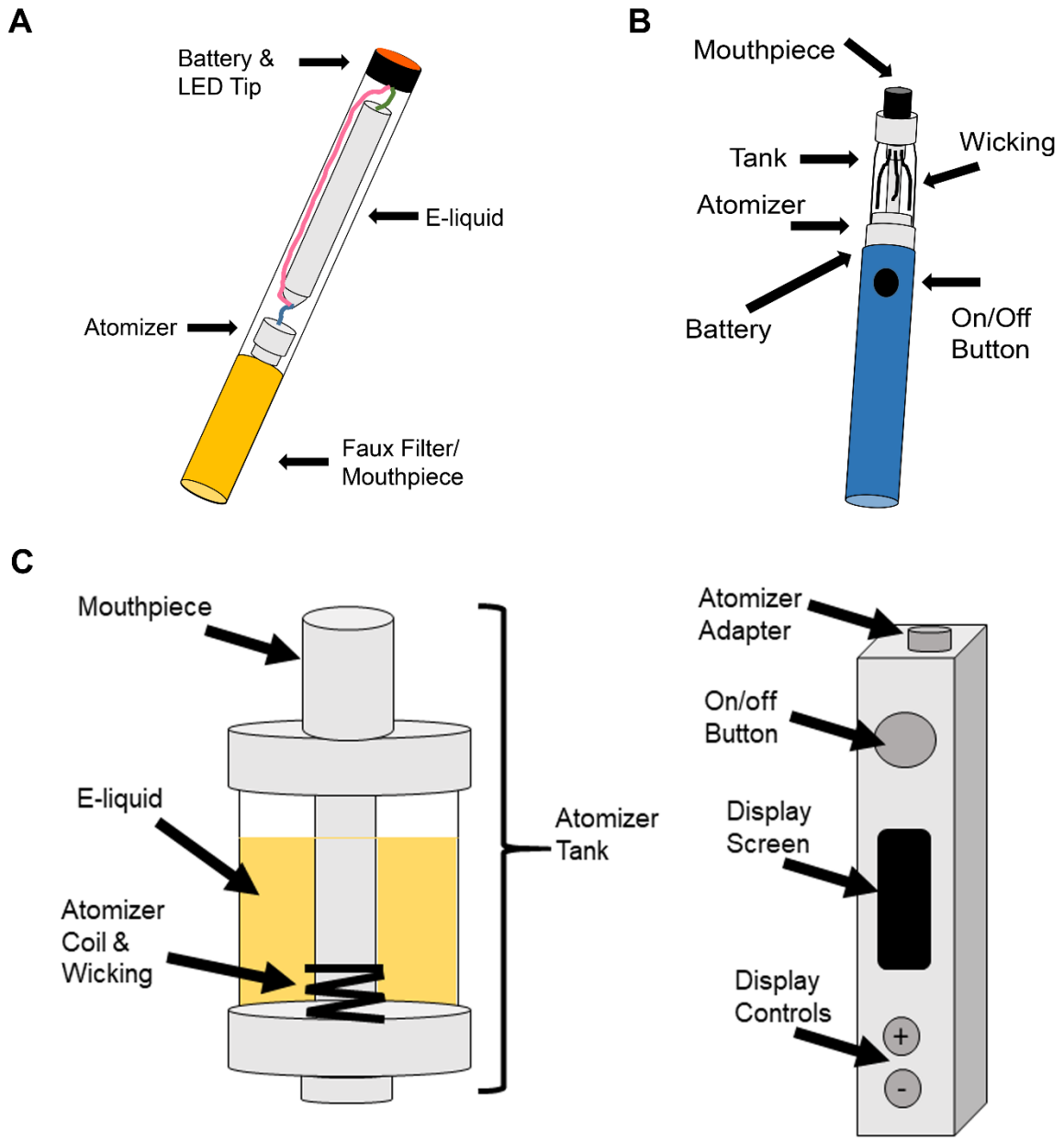

Figure 1.1. 1st-3rd generation e-cig device schematics. *A*: Schematic of 1st generation disposable 'cigalike' device. *B:* 2nd generation vape pen with refillable tank and rechargeable battery. *C*: Schematic of 3rd generation refillable atomizer tank with replaceable coil and corresponding mod device equipped with user controls and rechargeable battery.

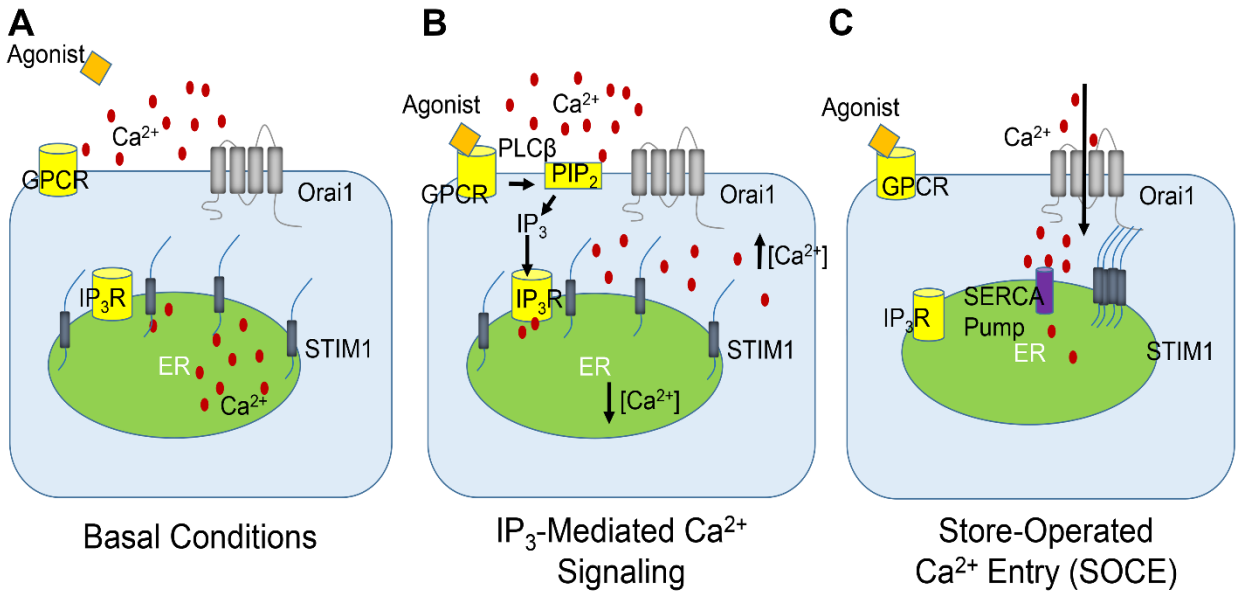

Figure 1.2. GPCR signaling pathway causes IP_3-mediated ER Ca^{2+} release and SOCE. *A*: At basal conditions, Ca^{2+} concentrations are low within the cytosol and high in the extracellular space and within the ER. *B*: GPCR activation elicits PLCβ cleavage of PIP_2 to generate IP_3, which acts on ER IP_3Rs to release ER Ca^{2+} and increase cytosolic Ca^{2+} concentrations. *C*: STIM1 senses ER Ca^{2+} depletion and forms aggregates and interacts with Orai1 to activate SOCE, prolonging the elevated Ca^{2+} concentration as the ER Ca^{2+} store is refilled by the SERCA pump.

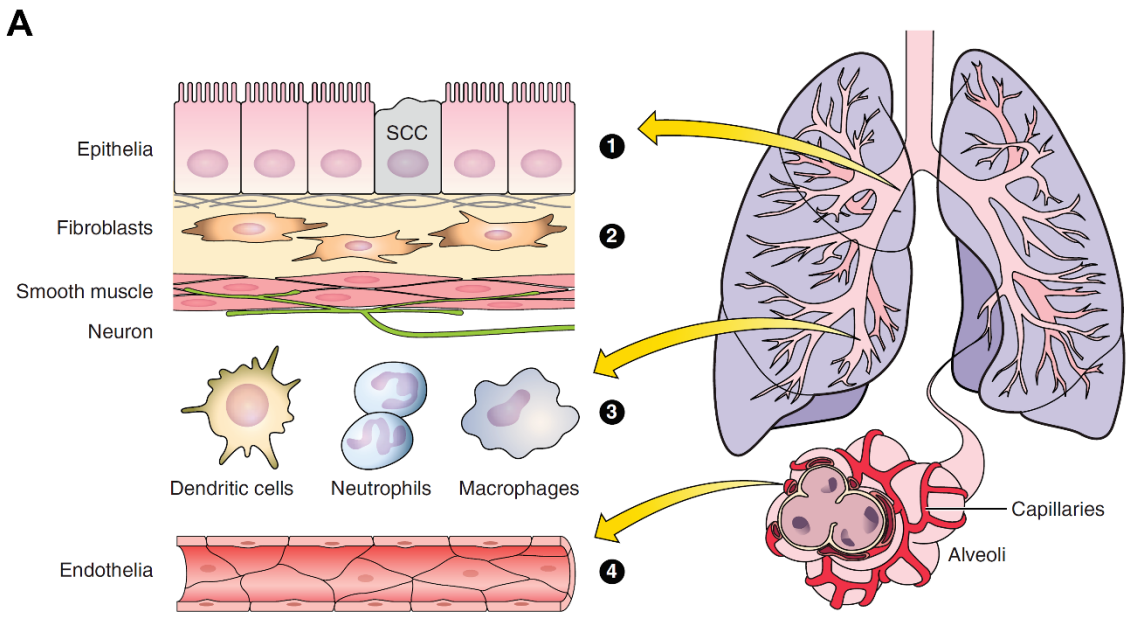

Current data for the effects of E-cigarettes/E-liquids on the lung	
Tissue/cell type	**Effects**
(1) Epithelia	↑Cytotoxicity ↓Cell viability ↑Inflammation ↑Infection
(2) Fibroblasts	↑Cytotoxicity ↓Cell viability Altered morphology
(3) Inflammatory cells (BALF)	↑Macrophages ↑Cytokine secretion ↑Infection
(4) Endothelia	↓Cell viability ↓Electrical resistance

Figure 1.3. Summary of the effects of e-cig and e-liquid exposures in pulmonary cell types. Included in the table is a short list of the current *in vitro* and *in vivo* study outcomes for lung-related cell types that are depicted in the cartoon and labeled appropriately.

Chapter 2: Flavored E-cigarette Liquids Reduce Proliferation and Viability in the CALU3 Airway Epithelial Cell Line

2.1. Overview

E-cigarettes are generally thought of as a safer smoking alternative to traditional cigarettes. However, little is known about the effects of e-cigarette liquids (e-liquids) on the lung. Since over 7,000 unique flavors have been identified for purchase in the United States, our goal was to conduct a screen that would test whether different flavored e-liquids exhibited different toxicant profiles. We tested the effects of 13 different flavored e-liquids [with nicotine and propylene glycol/vegetable glycerin (PG/VG) serving as controls] on a lung epithelial cell line (CALU3). Using the 3-(4,5-dimethylthiazol-2-yl)-2,5-diphenyltetrazolium bromide (MTT) assay as an indicator of cell proliferation/viability, we demonstrated a dose-dependent decrease of MTT metabolism by all flavors tested. However, a group of four flavors consistently showed significantly greater toxicity compared with the PG/VG control, indicating the potential for some flavors to elicit more harmful effects than others. We also tested the aerosolized vapor from select e-liquids on cells and found similar dose-dependent trends, suggesting that direct e-liquid exposures are a justifiable first-pass screening approach for determining relative e-liquid toxicity. We then identified individual chemical constituents for all 13 flavors using gas chromatography-mass spectrometry. These data revealed that beyond nicotine and PG/VG, the 13 flavored e-liquids have diverse chemical constituents. Since all of the flavors exhibited some degree of toxicity and a diverse

---

[2]This chapter previously appeared as an article published in American Journal of Physiology Lung Cell Molecular Physiology and is reprinted with permission. The original citation is as follows: **Rowell TR, Reeber SL, Lee SL, Harris RA, Nethery RC, Herring AH, Glish GL, Tarran R**. Flavored e-cigarette liquids reduce proliferation and viability in the CALU3 airway epithelial cell line. *Am J Physiol Lung Cell Mol Physiol* 313: L52-L66, 2017.

array of chemical constituents with little inhalation toxicity available, we conclude that flavored e-liquids should be extensively tested on a case-by-case basis to determine the potential for toxicity in the lung and elsewhere.

2.2. Introduction

E-cigarettes (e-cigs) have been growing in popularity since their debut in 2007 and are estimated to become a $50 billion global market by 2025 (202). E-cigs differ from tobacco cigarettes in that they do not contain tobacco, have varied nicotine concentrations (0–36 mg/ml), and produce an inhalable aerosol (vapor) that is generated without combustion. Instead, an e-cig liquid (e-liquid) is drawn and heated over a battery-operated coil as the user inhales. E-liquids are usually composed of a vehicle with varying ratios of propylene glycol (PG) and vegetable glycerin (VG) that contain nicotine and chemical flavors. Recently, the Food and Drug Administration (FDA) introduced rules to regulate e-cig products (https://www.fda.gov/TobaccoProducts/Labeling/ProductsIngredientsComponents/ucm456610.htm) (206, 209). Despite this legislation, there continues to be much debate over the safety and efficacy of these products. E-cigs have commonly been marketed as a safer smoking alternative because they lack the carcinogens from tobacco and presumably fewer of the pyrolysis products from combusting tobacco that are associated with smoking-related diseases. However, some e-cig devices are capable of producing pyrolysis products (i.e., reactive aldehydes) and oxidant species similar to traditional cigarettes (137, 218, 240), but the conditions under which users would actually be exposed to disease-causing levels of these products remain a source of controversy.

While the direct health effects of cigarette smoke exposure have been extensively studied with evidence-based links found between tobacco use and both lung cancer and chronic obstructive pulmonary disease, e-cig research is still lagging behind consumer use. A review of all known studies reporting effects of e-cig aerosols and e-liquids on the lung amounted to less than 15 in 2015 (212). Fortunately, the interest concerning lung health effects of e-cigs has led to many more research publications since then. However, there is still much that is unknown about the biological effects of e-cigs. Of particular concern, e-cig use in middle and high school students has tripled in just three years (156) and by 2015,

more than a quarter of middle and high students had tried e-cigs (254). Furthermore, the availability of over 7,000 unique flavors in the United States (276) alone may contribute to their popularity in adolescents (6).

It is currently unknown whether or not long-term e-cig use will cause respiratory diseases similar to cigarette smoke, none at all, or something entirely different. For example, bronchiolitis obliterans or "Popcorn Workers' Lung" is scarring of the small airways that can range from mild and reversible to severe and irreversible. Prolonged inhalation of diacetyl, a buttery-flavored chemical used in microwave popcorn manufacturing and elsewhere, can and has caused this disease in some workers at microwave popcorn manufacturing plants (17, 124). Although diacetyl is safe to eat and thus found on the "generally recognized as safe" list, it is clearly not safe to inhale. Diacetyl and many other flavorings have only been tested and approved for ingestion and have not been tested for inhalation toxicology. Despite the known link between diacetyl and bronchiolitis obliterans, Allen et al. reported that either diacetyl or 2 other prominent butter-flavored chemicals (2,3-pentanedione and acetoin) were detected in 47 of 51 flavored e-liquid aerosols tested (5). Thus there is the potential for e-liquid flavors to have as yet unknown and possibly negative effects on the lung, as has recently been discussed (19).

Given the variety of available flavors and devices, information is needed regarding the biological effects of different e-liquids and their individual constituent(s) on the different cell types in the respiratory system. Therefore, we used a high-throughput screening approach to assess the potential effects of 13 different flavored e-liquids and their respective controls on cell proliferation and an array of viability and toxicity markers over a range of doses following direct- and vaped- e-liquid exposure. Although several researchers have investigated the effects of e-liquids or e-cig aerosols on the lung, few studies have focused on *1*) identifying component chemicals and *2*) assessing their biological effects (15, 21, 79, 111, 112, 217, 226, 252). Therefore, we also conducted mass spectrometry analysis on all 13 flavors to pair biological outcomes with chemical constituent(s) identified in each flavor to understand which flavors and individual constituents may alter lung epithelial cell proliferation and/or viability.

2.3. Methods

Flavored e-cig liquids. All flavored e-cig liquids (e-liquids) were purchased from The Vapor Girl (https://www.thevaporgirl.com/). The tested flavors were Captain Black Cigar, Peanut Butter Cookie, T-bone, Popcorn, Black Licorice, Energon (orange energy drink), Vanilla Tobacco, Banana Pudding (Southern Style), Kola, Hot Cinnamon Candies, Menthol Tobacco, and Solid Menthol. All e-liquids were ordered to contain 12 mg/ml nicotine. An additional 0 mg/ml nicotine Captain Black Cigar was purchased as a nicotine-free control. At the time of purchase, the vehicle liquid was advertised as a 70/30 ratio of PG to VG. Thus a vehicle control was made in our laboratory using 70 PG/30 VG. For all aerosol experiments, additional Peanut Butter Cookies, Banana Pudding, and Hot Cinnamon Candies e-liquids were purchased from The Vapor Girl. All three additional e-liquids were ordered to contain 12 mg/ml nicotine and a 55/45 ratio of PG/VG. Therefore, we made an additional 55 PG/45 VG control for the aerosol experiments.

Chemicals and reagents. PG, VG, DMSO, probenecid, and methanol were purchased from Sigma-Aldrich. DAPI, calcein (AM), MitoTracker Red (CMXRos), fluo-4 (AM), and the Vybrant MTT Cell Proliferation Assay Kit were purchased from Life Technologies. Nicotine was purchased from Alfa Aesar. The Cytotoxicity Detection KitPLUS (LDH) was purchased from Roche. DAPI, calcein (AM), MitoTracker Red (CMXRos), and fluo-4 (AM) were reconstituted using DMSO and applied to cells in experiments where the final DMSO concentration was ≤0.1%.

Cell culture. CALU3 cells were cultured in MEM alpha with 10% FBS and penicillin/streptomycin (GIBCO) as described (49). For the 3-(4,5-dimethylthiazol-2-yl)-2,5-diphenyltetrazolium bromide (MTT) assay, MEM alpha without phenol was used per the manufacturer's guidelines. Cells were seeded into 96-well black-walled clear bottom plastic plates (Corning). For e-liquid 24-h studies, cells were seeded at 12,500 or 45,000 per well for 12 h overnight and the 24-h treatment began the next morning. E-liquids were diluted (%vol/vol) in CALU3 media. After 24 h, e-liquid-treated media was removed from cells and assays were performed. For aerosol 24-h studies, cells were seeded at 25,000 per well for 4–8 h and media were changed just before aerosol treatments were

performed. After aerosol exposures, cells were incubated for 24 h before aerosol-exposed media were removed and assays were performed.

Cell proliferation. The MTT assay was performed as instructed by the manufacturer after cells were treated for 24 h with either PBS, 70 PG/30 VG, nicotine, or flavored e-liquids. Cells were allowed to proliferate for 4 h after removal of the treatments. Data were calculated as percent absorbance of each treatment compared with the average of the 0% e-liquid (media control) treatments in each plate. Nonlinear regression curves were fit to each flavor or nicotine ± PG/VG dose responses in the MTT assays using GraphPad Prism to calculate IC_{50} values where appropriate.

Cell number and viability. Total cell number was measured at the end of the 24-h e-liquid and aerosol exposures. Cultures were rinsed with PBS and fixed with 100% methanol. After fixation, cells were rinsed again with PBS and stained with DAPI for 10 min. Cultures were rinsed following staining, and DAPI fluorescence intensity was measured using the Tecan Infinite Pro plate reader [excitation (ex): 360 ± 5 nm; emission (em): 460 ± 5 nm]. Total cell number was calculated as percent fluorescence of the e-liquid- or aerosol-treated cells compared with the average of the 0% e-liquid or 0 puff (media control) wells in each plate. Cell/mitochondrial viability was assessed using calcein and MitoTracker Red fluorescent indicators. After 24-h e-liquid or aerosol exposures, treated media were exchanged for fresh media containing either 3 µM calcein or 125 nM MitoTracker Red. Cultures were incubated for 30 min at 37°C. Cultures were then rinsed, media were replaced with a standard Ringer's solution, and fluorescence intensities were read using the Tecan Infinite Pro plate reader for calcein (ex: 495 ± 5 nm; em: 516 ± 5 nm) or MitoTracker Red (ex: 579 ± 5 nm; em: 599 ± 5 nm), respectively. Cell/mitochondrial viability was calculated as a percent fluorescence of e-liquid or aerosol-treated cells compared with the average of the 0% e-liquid or 0 puff (media control) wells in each plate.

Cytotoxicity (membrane permeability – LDH release). Membrane permeability due to e-liquid exposure was measured using the Cytotoxicity Detection Kit^{PLUS}. Media were collected from e-liquid-treated wells after 24-h exposure and the LDH assay was performed per manufacturer's instructions.

Data were calculated as percent LDH release compared with a lysed control and reported as %LDH release, where

$$\%LDH\ release = \frac{experimental\ value - low\ control}{high\ control - low\ control}\ x\ 100$$

Ca^{2+} signaling. Changes in cytosolic Ca^{2+} concentration were measured using 8 µM fluo-4 dye loaded into cells in the presence of 1 mM probenecid for 40 min at 37°C. Cultures were then rinsed, and media were replaced with a standard Ringer's solution and fluorescence intensities were read every 15 or 30 s using a Tecan Infinite Pro plate reader for fluo-4 (ex: 494 ± 5 nm; em: 516 ± 5 nm). A fluorescent baseline was established before the nicotine doses were added to the wells, and changes in fluorescence were normalized to the baseline (F/F_0). The peak change in F/F_0 was measured for each dose, and a nonlinear regression curve was fit using GraphPad Prism to calculate the EC_{50}.

RNA extraction, cDNA synthesis, and quantitative RT-PCR. RNA was extracted from untreated CALU3 cells using the Qiagen RNeasy kit following the manufacturer's protocol. cDNA was synthesized using the Bio-Rad iScript cDNA synthesis kit following the manufacturer's protocol. Gene expression was measured using Taqman gene expression assays from Applied Biosystems for *Orai1*, *Scnn1A*, *P2Y2R*, *GAPDH*, *CHRNA4*, *CHRNA5*, *CHRNA6*, *CHRNA7*, *CHRNB1*, *CHRNB2*, and *CHRNB3* using human primers. Genes of interest were normalized to *GAPDH* and fold change was calculated using ΔΔCT method relative to *Orai1*.

Aerosol exposures. E-liquids were heated to generate aerosols using Uwell Crown tanks with 0.25-Ω dual-coils and a Sigelei Fuchai 200W device. The power output was set to either 40 or 100 W, as indicated. Filter pads (GE Healthcare Life Sciences) with a 2-µm pore size were used to collect particulates from the aerosol. The filter pads were weighed before and after 15 or 35 puffs of either 40 W or 100 W, 55 PG/45 VG were passed through them. CALU3 cells seeded in 96-well plates were exposed to a range of puffs (0 –35) from either air, 55 PG/45 VG vehicle, 70 PG/30 VG vehicle, Peanut Butter Cookies, Banana Pudding, or Hot Cinnamon Candies. A syringe was used to collect, measure, and apply the aerosol to the wells. A 70-ml puff was applied once every 30 s and was distributed among six wells at

once using a three-dimensional printed acrylic six-channel manifold. After aerosol exposures, the cells were incubated for an additional 24 h before measuring total cell number or viability. These were calculated as percent fluorescence of the aerosol-treated cells compared with the average of the 0 puff (media control) wells per plate, which were covered with silicone strips to avoid aerosol exposures.

Mass spectrometry. Samples of e-liquids were diluted 10- or 50-fold in methanol and analyzed by gas chromatography-mass spectrometry (GC-MS) using an Agilent 6890 GC with an Agilent MSD mass spectrometer. One-microliter volumes were introduced by manual injection and were separated on an Agilent DB-5 column with helium carrier gas. The temperature was ramped from 60 to 300°C at a rate of 20°C/min. GC-MS spectra were analyzed using NIST AMDIS software coupled to the NIST 2008 mass spectral database for automated database searching. Constituent profiles of flavors were compared between all 13 e-liquid flavors using peak areas under the curve from GC-MS data that were discretized into a value of 0 (absent) or 1 (present) and compared using R software.

Statistical analyses. Data (see Figs. 2.1*A, C*; 2.3*A*–*D*; 2.4*A, B*; and 2.5*A, B*) were fit using a linear mixed model with main effects for flavor and dose, a flavor by dose interaction, and a random intercept to control for possible plate effect. A similar analysis was performed (see Fig. 2.5*C, D*), where puff number and wattage were analogous to flavor and dose. Based on these models, subanalyses were performed to investigate if there was an association between dose and response within a flavor. To reduce inflation of type 1 errors, a step-down approach was used in testing. Overall tests for a statistically significant dose and flavor interaction were performed first, and tests for the presence of a dose and response association within each individual flavor were performed only if the overall test was significant. Further tests to determine which doses were significantly different within a flavor were performed only if the previous test confirmed the existence of a dose and response association within that specific flavor. In the nicotine-dosing experiments, responses within each nicotine ± PG/VG treatment were compared with the respective 0 mg/ml. Graphpad Prism software was used to compare the log(IC_{50}) values between dose-response curves for select flavored e-liquids (%vol/vol) and nicotine (mg/ml) ± PG/VG (see Figs. 2.1*B, D;* Table 2.1).

For Fig. 2.2*A*, we fit a linear model to each log-transformed outcome with a fixed effect for gene type. Log transformations were used to ensure adherence to the modeling assumptions. If an overall test for the effect of gene type was found to be significant, we tested for pair-wise differences between each gene and *Orai1*. In Fig. 2.5*E* we fit a linear model with main effects for puff number and wattage and a puff number by wattage interaction term. Significant differences in puff numbers within each wattage level and significant differences in wattage levels within each puff number were identified using contrasts. Statistical modeling was performed using R statistical software (250) with the nlme package (185). Statistically significant relationships in all figures were reported (#,*$P \leq 0.05$; ##,**$P \leq 0.01$; ###,***$P \leq 0.001$).

2.4. Results

E-liquid exposures inhibit cell proliferation/viability in a dose-dependent manner. To compare the effects of different flavored e-liquids on airway epithelia, we selected a range of flavors that covered not only traditional menthol and tobacco cigarette flavors but a variety of foods and beverages. We also purchased the Captain Black Cigar flavor with and without nicotine to control for the effects of nicotine. Cells were exposed to a range of e-liquid dilutions directly into the culture media over 24 h to assess cell viability and proliferation after treatment, with 70 PG/30 VG serving as the vehicle control. To control for the possible effects of diluting the media, we also provided a PBS control group where we serially diluted media with PBS. We used the MTT assay to indirectly assess the number of viable cells and their ability to proliferate in each treatment. We found dose-dependent decreases in each e-liquid flavor tested, irrespective of nicotine, as well as our 70 PG/30 VG vehicle. These effects were not due to dilution of the growth media since the PBS dilutions had no effect on MTT absorbance (Fig. 2.1*A*). The T-bone flavored e-liquid was not tested at a 6 or 10% dose because our purchased stock had run out and the vendor discontinued this flavor before these experiments were completed. There were dose-dependent decreases in MTT metabolism for all flavors and the 70 PG/30 VG vehicle at ≥3% dose. Moreover, four flavors [Banana Pudding (Southern Style), Kola, Hot Cinnamon Candies, and Menthol Tobacco] showed significantly greater decreases in MTT metabolism compared with 70 PG/30 VG at 3% ($P \leq 0.001$).

When these four flavors were fitted with dose-response curves to calculate their IC_{50}s, these flavors had lower IC_{50}s than 70 PG/30 VG (Fig. 2.1*B;* Table 2.1), suggesting that they were more toxic. We also directly compared the responses of cells exposed to the Captain Black Cigar flavor ± nicotine and found that there were more severe effects in the nicotine-containing e-liquid compared with the nicotine-free e-liquid at ≥3% (Fig. 2.1*C*), suggesting that nicotine exerted additional effects beyond what was seen with the base e-liquid.

Nicotine decreases cell proliferation/viability dose dependently and is cytotoxic. Since we found additional dose-dependent effects of nicotine beyond what was seen with the Captain Black e-liquid alone, we sought to determine whether these negative effects were mediated by nicotinic acetylcholine receptors (nAChRs). We used quantitative RT-PCR to survey nAChR subtype gene expression in CALU3 cells relative to a common membrane Ca^{2+} channel (*Orai1*; Fig. 2.2*A*). As additional controls, we also looked at *Scnn1a* (epithelial sodium channel alpha subtype) and *P2Y2R* (purinergic receptor) expression. Five of 7 nAChR subtypes were detected in CALU3 cells, but only *CHRNA5* was expressed above the levels of *Orai1*, *Scnn1a, or P2Y2R* levels, while *CHRNA6*, *CHRNA7*, *CHRNB1*, and *CHRNB2* had much lower expression levels. nAChRs are ligand-gated ion channels that are permeable to Ca^{2+} ions, and since there was detectable nAChR subtype expression in CALU3 cells, we tested for functional activity using a fluorescent cytosolic Ca^{2+} indicator (fluo-4). The peak change in fluorescence per nicotine dose was plotted (Fig. 2.2*B*), and the EC_{50} was calculated (Table 2.1). The EC_{50} for nicotine was 2.89 mg/ml (17.8 mM) in CALU3 cells. However, the EC_{50} of nicotine for various nAChRs has been reported in the micromolar range (48, 92). Since increases in cytosolic Ca^{2+} can also be caused by cytotoxicity from permeabilized membranes, we measured cell viability and found a decrease in calcein fluorescence in cultures treated with ≥4.9 mg/ml nicotine (Fig. 2.2*C;* Table 2.1), suggesting that the effects of Ca^{2+} were due to cytotoxicity rather than being mediated by nAChRs.

Finally, we measured percent MTT absorbance in cells exposed to increasing doses of nicotine ± 1 or 3% 70 PG/30 VG to understand the potential negative role that nicotine ± vehicle might be having on CALU3 proliferation/viability. We chose a range of doses that encompassed the nicotine concentrations

in our e-liquid exposures (%vol/vol) from Fig. 2.1*A*. Irrespective of the presence of PG/VG, we found that there were dose-dependent decreases in percent absorbance with increasing doses of nicotine (Fig. 2.2*D*). Treating cells with 1% 70 PG/30 VG in combination with nicotine did not have additional effects. However, 3% 70 PG/30 VG decreased the threshold of MTT absorbance alone compared with either 0 mg/ml nicotine (media control) or 1% 70 PG/30 VG ($P \leq 0.001$). There was no difference between $\log_{10}(IC_{50})$ values of each nicotine treatment ± 70 PG/30 VG (Table 2.1), suggesting that adding nicotine to 70 PG/30 VG did not have a synergistic effect on cell proliferation. However, since most flavors caused a significant decrease in MTT absorbance at 3% (Fig. 2.1*A*), it is likely that 3% 70 PG/30 VG, rather than nicotine, caused the decrease, since 3% e-liquid contains 0.36 mg/ml nicotine, which is insufficient to affect MTT metabolism when combined with 70 PG/30 VG (Fig. 2.2*D*).

The four flavors of interest decreased cell number/viability in subconfluent CALU3 cultures. The initial screening of the 13 purchased e-liquid flavors on CALU3 cells directed our attention to four flavors of interest because of their lower IC_{50}s in the MTT assays compared with 70 PG/30 VG. Therefore, we continued screening the effects of all of the flavors on other measures of cell viability and toxicity but focused on the effects of these four flavors in this paper [i.e., Banana Pudding (Southern Style), Kola, Hot Cinnamon Candies, and Menthol Tobacco]. We also tested Peanut Butter Cookies, a less toxic flavor, as well as Captain Black Cigar ± nicotine to control for the potential effects of nicotine. We performed additional analyses by measuring total cell number using DAPI staining (Fig. 2.3*A*). We found dose-dependent decreases in cell number 24 h after exposure to 70 PG/30 VG, Captain Black Cigar ± nicotine, Peanut Butter Cookies, as well as our four flavors of interest. We then used the fluorescent dyes calcein (Fig. 2.3*B*) and MitoTracker Red (Fig. 2.3*C*) as indicators of viable cells and active mitochondria, respectively (62, 102). Overall, 70 PG/30 VG only exerted effects on total cell number at 3% (Fig. 2.3*A*). However, the Captain Black Cigar e-liquids, irrespective of nicotine, as well as the four more toxic flavors of interest, showed dose-dependent decreases in all three measures (Fig. 2.3*A*–*C*). Moreover, the four flavors of interest were significantly more toxic than either 70 PG/30 VG or Captain Black Cigar ± nicotine at the 3% dose ($P \leq 0.0001$). Since cell density and viability were reduced, we further

investigated the potential for cytotoxicity using LDH release as a marker (Legrand et al., 1992). A 24-h exposure to 70 PG/30 VG, Captain Black Cigar ± nicotine, Peanut Butter Cookies, or Banana Pudding (Southern Style) did not induce LDH release. However, there were significant dose-dependent increases in LDH release following exposure to Kola, Hot Cinnamon Candies, and Menthol Tobacco flavors (Fig. 2.3*D*).

Hot Cinnamon Candies and Menthol Tobacco 24-h e-liquid exposures show cytotoxicity in confluent CALU3 cultures. Since the previous experiments were performed on subconfluent, proliferating cultures to accommodate the MTT assay (Figs. 2.1–3), we next assessed the effects of the flavors on confluent, non-proliferating cultures to ascertain whether decreases in cell number/viability were due to cytotoxicity or decreased cell growth. We seeded CALU3 cells into 96-well plates at a higher density where they formed confluent monolayers before conducting the 24-h e-liquid exposures. We found that there were dose-dependent decreases in DAPI fluorescence following exposure to the 70 PG/30 VG vehicle, Peanut Butter Cookies, and the 4 flavors of interest (Fig. 2.4*A*). However, the decreases in Peanut Butter Cookies, Banana Pudding (Southern Style), and Kola were not significantly greater than that seen with 70 PG/30 VG, while those seen with Hot Cinnamon Candies and Menthol Tobacco were significantly different. Additionally, there were dose-dependent decreases in calcein fluorescence with the 70 PG/30 VG vehicle, Hot Cinnamon Candies, and Menthol Tobacco at 3% (Fig. 2.4*B*). However, the decreases in 3% Hot Cinnamon Candies and Menthol Tobacco were greater than those seen for 70 PG/30 VG ($P \leq 0.001$).

Aerosolized e-liquids have similar toxicity profiles as neat e-liquids. We next exposed CALU3 cells to aerosolized e-liquid vapor from the PG/VG controls (70 PG/30 VG and 55 PG/45 VG), Peanut Butter Cookies (less harmful flavor), and two of our more toxic flavors (Banana Pudding and Hot Cinnamon Candies). E-liquids were loaded into a tank attached to an e-cig device, and a syringe was used to collect and measure out 4 s/70 ml puffs that were then manually administered to cells at 30-s intervals. Cells were given 100 µl new media before exposure and then left in the aerosol-exposed media for 24 h before total cell number (%DAPI fluorescence) and cell viability (%calcein fluorescence) were

measured. A media control group (0 puffs) was run in every plate, and wells were covered with fitted silicone strips during the exposure to ensure no unwanted exposures. Control groups with equal numbers of air puffs were also run. A 55 PG/45 VG vehicle group was added because the vendor had shifted from a 70 PG/30 VG to 55 PG/45 VG ratio and additional Peanut Butter Cookies, Banana Pudding, and Hot Cinnamon Candies e-liquids were required to conduct our experiments.

We found that all of the flavors and the PG/VG vehicle controls caused dose-dependent decreases in cell number (Fig. 2.5*A*). However, there was no effect of our air control group. We also found that both Banana Pudding and Hot Cinnamon Candies were more toxic than either Peanut Butter Cookies or the PG/VG groups after aerosol exposure at greater or equal to five puffs (Fig. 2.5*A*; $P \leq 0.001$). We also found again that all flavors and PG/VG vehicle controls caused dose-dependent decreases in cell viability (Fig. 2.5*B*), and again, there was no effect of air exposure. Both Banana Pudding and Hot Cinnamon Candies were more toxic than either Peanut Butter Cookies or the PG/VG groups after aerosol exposure at greater or equal to five puffs (Fig. 2.5*B*; $P \leq 0.001$). Importantly, the same order of toxicity demonstrated after aerosol (vape) exposure was also seen after e-liquid exposures, suggesting that direct e-liquid exposure is valid for determining relative toxicity.

Since many e-cig devices have adjustable power settings, we decided to investigate the impact of this parameter of aerosol output on cell number and viability as well. The aerosol data in Fig. 2.5*A-B*, were generated at 40 W. We next compared the effects of the 55 PG/45 VG vehicle produced at 40 vs. 100 W. We found that aerosol generated at 100 W exerted significant biological effects after 5 puffs, while the threshold for the 40 W setting was 15 puffs (Fig. 2.5*C-D*). We also observed significant differences in the DAPI and calcein outcomes for 40 vs. 100 W settings at 15 and 25 puffs. However, wattage no longer had any effect at 35 puffs. We then passed either 15 or 35 puffs of the 55 PG/45 VG vehicle at either 40 or 100 W through preweighed Cambridge filter pads (2-µm pores) to collect aerosol particles. We observed a significant increase in weight for both wattage settings, indicating that the filter pads were collecting aerosolized e-liquid. We also detected a significantly greater weight when aerosol was generated at 100 W than at 40 W per puff number. Taken together, these data suggest that either

increasing the number of puffs or the wattage increases the amount of aerosol that cells are exposed to. There was no significant difference in the weight of filter pads exposed to fifteen, 100-W puffs or 35, 40-W puffs 55 PG/45 VG (Fig. 2.5*E*), suggesting that cells were exposed to a similar toxic burden with either setting (Fig. 2.5*C*-*D*).

GC spectra identify a range of chemical constituents per flavor, displaying the variety of unique flavor profiles in commercially available e-liquids. GC-MS was conducted on all 13 e-liquids flavors. Annotated gas chromatograms for representative flavors are shown in Fig. 2.6*A*–*E*. Between 9 and 25 individual chemical constituents were identified in each e-liquid flavor that we investigated. Flavors in this screen were grouped using hierarchical clustering based on the presence or absence of all constituents detected (Fig. 2.7). For example, our analysis demonstrated that Banana Pudding (Southern Style) is least similar to Captain Black Cigar (12 mg/ml nicotine) and most similar to Peanut Butter Cookies and Vanilla Tobacco based on their constituent profiles.

Comparing flavor profiles in our four flavors of interest to identify potential shared or unique constituents that could contribute to cytotoxicity or inhibition of cell proliferation. Since we reported that Banana Pudding (Southern Style), Kola, Hot Cinnamon Candies, and Menthol Tobacco had the most negative effects on cell proliferation and viability, we chose to focus on comparing their constituent profiles to potentially target unique or shared constituents that could be causing cytotoxicity or inhibiting cell proliferation in CALU3 cells for future studies. Hot Cinnamon Candies and Menthol Tobacco showed cytotoxicity in confluent CALU3 cultures and when compared, their flavor profiles shared 8 constituents and have 9 and 11 unique constituents, respectively (Fig. 2.8*A*). Since Banana Pudding (Southern Style) and Kola inhibited cell proliferation, we compared these 2 flavors and found 3 shared constituents and 14 and 15 unique constituents, respectively (Fig. 2.8*B*). A detailed list of the constituents identified in these comparisons can be found in Table 2.2. When all four of these flavors were compared, they only shared three constituents (Fig. 2.8*C*). However, there were 9, 6, 7, and 11 unique constituents in Banana Pudding (Southern Style), Menthol Tobacco, Hot Cinnamon Candies, and Kola, respectively (Table 2.3).

2.5. Discussion

In this study, we found that all 13 flavors of e-liquids, as well as the PG/VG vehicle, caused dose-dependent decreases in MTT absorbance in CALU3 cells, indicating that all e-liquids negatively affected cell proliferation. These effects were not due to the dilution of growth media since comparable dilutions with PBS were without effect (Fig. 2.1*A*-*B*). Using this process, we also identified flavors of interest [Banana Pudding (Southern Style), Kola, Hot Cinnamon Candies, and Menthol Tobacco] that were significantly more toxic than the 70 PG/30 VG vehicle, indicating that some flavors are more harmful than others (Table 2.1). Similar dose-dependent effects have previously been reported. For instance, Bahl et al. tested the effects of 40 flavored e-liquids and categorized them as "noncytotoxic," "moderately cytotoxic," and "highly cytotoxic" based on their effects on human embryonic stem cells, mouse neural stem cells, and human pulmonary fibroblasts (15). They also found that cytotoxicity was caused by certain chemical constituents found in these e-liquids rather than by nicotine. Behar et al. also tested the effects of 10 cinnamon flavored e-liquids on human embryonic stem cells and pulmonary fibroblasts, using the MTT assay, and found that all flavors exhibited cytotoxicity with stem cells being more sensitive than fibroblasts (21). Sherwood and Boitano screened specific flavored constituents on immortalized human bronchial epithelial cells (16HBE14o-) for toxicity thresholds and found cytotoxic threshold for five of the seven chemicals tested (226). Taken together, both the data reported here and the published data all suggest a broad heterogeneity of responses that is e-liquid dependent.

We also characterized the effects of flavored e-liquids using other well-established markers of exposure including cell number (DAPI), cell viability (calcein, MitoTracker Red), and cytotoxicity (LDH release). We also chose to measure total cell number and cell viability in both subconfluent (Fig. 2.3*A*–*D*) and confluent (Fig. 2.4*A*-*B*) cultures to assess whether these flavored e-liquids inhibited proliferation or elicited a cytotoxic response, respectively. Using these complementary techniques, we again found that Banana Pudding (Southern Style), Kola, Hot Cinnamon Candies, and Menthol Tobacco caused dose-dependent decreases in DAPI, calcein, and MitoTracker Red fluorescence that were greater than what was induced by the 70 PG/30 VG vehicle (Figs. 2.3*A*–*C*). However, only Hot Cinnamon Candies and

Menthol Tobacco exerted effects on confluent cultures (Fig. 2.4*A*-*B*). These data suggest that some flavors (i.e., Banana Pudding Southern Style and Kola) tend to inhibit cell proliferation, while other flavors (i.e., Hot Cinnamon Candies and Menthol Tobacco) are more cytotoxic. Importantly, our data indicate that the growth phase must be taken into consideration when measuring the effects of e-liquids and when comparing different studies.

E-liquids are typically heated to temperatures (100–250°C) at which glycerin can decompose (274) and form reactive aldehydes. However, whether or not e-liquids undergo significant chemical transformation, including pyrolysis and degradation, following the heating required for aerosol formation is controversial. Thus, to test the effects of heating/aerosolization, we vaped e-liquids using a common third generation tank-style e-cig device using 4 s/70 ml puffs, based on existing topography (74, 78, 208). Using DAPI and calcein staining in subconfluent cultures as our markers of exposure, we found that all except the air treatment were sensitive to aerosolized e-liquid exposure. Moreover, the Peanut Butter Cookies flavor had similar dose responses to the PG/VG vehicle treatments, while Banana Pudding and Hot Cinnamon Candies exposures were more toxic (Fig. 2.5*A*-*B*). Importantly, we observed the same trends in decreasing cell number and viability with aerosol exposure (Fig. 2.5*A*-*B*) as seen with direct e-liquid exposure (Figs. 2.1–4). That is, Banana Pudding and Hot Cinnamon Candies flavors were more toxic than Peanut Butter Cookies and the PG/VG vehicle both after neat e-liquid exposure and after vaping.

We also investigated the effect of wattage on aerosol output and subsequent cellular toxicity. When we compared the effects of multiple 70 ml puffs of 55 PG/45 VG on cells generated at either 40 or 100 W, we found that the 100-W setting left-shifted the dose-dependent effects, compared with the 40-W setting (Fig. 2.5*C*-*D*). Indeed, when we passed 55 PG/45 VG through a filter pad to collect aerosol-phase particles, an increase in weight, as a proxy for aerosol output, could be achieved by both increasing the puff number and by increasing the wattage (Fig. 2.5*E*). Thus the effects that we saw are likely due to an increase in aerosol produced by increasing the wattage (power). These observations also follow online e-cig forums on subohm vaping that describe 40 W as being on the cooler side with less aerosol produced,

while 100 W is on the hotter side with more aerosol produced using the UWell Crown tanks [http://vaping360.com/crown-sub-ohm-tank-review-topfilling-sub-ohm-tank-uwell/, http://ecigarettereviewed.com/uwell-crown-review/]. Our data are similar to other studies that have exposed cells to either e-cig aerosols or aerosol that has been condensed back to a liquid, where both e-cig aerosol or condensate exposures result in measurable toxicity and/or oxidative stress (111, 137, 172, 217, 218, 222). However, ours is one of the only studies to investigate and compare the effects of both neat e-liquids and their respective aerosols in a variety of flavors.

Nicotine is the addictive substance in tobacco smoke and e-liquids that drives addiction and maintenance of use (24). Nicotine exerts its physiological effects through nAChRs, which are ligand-gated ion channels that are expressed both in the nervous systems and the lung (3, 52, 155, 166, 277). We found that CALU3 cells expressed a number of nAChR subunits, with α5 being the most abundant (Fig. 2.2*A*). Stimulation of nAChR with nicotine elicits an increase in cytoplasmic Ca^{2+} levels, with an EC_{50} in the low micromolar range (48, 92). We tested the effects of nicotine on cytoplasmic Ca^{2+} homeostasis by measuring the change in fluo-4 fluorescence and found the EC_{50} to be 2.89 mg/ml nicotine (17.8 mM) with nicotine levels greater than ~2 mg/ml causing acute cytotoxicity (Fig. 2.2*C-D;* Table 2.1). Since we found a difference in the Captain Black Cigar flavor ± nicotine on MTT metabolism (Fig. 2.1*C*), we then investigated the effects of nicotine on our cells. We tested the effects of nicotine alone and in combination with 1 or 3% PG/VG using the MTT assay (Fig. 2.2*D*). We found a dose-dependent decrease in percent absorbance with an IC_{50} of ~1.7 mg/ml (10 mM; Table 2.1). Although adding 3% PG/VG with nicotine decreased the magnitude of the response, the IC_{50}s were not different (Fig. 2.2*D;* Table 2.1). Thus, although nicotine and 3% PG/VG individually reduced MTT metabolism, together, they were not synergistic. Furthermore, since 3% e-liquid contains ~0.36 mg/ml nicotine (2.2 mM), at this dose, it is likely that PG/VG rather than nicotine caused the decrease in cell proliferation since this value was below the thresholds at which nicotine increased cytoplasmic Ca^{2+} and induced cytotoxicity (Fig. 2.2*B-C*). We included concentrations of nicotine used in our dilutions (i.e., 0–1.2 mg/ml nicotine) as well as those reported in the literature. For example, e-liquids with up to 36 mg/ml are commercially

available and nicotine delivery can vary depending on the device itself (77-79, 220). Similarly, Schweitzer et al. found dose-dependent decreases in cell proliferation in lung endothelial cells exposed to 1–20 mM nicotine, which falls within our dose-response range (222). Garcia-Acros et al. administered aerosol containing PG/VG ± 36 mg/ml nicotine to bronchial epithelia and found that nicotine alone reduced ciliary beat frequency and reduced CFTR activity, suggesting a failure of mucus clearance and impaired host defense against pathogens (83). However, Lam et al. found that ~100 nM nicotine increased gene expression of nAChRs (128), while West et al. found an increase in cell number after 1 nM–10 mM of nicotine exposure in human bronchial epithelia (263). It is possible that increased proliferation could occur via nAChRs with lower more physiological levels of nicotine (1 nM–1 mM), while our results, and those of Garcia-Acros et al., may have been nonspecific cytotoxic effects from the extremely high (i.e., mM) nicotine levels seen in e-liquids (83). Further studies will be required to differentiate between receptor-mediated and nonspecific effects of nicotine, and to understand the contribution of nicotine to the potential toxicity of e-liquids.

In our study, we conducted GC-MS analysis on all 13 flavors (Fig. 2.6) and performed hierarchical clustering (Fig. 2.7) before focusing on the individual constituents found in our 4 more toxic flavors of interest (Fig. 2.8). In this approach, we found that Banana Pudding (Southern Style) was more similar to Peanut Butter Cookies than to Captain Black Cigar. Further comparisons of just the four more toxic flavors of interest identified flavoring constituents such as cinnamaldehyde and vanillin, which were shown to have potentially cytotoxic properties elsewhere (21, 112, 137, 226, 252). We also found that benzene derivatives were identified in several e-liquids (Fig. 2.7). Of note, benzene has been directly linked with the induction of cancer (159). We also identified 9, 11, 7, and 6 unique constituents, respectively (Table 2.3), most of which have no available toxicity data. Importantly, our data indicate the list of constituents for each e-liquid should be made available to the consumers to better make informed choices.

In conclusion, our study provides biological data from direct and aerosol based exposures to a diverse range of e-liquid flavors, PG/VG, and nicotine. While we do not yet know the concentrations of

e-liquid in the lungs after inhalation, recent studies have found that particle size from e-cig aerosols is similar (164) or slightly smaller (151), than cigarette smoke, suggesting that it may deposit in the same fashion (148). Moreover, based on aerosol particle size, the predicted deposition of e-cig aerosol in the lungs is 15–45% (232), which is similar to the reported range of some jet nebulizers (~13–25%) (53). Thus, if 10 ml of e-liquid is vaped, and given that the airway surface liquid volume in the lung is ~3 ml, this could lead to a dilution of 5–15%, suggesting that our dosing range of ≤10% e-liquid (vol/vol) is appropriate. However, additional experiments will be needed to directly measure e-liquid deposition patterns in the lung. Since our biological results were paired to analytical data, this has enabled the identification of a wide range of e-liquid constituents. We also provided evidence that direct e-liquid exposures are comparable to the more realistic, but more time-consuming, aerosol exposures. Thus we are providing a data set that informs as to the basic toxicological parameters of flavored e-liquids on a lung epithelial cell line that could potentially harm the lung of flavored e-cigs users.

Table 2.1. List of $Log_{10}(IC_{50})/Log_{10}(EC_{50})$ and IC_{50}/EC_{50} values for dose response curves in Figures 2.1 and 2.2. Nonlinear regression curves were fit to the mean % absorbance values of all doses within each flavored e-liquid (Figure 2.1*B*) and nicotine ± 70 PG/30 VG (Figure 2.2*D*). A nonlinear regression curve was fit to mean peak changes in cytosolic Ca^{2+} fluorescence with nicotine dosing (Figure 2.2*B*). A nonlinear regression curve was fit to mean %calcein fluorescence with nicotine dosing (Figure 2.2*C*). The $Log_{10}(IC_{50})$ ± SEM was reported where appropriate for all treatments. The $Log_{10}(EC_{50})$ ± SEM was reported for where appropriate. ND represents 'not determined', where curves could not be fit in the range of doses tested. The IC_{50} and EC_{50} were reported, where appropriate, in either % v/v for flavored e-liquids or mg/ml for nicotine ± 70 PG/30 VG treatments. Statistics were calculated using Prism software to compare $Log_{10}IC_{50}$ values where applicable. ***$p<0.001$ in the above flavors compared to the 70 PG/30 VG vehicle.

Treatment	**$Log_{10}(IC_{50})$ ± SEM**	**IC_{50} (% v/v)**
PBS	ND	ND
Vehicle (70 PG/30 VG)	0.5755 ± 0.02	3.763
Captain Black Cigar (0 mg/ml nicotine)	ND	ND
Captain Black Cigar	ND	ND
Peanut Butter Cookies	ND	ND
T-bone	ND	ND
Popcorn	ND	ND
Black Licorice	ND	ND
Energon	ND	ND
Vanilla Tobacco	0.4730 ± 14.79	2.792
Banana Pudding, Southern Style	0.0094 ± 0.02	1.022
Kola	-0.0005 ± 0.02***	0.999
Hot Cinnamon Candies	-0.4908 ± 0.02***	0.323
Menthol Tobacco	0.0714 ± 14.18	1.179
Solid Menthol	ND	ND
Treatment	**$Log_{10}(IC_{50})$ ± SEM**	**IC_{50} (mg/ml)**
Nicotine Only	0.2513 ± 0.07	1.784
Nicotine + 1% PG/VG	0.2157 ± 0.04	1.643
Nicotine + 3% PG/VG	0.2048 ± 0.08	1.603
Treatment	**$Log_{10}(EC_{50})$ ± SEM**	**EC_{50} (mg/ml)**
Nicotine Only	0.4605 ± 0.05	2.887
Treatment	**$Log_{10}(EC_{50})$ ± SEM**	**EC_{50} (mg/ml)**
Nicotine Only	~0.4431 ± ND	ND

Table 2.2. List of chemical constituents identified and compared using Venn diagrams in Figure 2.8*A*-*B*. Chemical constituents identified from GC-MS of e-liquids in 4 flavors of interest. Data were compared using R software and lists were generated of unique and shared constituents between grouping 1 (Menthol Tobacco and Hot Cinnamon Candies) or grouping 2 [Kola and Banana Pudding (Southern Style)] (*A*-*F*).

(A) Menthol Tobacco Only	**(B) Hot Cinnamon Candies Only**	**(C) Both Menthol Tobacco & Hot Cinnamon Candies**	**(D) Kola Only**	**(E) Banana Pudding (Southern Style) Only**	**(F) Kola & Banana Pudding (Southern Style)**
1,2-Cyclopentanedione, 3-methyl-	1H-Inden-2-ol, 2,3-dihydro-1-methoxy-, cis-	1,2,3-Propanetriol, monoacetate	1,4-Cyclohexadiene, 1-methyl-4-(1-methylethyl)-	1,2-Cyclopentanedione, 3-methyl-	2-Propanol, 1,1'oxybis-
Cyclopentane, 1,1,3-trimethyl-	2,2-Dimethoxybutane	2,4-Dimethyl-1-heptene	1,6-Octadien-3-ol, 3,7-dimethyl-	1-Butanol, 3-methyl-, acetate	Glycerin
D-menthone	2-Propen-1-ol, 3-phenyl-, acetate	2-Propanol, 1,1'-oxybis-	1-Propanol, 2-(2-hydroxypropoxy)-	2(3H)-Furanone, 5-ethyldihydro-	Nicotine
Decane, 3,7-dimethyl-	4-Nonene, 3-methyl-, (Z)-	Acetic acid, methyl ester	2,4-Dimethyl-1-heptene	2,6-Octadien-1-ol, 3,7-dimethyl-, acetate, (Z)-	
Benzoic acid, 3,4-methylenedioxy-, 3-formylphenyl ester	Benzaldehyde, 3,4-dimethoxy-, methylmonoacetal	Benzoic acid, 4-ethoxy-, ethyl ester	3-Cyclohexen-1-ol, 4-methyl-1-(1-methylethyl)-	3-Acetyl-2,5-dimethyl furan	
Ethyl Vanillin	Cinnamaldehyde	Glycerin	Benzene, 1-methyl-3-(1-methethyl)-	3-Hexen-1-ol	
Menthol	Eugenol	Hexane, 3-ethyl-	Benzoic acid, 4-ethoxy-, ethyl ester	4-Methoxycarbonyl-4-butanolide	
Phenol, 2-methoxy-	Maltol	Nicotine	Bicyclo[2.2.1]heptan-2-ol, 1,3,3-trimethyl-, (1R-endo)-	4H-Pyran-4-one, 2-ethyl-3-hydroxy-	
Pyrazine, trimethyl-	Pentanoic acid, 1,1-dimethylpropyl ester		Cyclotrisiloxane, hexamethyl-	5-Thiazoleethanol, 4-methyl-	
	Propylene Glycol		Cinnamaldehyde	Benzaldehyde, 4-methoxy-	
	Vanillin		D-limonene	Ethyl Vanillin	
			Eucalyptol	Eugenol	
			Triacetin	Pentanoic acid, 1,1-dimethylpropyl ester	
			Beta pinene	Phenol, 2-methoxy-	
				Vanillin	

Table 2.3. List of unique chemical constituents identified from Venn diagram comparisons in Figure 2.8*C*. Chemical constituents identified from GC-MS of e-liquids in 4 flavors of interest. Data was compared using R software and lists were generated of unique and shared constituents between all 4 flavors of interest Banana Pudding (Southern Style), Kola, Hot Cinnamon Candies, and Menthol Tobacco.

Banana Pudding (Southern Style)	Kola	Hot Cinnamon Candies	Menthol Tobacco
4H-Pyran-4-one 2-ethyl-3-hydroxy-	1,4-Cyclohexadiene, 1-methyl-4-(1-methylethyl)-	1H-Inden-2-ol, 2,3-dihydro-1-methoxy-, cis-	Pyrazine, trimethyl-
1-Butanol, 3-methyl-, acetate	beta pinene	2,2-Dimethoxybutane	Cyclopentane, 1,1,3-trimethyl-
3-Hexen-1-ol	Eucalyptol	Maltol	D-menthone
4-Methoxycarbonyl-4-butanolide	1,6-Octadien-3-ol, 3,7-dimethyl-	Benzaldehyde, 3,4-dimethoxy-, methylmonoacetal	Decane, 3,7-dimethyl-
2(3H)-Furanone, 5-ethyldihydro-	3-Cyclohexen-1-ol, 4-methyl-1-(1-methylethyl)-	Propylene Glycol	Menthol
Benzaldehyde, 4-methoxy-	Bicyclo[2.2.1]heptan-2-ol, 1,3,3-trimethyl-, (1R-endo)-	4-Nonene, 3-methyl-, (Z)-	Benzoic acid, 3,4-methylenedioxy-, 3-formylphenyl ester
3-Acetyl-2,5-dimethyl furan	Benzene, 1-methyl-3-(1-methylethyl)-	2-Propen-1-ol, 3-phenyl-, acetate	
2,6-Octadien-1-ol, 3,7-dimethyl-, acetate, (Z)-	Cyclotrisiloxane, hexamethyl-		
5-Thiazoleethanol, 4-methyl-	D-Limonene		
	1-Propanol, 2-(2-hydroxypropoxy)-		
	Triacetin		

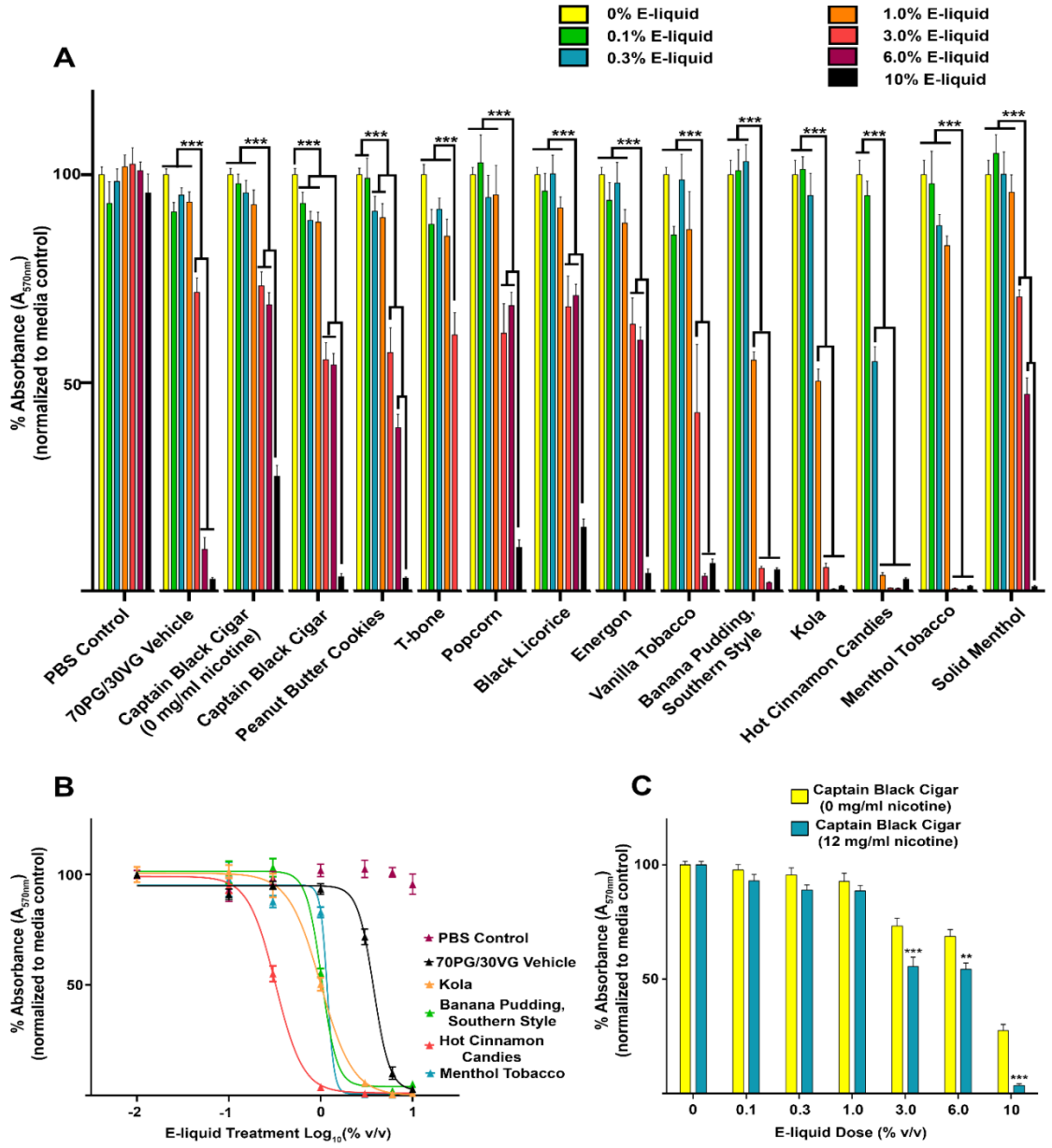

Figure 2.1. Flavored e-liquids cause dose-dependent decreases in cell proliferation and viability. CALU3 cells were seeded at 12,500 per well in 96-well plates and were challenged with increasing doses of e-liquid flavors diluted in media (% vol/vol) for 24 h. Cell proliferation/viability was measured at the end of the 24 h treatment using the MTT assay. *A*: mean %absorbance was plotted for all flavors and controls in all doses. *B*: nonlinear regression curves were fit to calculate the IC_{50} of each flavor. *C*: MTT responses were compared in Captain Black Cigar containing either 0 or 12 mg/ml nicotine to determine the effects of nicotine. Bars and triangles represent average %absorbance measured normalized to 0% e-liquid (media control) treatment per plate ± SEM. n = 12-24 wells run in 4-8 independent experiments per treatment. Statistics were calculated using a linear mixed model with pairwise comparisons for doses within flavor (*A*) or between flavors in each dose (*C*). *A*: P values for overall tests of dose within flavor denoted (***$P < 0.001$), and, where applicable, further pairwise significant differences ($P < 0.05$) are

indicated using cluster lines above the graph. *C*: *P* values for pairwise differences denoted (**$P < 0.01$, ***$P < 0.001$).

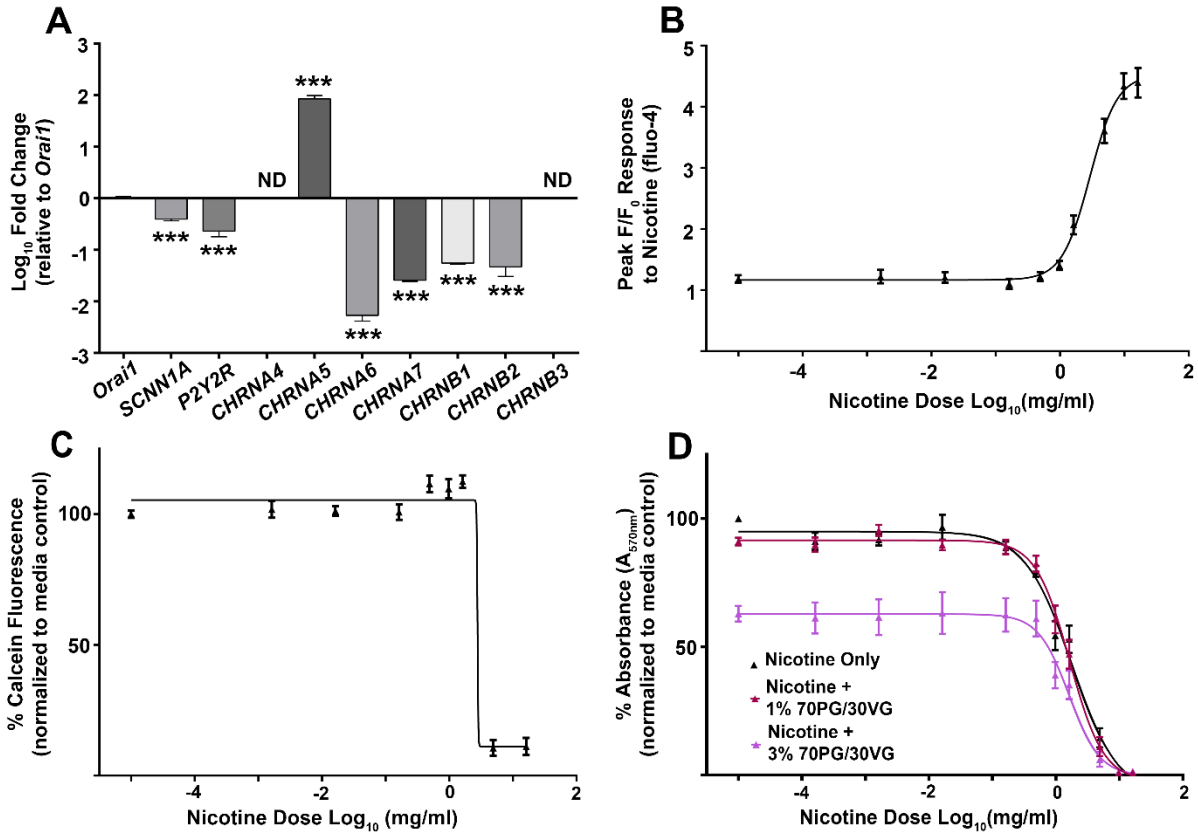

Figure 2.2. Nicotine alone decreases cell proliferation and cytotoxicity that is independent of nAChR stimulation. *A*: RNA was isolated from untreated CALU3 cells and mRNA expression of nAChR subunits relative to *Orai1*, a Ca^{2+} channel, were measured (n = 4-10 wells per gene). *B* and *C*: CALU3 cells were seeded at 45,000 per well in 96-well plates overnight and were challenged with nicotine doses acutely to measure Ca^{2+} activity (fluo-4) or measure viability (calcein). Peak changes in fluo-4 fluorescence (F/F_0) per nicotine dose was plotted and fit with a nonlinear regression curve to calculate the EC_{50} (n = 14-30 wells per treatment). Cell viability was measured 1 h post-nicotine exposure by measuring calcein fluorescence and fitting dose response with a nonlinear regression curve (n = 11-18 wells per treatment). *D*: Cells were seeded at 12,500 per well in 96-well plates overnight and were challenged with varying doses of nicotine ± 70 PG/30 VG diluted in media for an additional 24 h. Cell proliferation/viability was measured at the end of the 24 h treatment using the MTT assay. Mean %absorbance were plotted for all treatments and doses and fit with nonlinear regression curves to calculate the IC_{50} of each treatment (Table 2.1) (n = 12-15 wells per treatment). Bars represent average gene expression relative to Orai1 ± SEM (*A*). Triangles represent average %fluorescence or %fluorescence measured normalized to 0 mg/ml dose (media control) per plate ± SEM (*B-D*). Statistics were calculated using a linear model of log-transformed outcomes with a fixed effect for gene type and pair-wise comparisons between genes (*A*) (***$P < 0.001$; ND, not determined).

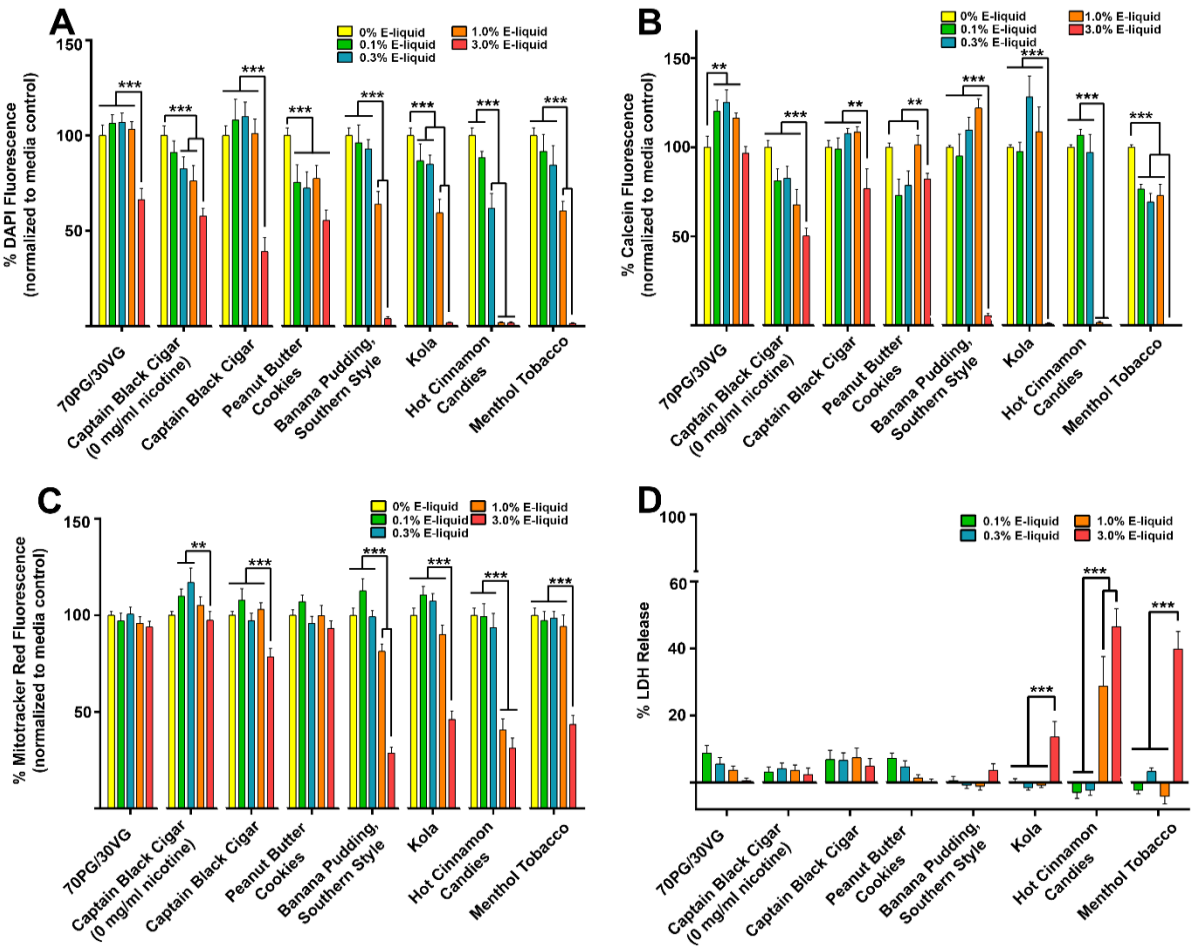

Figure 2.3. E-liquids decrease cell number/viability in sub-confluent CALU3 cultures. CALU3 cells were seeded at 12,500 per well in 96-well plates for 12 h before e-liquids were diluted in media in a dose-dependent manner (% vol/vol) and cells challenged for 24 h. *A*: Cell number was measured by fixing cells and measuring DAPI fluorescence. Cell/mitochondrial viability was measured using calcein (*B*) and MitoTracker Red (*C*). *D*: Cytotoxicity was measured from the cell supernatants collected at 24 h and compared to lysed cell positive controls. Bars represent average fluorescence or absorbance measured normalized to 0% e-liquid (media control) treatment per plate + SEM. n = 9-15 wells run in 3-5 independent experiments per treatment. Statistics were calculated using a linear mixed model with pairwise comparisons for doses within flavor (*A-D*). P values for overall tests of dose within flavor denoted (**$P < 0.01$, ***$P < 0.001$), and, where applicable, further pairwise significant differences ($P < 0.05$) are indicated using cluster lines above the graph.

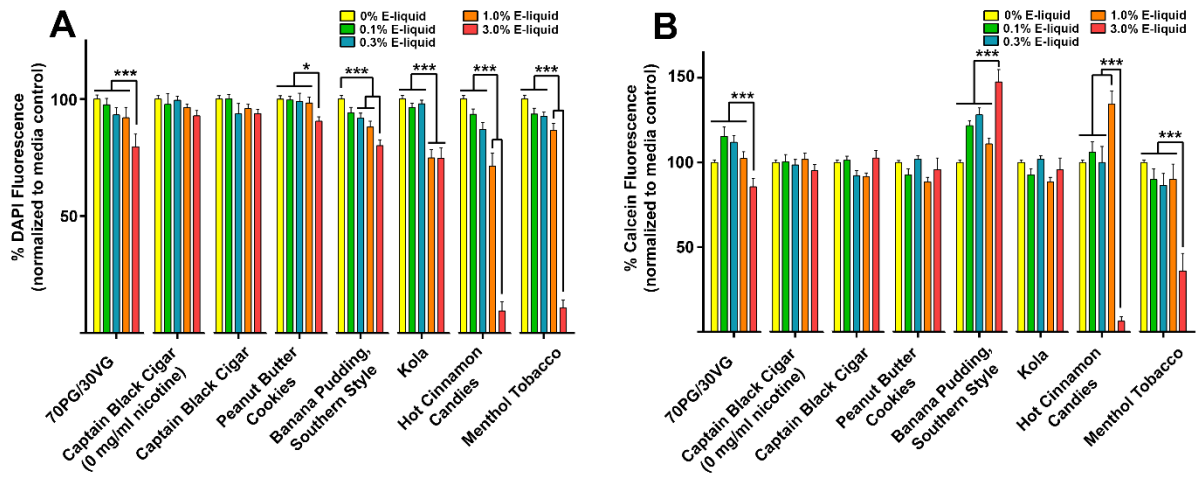

Figure 2.4. Confluent CALU3 cultures show cytotoxicity after Hot Cinnamon Candies and Menthol Tobacco flavor exposure. CALU3 cells were seeded at 45,000 per well in 96-well plates for 12 h until confluent monolayers were formed. E-liquids were diluted in media in a dose-dependent manner (% vol/vol) and cells were challenged for 24 h. Cell number was measured by fixing cells and measuring DAPI fluorescence (*A*) and cell viability was measured using calcein (*B*). Bars represent average fluorescence measured normalized to 0% e-liquid (media control) treatment per plate + SEM. *n* = 12 wells run in 4 independent experiments per treatment. Statistics were calculated using a linear mixed model with pairwise comparisons for doses within flavor (*A*-*B*). *P* values for overall tests of dose within flavor denoted (**P* < 0.05, ***P* < 0.01, ****P* < 0.001), and, where applicable, further pairwise significant differences (*P* < 0.05) are indicated using cluster lines above the graph.

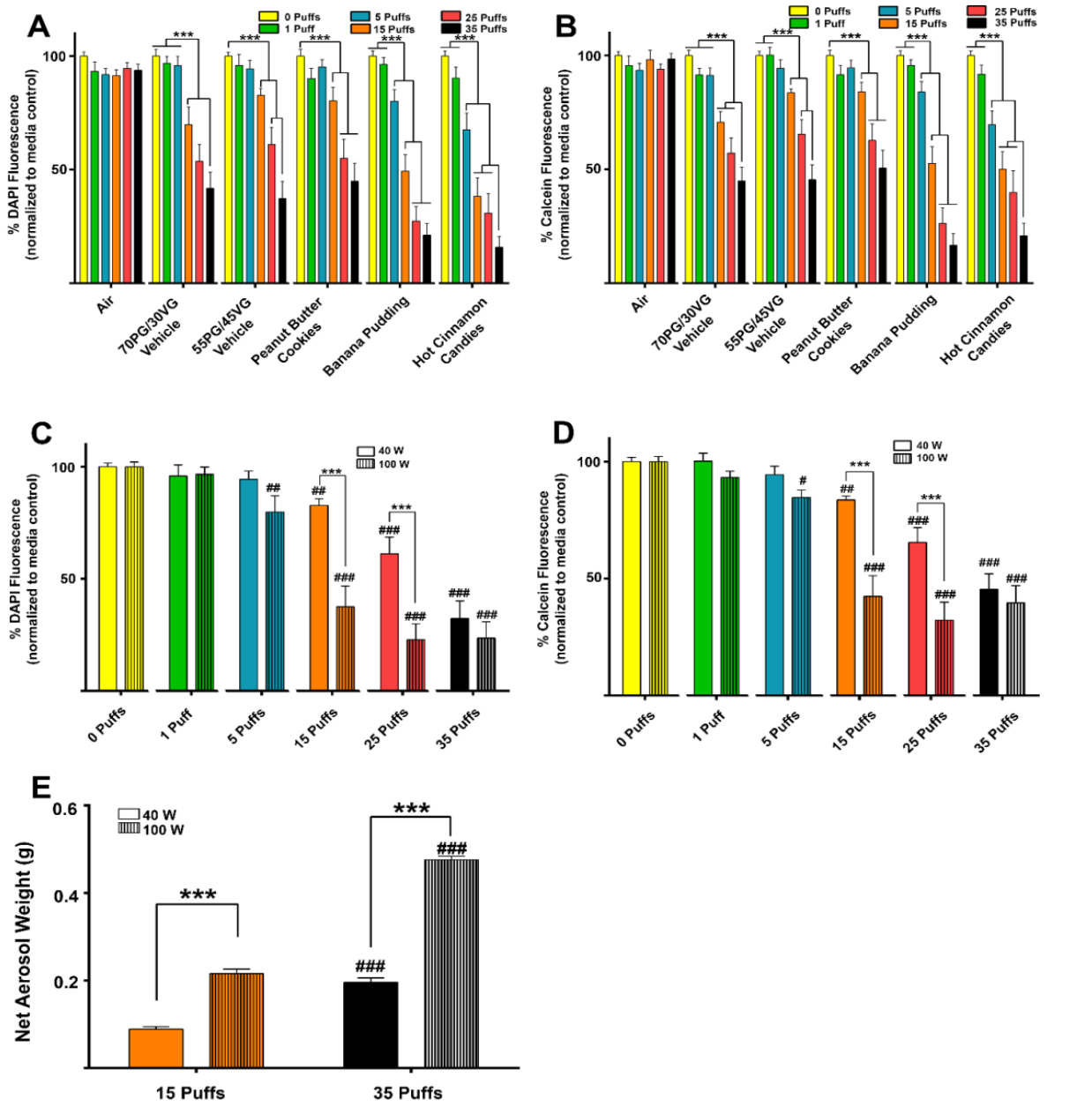

Figure 2.5. E-cigarette aerosols dose-dependently decrease cell number/viability in sub-confluent CALU3 cultures. CALU3 cells were seeded at 25,000 per well in 96-well plates for 4-8 h before aerosol exposure. Aerosols were generated at 40 or 100 W and each 70 ml puff was distributed among 6 wells using a multi-channel manifold at a rate of 1 puff/30 s. Media was not changed for 24 h following aerosol exposure. *A-D*: Dose-dependent outcomes of cell number (DAPI) or cell viability (calcein) between flavors or PG/VG controls were measured (n = 18-54 wells per treatment). *C* and *D*: Effects of wattage (40 and 100 W) were compared in the 55 PG/45 VG treatment where %DAPI and calcein fluorescence were measured (n = 18-48 wells per treatment). Aerosol phase particles were captured from 55 PG/45 VG at either the 40 or 100 W settings for 15 and 35 puffs using Cambridge filter pads. *E*: Aerosol was collected on pre-weighed filter pads and the net weight (g) of aerosol-phase particles were plotted (*n* = 7 per treatment). Bars represent average %fluorescence measured normalized to 0 puff (media control) treatment per plate + SEM (*A-D*) or average net weight of filter pads per treatment + SEM (*E*). Statistics were calculated using a linear mixed model with pairwise comparisons for doses within exposure

treatment (*A*-*D*). A linear model was used to obtain the statistical results in (*E*). *A*-*E*: *P* values for overall test of dose within flavor denoted (***$P < 0.001$) with further pairwise significant differences ($P < 0.05$) indicated using cluster lines above the graph. Differences shown without brackets were compared to either the 0 puff control for respective treatments (*C* and *D*) or between puff numbers within a wattage setting (*E*) (#$P < 0.05$, ##$P < 0.01$, ###$P < 0.001$).

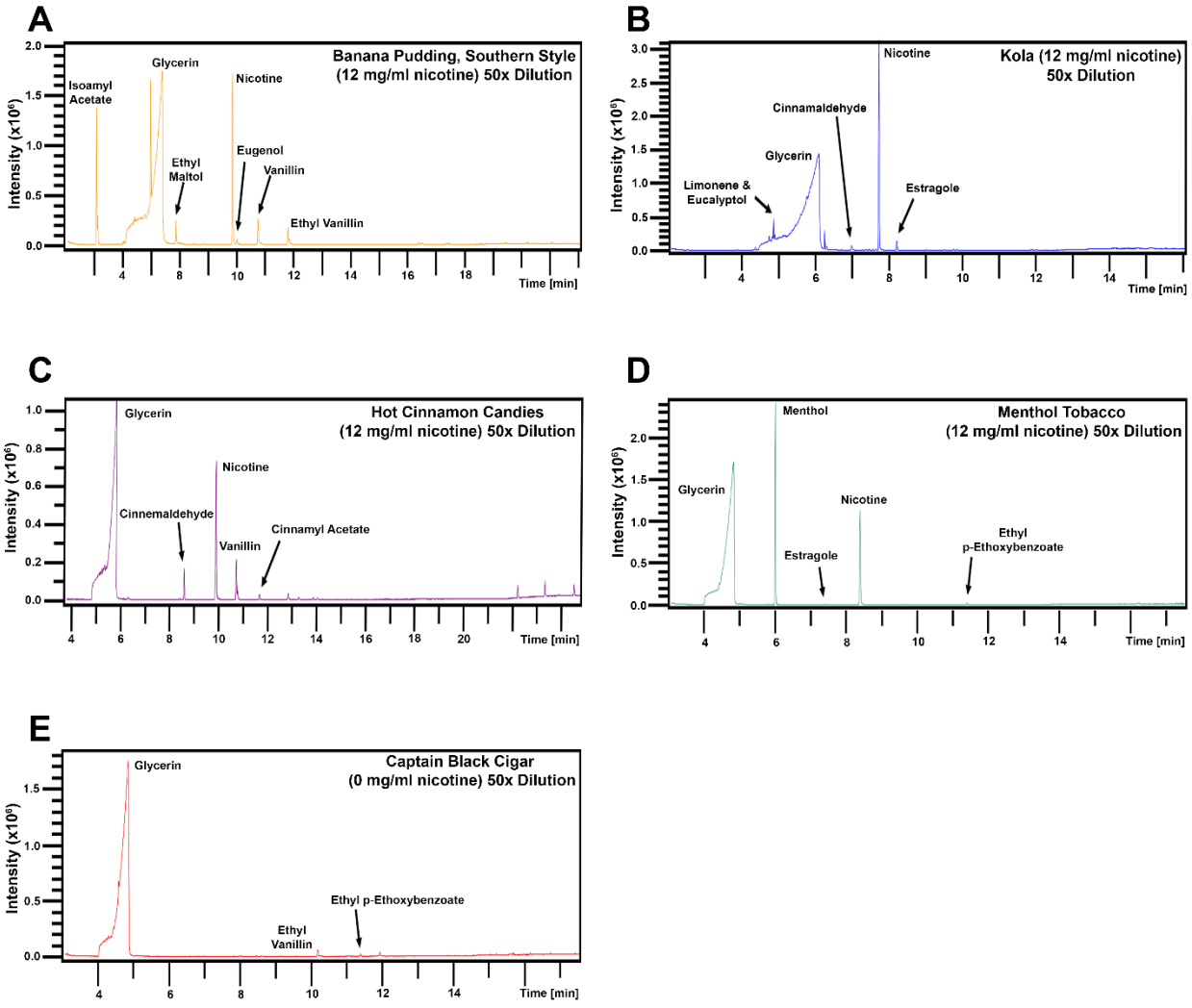

Figure 2.6. Gas chromatography-mass spectrometry (GC-MS) identified individual chemical constituents in the 13 different e-liquids. GC-MS was used to detect between 9 and 25 individual chemical constituents for individual e-liquid flavors across all 13 flavors tested. Annotated gas chromatograms of Banana Pudding (Southern Style) (*A*), Kola (*B*), Hot Cinnamon Candies (*C*), Menthol Tobacco (*D*), and Captain Black Cigar (0 mg/ml nicotine) (*E*) depict examples of peaks derived for individual constituent identification in e-liquids diluted 50x.

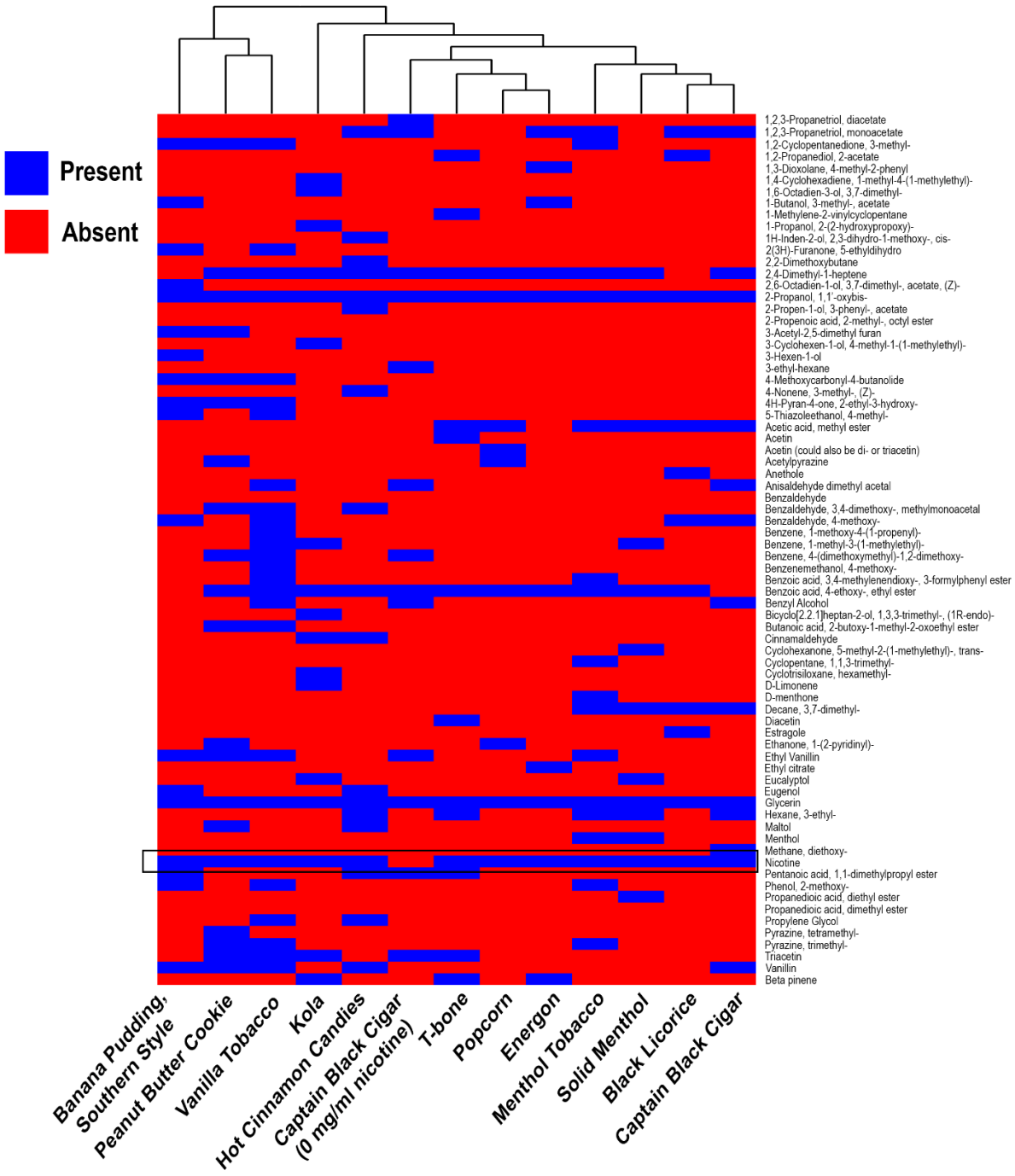

Figure 2.7. Heat map compares individual chemical constituent profiles from 13 different e-liquid flavors tested. All e-liquid flavors were compared for constituent flavor profile using a heat map showing presence (blue) or absence (red) of a single constituent detected respectively. The black box indicates the presence or absence of nicotine in each flavor as an example. All identified constituents are listed on the right and brackets group flavors by 'likeness' using hierarchical clustering.

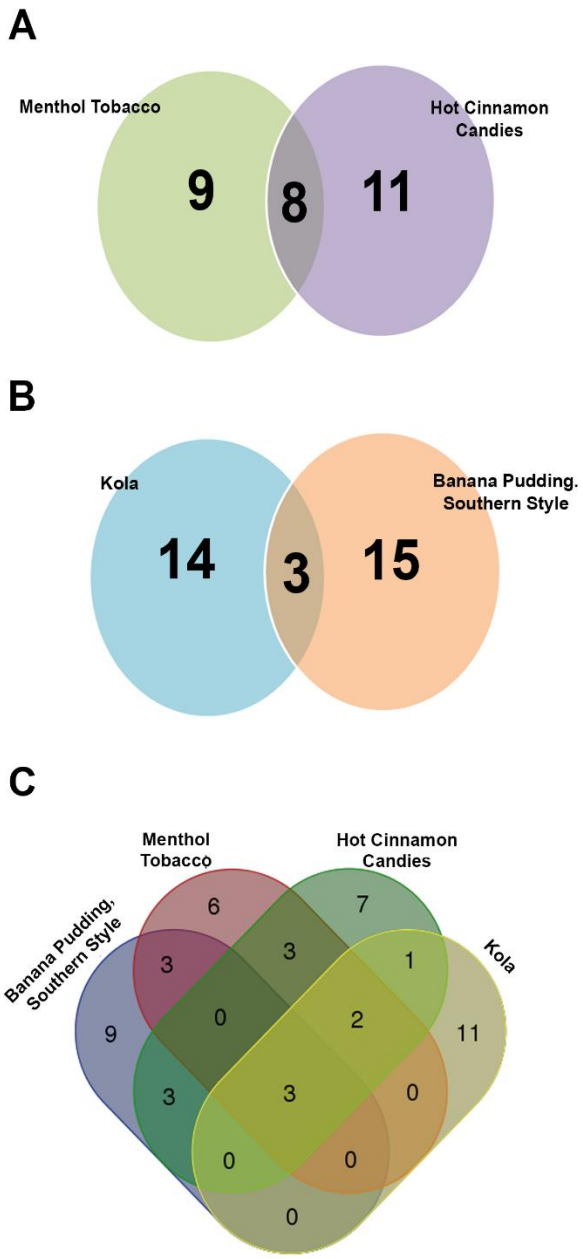

Figure 2.8. Flavor profiles for the 4 flavors of interest compared to identify potential constituents responsible for either cytotoxicity or cell proliferation inhibition. Comparing between Menthol Tobacco and Hot Cinnamon Candies e-liquid flavor profiles, only 8 constituents are shared (*A*) while Kola and Banana Pudding (Southern Style) only share 3 constituents (*B*). When all 4 are compared against each other, Banana Pudding (Southern Style), Menthol Tobacco, Hot Cinnamon Candies, and Kola have 9, 6, 7, and 11 unique constituents respectively (*C*).

Chapter 3: Banana Pudding-Flavored E-liquid Activates Phospholipase C and Store-Operated Ca^{2+} Entry in Lung Epithelia

3.1. Overview

E-cigarettes (e-cigs) are available in over 7,000 flavors and there is still much to understand regarding their potential biological effects. Calcium (Ca^{2+}) is a ubiquitous second messenger, which regulates cell homeostasis. Chronic changes to Ca^{2+} homeostasis can have dramatic cellular effects, including the facilitation of chronic inflammation (e.g., increased cytokine/mucin secretion) and altered cell growth/proliferation. Therefore, we characterized the novel effects of a Banana Pudding (BP)-flavored e-liquid on Ca^{2+} metabolism. We found that acute BP exposure caused inositol 1,4,5-triphosphate (IP_3) formation, ER Ca^{2+} release, and store-operated Ca^{2+} entry (SOCE), followed by protein kinase C (PKCα) phosphorylation. However, longer BP exposures blunted thapsigargin-induced ER Ca^{2+} release and SOCE, suggesting that BP may alter Ca^{2+} homeostasis with time. We have not identified the upstream target of phospholipase C stimulated IP_3 generation, though we determined that the response is independent of receptor tyrosine kinase activation. Further studies are needed to understand both the upstream target of Ca^{2+} activation, as well as the widespread nature of altered Ca^{2+} homeostasis signaling with flavored e-liquid exposure and the potential effects of individual chemical flavorings common to these products. However, dysregulation of Ca^{2+} signaling can cause chronic inflammation and/or cancer, flavored e-cig products should be further evaluated for potential toxicity.

---

[3]Contributing authors: Temperance R Rowell, Andrew Kennedy, Stephen B Shears, and Robert Tarran.

3.2. Introduction

E-cigs are electronic nicotine delivery systems (ENDS) that utilize a battery-powered coil to heat flavored e-liquids into an inhalable aerosol. E-liquids are usually composed of a propylene glycol/vegetable glycerin (PG/VG) base to which nicotine and a number of individual flavoring chemicals are added to create flavored e-liquids for purchase. E-cig use in adolescent populations has particularly increased over time (13). Interestingly, the availability of flavors, especially sweet flavors, may contribute to e-cig use in adolescents and young adults (6, 98). With over 7,000 flavored e-liquids commercially available in the United States (276) and little information available about the inhalation toxicity for many flavored e-liquids or their constituent chemicals (19, 212), e-cig health effects and safety are widely debated. Concern regarding inhalation safety for individual flavoring chemicals stems from cases of chronic diacetyl inhalation in manufacturing plant workers (124). Though diacetyl, a butter flavor, is 'generally recognized as safe' (GRAS) for ingestion, chronic inhalation exposure can lead to the development of bronchiolitis obliterans or 'Popcorn Lung', which causes scarring and fibrosis of the airways (17). Interestingly, several recent studies have implicated flavored e-liquids and individual flavoring chemicals in causing toxicity or altering other biological functions of respiratory cells in addition to PG/VG (21, 47, 85, 211, 226, 252).

Pulmonary epithelia are one of the first lines of defense against inhaled toxicants. They serve as a physical barrier and are integral in coordinating innate defenses, often through second messenger signaling molecules such as intracellular Ca^{2+} (97, 139, 153). Typically, cells rely upon a number of pumps, receptors, and channels to control fluctuations in cytosolic Ca^{2+} and sequester it in specific organelles (26). Following activation, canonical G protein-coupled receptors (GPCRs) can activate phospholipase Cβ (PLCβ) to generate inositol 1,4,5-triphosphate (IP_3). The subsequent stimulation of IP_3 receptors (IP_3Rs) triggers ER Ca^{2+} release, often followed by store-operated Ca^{2+} entry (SOCE) to replenish ER Ca^{2+} stores. SOCE requires the translocation of stromal interaction molecule 1 (STIM1) to ER plasma membrane junctions where it activates Orai1, a plasma membrane Ca^{2+} release-activated Ca^{2+} channel to permit Ca^{2+} entry (141, 189). The signaling cascade continues downstream of SOCE and

increases the phosphorylation of kinases such as protein kinase C (PKC). The PKCα isoform is canonically activated downstream of both PLC activation (i.e., diacylglycerol formation) and Ca^{2+} release (122, 241), and its activation in turn can cause cellular responses (e.g., cell proliferation or apoptosis) (146, 261). Some membrane receptor tyrosine kinases (RTK) have also been shown to activate a similar response (i.e., IP_3 formation, ER/SOCE-dependent Ca^{2+} release, and PKCα phosphorylation) through PLCγ (161, 173). Activating Ca^{2+} pathways can have profound effects on cell function. For example, the ability to maintain Ca^{2+} homeostasis is paramount to cell survival and regulation of many important processes (i.e., exocytosis, enzyme activity, transcription, cell cycle, apoptosis). Dysregulation of any of these key components of Ca^{2+} signaling can result in pathophysiology (i.e., overexpression or hyperactivity of some PLC isoforms has been linked to cancer) (27, 231).

Given the number of flavored e-cig products that are available for purchase, and the lack of safety information regarding their effects on the lung, we tested the effects of commercially available e-liquids for their ability to alter an important universal cell signaling pathway (i.e., PLC-activated Ca^{2+} signaling). We initially characterized one flavored e-liquid (BP) that had previously been shown to inhibit cell proliferation (211). We then tested the hypothesis that e-liquids with similar flavoring constituents could also affect cytoplasmic Ca^{2+} levels.

3.3. Methods

Flavored e-cig liquids (e-liquids). Experiments were performed using the Banana Pudding (BP)-flavored e-liquid purchased from The Vapor Girl (www.thevaporgirl.com). Two different lots (or batches) of BP (designated #09 or #165) were used after they were verified for chemical composition (not shown), toxicity, and cytosolic Ca^{2+} responses (Fig. 3.2). BP-flavored e-liquid was purchased ± 12 mg/ml nicotine. The e-liquid vehicle was advertised as 55/45 propylene glycol (PG) to vegetable glycerin (VG) mixture. Thus, a vehicle control was made in our laboratory using 55 PG/45 VG.

Chemicals and reagents. PG, VG, DMSO, human placental type VI collagen, probenecid, thapsigargin, methanol, uridine triphosphate (UTP), and carbonyl cyanide m-chlorophenyl hydrazine (CCCP) were purchased from Sigma-Aldrich. DAPI, calcein (AM), fura-2 (AM), fluo-4 (AM), rhod-2

(AM), and lipofectamine 2000 were purchased from ThermoFisher. Paraformaldehyde (PFA) was purchased from Affymetrix. 2-aminoethoxydiphenyl borate (2-APB) was purchased from Tocris. DAPI, calcein (AM), thapsigargin, fura-2 (AM), fluo-4 (AM), and rhod-2 (AM) were reconstituted using DMSO and applied to cells in experiments where the final DMSO concentration was ≤ 0.1%. STIM1 tagged with mCherry on the C-terminus was kindly provided by Dr. Ricardo Dolmetsch (181). Orai1 labelled with YFP on the C-terminus was purchased from Addgene (19756) (189).

Cell culture and transfections. Primary human bronchial epithelial cells (HBECs) were procured from non-smoker human excess donor lungs under a protocol approved by the University of North Carolina Institutional Review Board as described previously (196). HBECs were grown on glass coverslips coated with human placental type VI collagen, cultured in bronchial epithelial growth medium (BEGM) with 5% CO_2 at 37°C, and assayed within a week of plating. CALU3 cells were cultured in Minimum Essential Media (MEM) alpha with 10% FBS and penicillin/streptomycin (Gibco) with 5% CO_2 at 37°C. CALU3 cells were seeded onto glass coverslips for fura-2 experiments or 12 and 96 well and 60 mm plastic dishes (Corning) for all other experiments. HEK293T cells were cultured in D-MEM (high glucose) with 10% FBS and penicillin/streptomycin (Gibco) with 5% CO_2 at 37°C. HEK293T cells were plated onto glass coverslips for fura-2 and STIM1/Orai1 puncta imaging experiments. HEK293T cells were seeded into 12 and 24 well plastic dishes (Corning) for fluo-4 and total inositol phosphate activation experiments.

Ca^{2+} signaling. Changes in cytosolic [Ca^{2+}] were measured using either fura-2 or fluo-4 dyes. HBECs and CALU3 cells were loaded with 8 μM fura-2 in the presence of 1-2.5 mM probenecid for 40 min at 37°C prior to experiments. HEK293T cells were loaded with 5 μM fura-2 for 20 min at 37°C prior to experiments. All cultures were then rinsed with PBS and replaced with a standard Ringer's solution as described (198). Fura-2 fluorescence intensities were measured every 15 or 30 sec using a 40 x 1.3 NA oil objective on a Nikon Ti-S inverted microscope using alternating excitation at 340 and 380 nm (emission > 450 nm) using LUDL filter wheels at room temperature. Images were captured with an Orca CCD camera (Hammamatsu) and analyzed using HCImage software. Fura-2 signals were calculated

using the ratio (340/380). Thapsigargin was added to cultures in to a final concentration of 2 μM. In some cases, nominally Ca^{2+}-free Ringer's solution was added extracellularly as described (198).

In some cases, CALU3 and HEK293T cells were loaded with fluo-4 in the same fashion as fura-2. Fluorescence intensities were measured every 15 or 30 sec using a Tecan Infinite Pro plate reader (ex: 490 ± 10 nm, em: 516 ± 5 nm) at room temperature. Changes in fluo-4 fluorescence were normalized to the baseline (F/F_0) after subtracting background light levels. Traces were plotted to show F/F_0 over time and the peak F/F_0 was measured for each dose and compared between treatments. Thapsigargin was added to cultures at a final concentration of 2 μM. Neat e-liquids were diluted in Ringer's solution and exposed to cells at final concentration (%vol/vol). CALU3 cells were pretreated with 10 μM CCCP for 1 h at 37°C as designated (Fig 3.5*C-D*). HEK293T cells were pretreated with 100 μM 2-APB for 1 min prior to UTP or e-liquid treatment (Fig 3.7*B-C*).

Changes in mitochondrial Ca^{2+} signals were measured in CALU3 cells ± CCCP pretreatment. Cells were loaded with 3 μM rhod-2 for 1 h at 37°C, rinsed with PBS, and incubated in media for 12-24 h as described (198). Cultures were rinsed and media was replaced with a standard Ringer's solution. Fluorescence intensities were measured every 15 or 30 sec using a Tecan Infinite Pro plate reader (ex: 550 ± 5 nm, em: 580 ± 5 nm) at room temperature. Changes in rhod-2 fluorescence were plotted as peak changes in arbitrary fluorescence units (AFU) after subtracting background light levels.

Aerosol exposures. Aerosol exposures were conducted in 96 well plates using a Sigelei Fuchai 200W device and Uwell Crown tanks as before (57, 211, 216). BP (12 mg/ml nicotine) or PG/VG were heated to generate aerosols with the power output set to 100 W. CALU3 cells were seeded into 96 well plates and loaded with fluo-4 prior to the aerosol exposures. Cells were submerged in 100 μl Ringer's solution per well and baseline fluorescence was measured for 1 min before cells were moved to a dark chemical hood and exposed to 0-25 puffs of air or heated aerosols. A 70 ml aerosol or air puff was applied manually (1 puff every 30 sec) using a 100 ml syringe and a three-dimensional printed acrylic six-channel manifold (57). Naïve wells were run on each plate and covered with silicone strips to avoid aerosol exposures. Plates were returned to the plate reader and fluorescence was read over time.

Total cell number (DAPI) and viability (calcein). As an indicator of total cell number, cultures were fixed with 100% methanol for 10 min at room temperature, rinsed with PBS, and stained with 1:1000 DAPI for 5-10 min. DAPI fluorescence was measured using a Tecan Infinite Pro plate reader (ex: 360 ± 5 nm, em: 460 ± 5 nm) at room temperature. Fluorescence intensities were plotted as DAPI fluorescence (AFU) after background subtraction (Fig 3.11*E-F*) or calculated as percent fluorescence of the e-liquid-treated cells compared to the average of the 0% e-liquid control (Fig. 3.2*C*) (211). Cell viability was measured using the fluorescent indicator calcein. After 24 h BP e-liquid exposure, media was replaced and cells were incubated with 3 μM calcein for 30 min at 37°C. Then cultures were rinsed and replaced with Ringer's solution and fluorescence intensities were read using the Tecan Infinite Pro plate reader (ex: 495 ± 5 nm; em: 516 ± 5 nm). Cell viability was calculated as percent fluorescence of e-liquid-treated cells compared with the average of the 0% e-liquid control group (Fig. 3.2*D*).

Measurement of total intracellular inositol phosphates. HEK293T cells were plated in 24 well plates for 6 h before an 18 h incubation with [^{3}H]inositol (4 μCi/ml; American Radiolabeled Chemicals; Saint Louis, MO) in culture media. Cells were then rinsed and given fresh incubation media (115 mM NaCl, 25 mM HEPES, 10 mM glucose, 5 mM KCl, 1.35 mM $CaCl_2$, 1 mM NaH_2PO_4, and 0.5 mM $MgSO_4$) for 2 h at 37°C. 10 mM LiCl was added to each culture before initiating the experiment where cells were exposed to buffer only, 200 μM UTP, 3% PG/VG, 3% BP (12 mg/ml nicotine), or 3% BP (0 mg/ml nicotine) for 2 min. Assays were quenched by aspiration of the media and addition of 0.4 ml of ice-cold 2 M perchloric acid / 0.2 mg/ml inositol phosphate 6 (InsP6). Culture plates were left on ice for 10 min before media was transferred to microcentrifuge tubes and neutralized with 1M KCO_3 and 40 mM EDTA. Samples were left overnight at 4°C and perchlorate precipitate was removed via centrifugation. Gravity-fed ion-exchange chromatography was used to separate [^{3}H]inositol (Ins) from the [^{3}H]inositol-labeled inositol phosphates ("InsP", i.e, InsP1 + InsP2 + InsP3 + InsP4) (225). Data were calculated as 1000 x (InsP / Ins) and then transformed to percent activation at 2 min for each experiment.

$$\%\ Activation = \frac{experimental\ value - average\ PG/VG\ value}{average\ PG/VG\ value} * 100$$

STIM1 and Orai1 puncta quantification. HEK293T cells were plated onto glass coverslips and transfected with Orai1-YFP and STIM1-mCherry using lipofectamine 2000 per manufacturer's protocol as described (198). Cells expressing STIM1-mCherry or Orai1-YFP were treated with 0% BP (media), 3% PG/VG, 2 μM thapsigargin, 3% BP (0 mg/ml nicotine), or 3% (12 mg/ml nicotine) for 5-10 min. Cells were fixed with 4% PFA for 10 min following treatment and rinsed with PBS before imaging. All puncta imaging was conducted on a Leica SP8 confocal microscope with a 63 x 1.4 NA oil immersion objective. Multiple images were taken per coverslip from different parts of the coverslip and ≥ 12 transfected cells were visually analyzed for the percentage of puncta positive cells per coverslip.

Immunoblots. Rabbit anti-phospho-PKCα (1:1000) and anti-PKCα (1:1000) (Abcam); mouse anti-phospho-tyrosine (1:2000) (Cell Signaling); mouse anti-GAPDH (glyceraldehyde-3-phosphate dehydrogenase) (1:1000) (Santa Cruz); peroxidase-conjugated-rabbit or mouse (all 1:3000, Jackson ImmunoResearch) were purchased from commercial sources. CALU3 cells were plated in 60 mm dishes and exposed to 3% BP (12 mg/ml nicotine) for 0-60 min. Cells were lysed in modified Pierce IP lysis buffer with 25 mM Tris-HCl pH 7.4, 150 mM NaCl, 1% NP-40, 1 mM EDTA and supplemented with 1X proteinase inhibitor cocktail and 1X phosphatase inhibitor cocktail (Roche) to detect protein expression from total cell lysates. Lysates were processed by sodium dodecyl sulfate (SDS)-polyacrylamide electrophoresis and immunoblot.

RNA extraction, cDNA synthesis, and quantitative RT-PCR. RNA was extracted from untreated primary whole lung tissue and HBECs, as well as immortalized CALU3 and HEK293T cells using the Qiagen RNeasy kit following the manufacturer's protocol. cDNA was synthesized using the Bio-Rad iScript cDNA synthesis kit following the manufacturer's protocol. Gene expression was measured using Taqman gene expression assays from Applied Biosystems for *CFTR, ADRB2, ORAI1,GNAT3, TAS1R1, TAS1R2, TAS1R3, TAS2R1, TAS2R3, TAS2R4, TAS2R5, TAS2R7, TAS2R8, TAS2R9, TAS2R10, TAS2R13, TAS2R14, TAS2R16, TAS2R19, TAS2R20, TAS2R30, TAS2R31, TAS2R38, TAS2R42, TAS2R43, TAS2R45, TAS2R46, TAS2R50,* and *TAS2R60* using human primers. Genes of interest were normalized to *GAPDH* and fold change was calculated using ΔΔCT method relative to *CFTR* or *ORAI1*.

E-liquid internalization imaging. CALU3 cells were plated onto glass coverslips and media was rinsed and replaced with Ringer's solution prior to imaging. All imaging was conducted on a Leica SP8 confocal microscope with a 63 x 1.4 NA oil immersion objective similar to (88). Bright field and fluorescent (ex: 405 nm, em: 460 nm) images were taken before and after cells were exposed to BP e-liquid. Images were compiled into Z-stacks.

Statistical analyses. All statistics were run using Prism Graphpad (San Diego) software. Data were analyzed using the Kruskal-Wallis test with Dunn's multiple comparisons test or Mann-Whitney test as appropriate. *P*-values ≤ 0.05 were found to be significant and reported (*$P \leq 0.05$, **$P \leq 0.01$, ***$P \leq 0.001$; #$P \leq 0.05$, ##$P \leq 0.01$, ###$P \leq 0.001$). All experiments were performed on at least three separate occasions. Whole lung and HBECs were obtained from three or more normal donors (Fig. 3.1*A*,*D;* 3.9*A*; Table 3.1).

3.4. Results

BP-flavored neat e-liquid elicits acute dose-dependent cytosolic Ca^{2+} responses in both primary and immortalized epithelial cells. We loaded cells with cytosolic Ca^{2+} indicators (fura-2 or fluo-4) as specified and exposed them to the BP e-liquid diluted (%vol/vol) in Ringer's solution. We found that primary HBECs, CALU3 cells, and HEK293T cells increased cytosolic Ca^{2+} after BP addition (Fig. 3.1*A-C*). An additional 3% PG/VG vehicle control was run in both CALU3 and HEK293T cells and did not elicit a response. Peak responses to each treatment were grouped by cell type and compared (Fig. 3.1*D*). Addition of 3% BP diminished the response to thapsigargin, suggesting that BP was causing ER Ca^{2+} release (Fig. 3.1*A-D*).

BP e-liquid lot (batch) testing reveals similar acute cytosolic Ca^{2+} and 24 h cell viability/proliferation responses. Since the e-liquids used in this study were purchased from commercial vendors, our BP-flavored e-liquid results were performed using two different lots (batches) prepared at different times, and thus were tested for chemical composition and functional similarities before continuing the study. GC-MS analysis verified that both BP e-liquids has similar chemical constituent profiles (not shown). Figure 3.1 data included lots of BP (designated #09 or #165), so we compared

responses by lot and found that both lots displayed similar dose-dependent responses in CALU3 cells (Fig. 3.2*A*-*B*). Our previous study also showed BP e-liquid affected cell viability/proliferation at similar doses (%vol/vol) following 24 h exposure, so we compared total cell number and viability data between the lots and found those responses to be similar as well (Fig. 3.2*C*-*D*).

Cytosolic Ca^{2+} responses following BP exposure independent of nicotine. The BP e-liquid used in Fig. 3.1 contained 12 mg/ml nicotine. To control for the potential effects of nicotine on cytosolic Ca^{2+} responses, a separate BP e-liquid was purchased that contained 0 mg/ml nicotine. CALU3 cultures were loaded with fluo-4, exposed to 3% BP ± 12 mg/ml nicotine ± wash out, and the cytosolic Ca^{2+} responses were measured (Fig. 3.3*A*-*B*). BP with nicotine caused a peak response, followed by a sustained plateau that was removed following wash out (Fig. 3.3*C*-*D*). In contrast, BP without nicotine had a similar peak response. However, the plateau phase was diminished in the absence of nicotine ± wash out, suggesting that nicotine contributed to the plateau but not the peak phase.

BP aerosol exposure to submerged CALU3 cultures acutely elicits cytosolic Ca^{2+} responses, similar to unheated e-liquids. Since we found dose-dependent increases in cytosolic Ca^{2+} following direct BP exposure, we sought to determine whether aerosolized BP would also increase cytosolic Ca^{2+}. We loaded CALU3 cells with fluo-4 and measured cytosolic Ca^{2+} responses following 0-25 puffs of aerosol as indicated. Neither puffs of air nor PG/VG (vehicle) elicited a change in cytosolic Ca^{2+} (Fig. 3.4*A*-*B*). In contrast, addition of thapsigargin elevated Ca^{2+}, suggesting that the cells were responsive to stimuli. However, exposure to 5-25 puffs of BP aerosol elicited robust increases in cytosolic Ca^{2+} and diminished the thapsigargin response, indicating that the ability of BP to affect thapsigargin-sensitive stores was maintained when BP was exposed to cells as an aerosol (Fig. 3.4*C*-*D*).

BP e-liquid cytosolic responses are ER/SOCE-dependent and do not involve mitochondrial Ca^{2+}. Ca^{2+} is sequestered into multiple intracellular stores, including the ER (242). Thapsigargin is a sarco/endoplasmic reticulum Ca^{2+}-ATPase (SERCA) pump inhibitor that depletes ER stores to activate SOCE (144). Since cultures did not respond to thapsigargin after BP exposure, we decided to test whether this signal was dependent on the ER/SOCE pathway. We performed Ca^{2+} replacement studies to

measure cytosolic Ca^{2+}, where cells were placed in Ca^{2+}-free Ringer's solution then, after ER Ca^{2+} was depleted, 2 mM Ca^{2+} was added extracellularly. Following this protocol, thapsigargin caused a small peak due to ER Ca^{2+} release that was followed by a second, larger SOCE response when Ca^{2+} was returned extracellularly (Fig. 3.5*A*). 3% BP (12 mg/ml nicotine) elicited a similar peak in nominal Ca^{2+}-free solution and a second larger peak in the presence of extracellular Ca^{2+} solution that was thapsigargin-insensitive (Fig. 3.5*A*). Taken together, these data suggested that BP activated a classic ER-dependent SOCE response. Moreover, pretreating cells with thapsigargin abolished the 3% BP Ca^{2+} response (Fig. 3.5*B*).

The mitochondria are also a significant store of intracellular Ca^{2+} (203). To test for mitochondrial Ca^{2+} contributions to the BP response, we pretreated cells with CCCP, which caused mitochondrial Ca^{2+} depletion. We found that there was a similar cytosolic Ca^{2+} response with CCCP pretreatment in CALU3 cells (Fig. 3.5*C*). Additionally, we loaded CALU3 cells with the mitochondrial Ca^{2+} indicator rhod-2 to directly measure mitochondrial Ca^{2+} stores. There was no significant difference in rhod-2 fluorescence following 3% BP or PG/VG compared to 0% BP ± CCCP pretreatment (Fig. 3.5*D*). In contrast, CCCP diminished rhod-2 mitochondrial Ca^{2+} levels (Fig. 3.5*D*).

Ca^{2+}-eliciting BP e-liquid initiates STIM1 and Orai1 puncta formation (SOCE) and downstream protein kinase Cα (PKCα) phosphorylation. IP_3-dependent ER Ca^{2+} release causes aggregation of the ER membrane protein STIM1 into discrete puncta at the ER-plasma membrane junction, which then activates Orai1 and is required for subsequent plasma membrane Ca^{2+} influx (SOCE) (141, 189). We transfected HEK293T cells with STIM1-mCherry or Orai1-YFP and looked for the puncta formation of these proteins following BP exposure. Transfected cells were treated with 0% BP, 3% PG/VG, thapsigargin, or 3% BP (± 12 mg/ml nicotine) and both STIM1-mCherry and Orai1-YFP were imaged by confocal microscopy (Fig. 3.6*A*). 3% BP treatment increased both STIM1 and Orai1 puncta formation to a similar degree as thapsigargin, independent of the presence of nicotine (Fig. 3.6*B*-*C*). Thus, BP e-liquid caused downstream activation of STIM1 and Orai1. Downstream of ER/SOCE activation, Ca^{2+} alters the phosphorylation of key protein kinases, which further impacts cell function, including gene expression

and protein translation (65, 73). For example, protein kinase Cα (PKCα) is canonically activated downstream of IP_3 formation and Ca^{2+} signaling and plays a role in many biological functions (e.g., cell proliferation) (122, 146, 241, 261). We tested whether BP could induce phosphorylation of PKCα. Western blots for phosphorylated-PKCα (p-PKCα), total PKCα, and GAPDH were generated from CALU3 cells treated with 3% BP (12 mg/ml nicotine) over time (Fig. 3.6*D*). There was a significant increase in PKCα phosphorylation at 15-30 min, indicating that BP e-liquid has the ability not only to induce SOCE, but to phosphorylate important downstream protein kinases (Fig. 3.6*E*).

BP e-liquid produces inositol phosphate (InsP) accumulation upstream of ER/SOCE Ca^{2+} response. Since we determined that the Ca^{2+} response was ER/SOCE-dependent, we next sought to identify upstream signaling components. IP_3 is a common cellular messenger that is produced by PLC-dependent cleavage of phosphatidylinositol 4,5-biphosphate (PIP_2) and causes ER Ca^{2+} release after activating the IP_3Rs on ER membranes. To determine whether BP generated IP_3 formation, total InsP accumulation was measured following a 2 min exposure to either 3% PG/VG, buffer control, UTP, or 3% BP ± 12 mg/ml nicotine. 3% BP significantly increased total InsP production (percent activation) compared to 3% PG/VG independently of nicotine (Fig. 3.7*A*). The response was similar to UTP, which is known to induce IP_3 formation following activation of the $P2Y_2$ receptor (G_q-linked GPCR) (64). Additionally, we exposed HEK293T cells to the IP_3R antagonist 2-APB (152, 228) to test the involvement of IP_3 formation in eliciting the BP Ca^{2+} response. Traces of cytosolic Ca^{2+} in response to UTP or 1% BP ± 2-APB pretreatment were shown (Fig. 3.7*B*). UTP and 1% BP treatments elicited a cytosolic Ca^{2+} signal compared to 0% BP (Fig. 3.7*C*). 2-APB pretreatment blunted the Ca^{2+} response of UTP and 1% BP.

BP-initiated IP_3 formation, ER Ca^{2+}/SOCE response, and PKCα phosphorylation are independent of upstream receptor tyrosine kinase (RTK) activation. RTKs are a large family of kinases that phosphorylate proteins on tyrosine residues to regulate important cellular functions and can involve pathways such as the one activated by 3% BP exposure (161, 173). We used a phospho-tyrosine (p-Tyr) antibody to measure phosphorylation in protein lysates collected from 3% BP-treated CALU3 cells over

time (Fig. 3.8*A*). We found that BP treatment did not increase p-Tyr among detected proteins in our gel (normalized to GAPDH), suggesting that BP does not activate RTKs and PLCγ upstream of IP_3 formation (Fig. 3.8*B*).

Low endogenous mRNA expression in primary lung epithelia suggests that BP signaling is independent of taste receptor activation. Since our previous data showed that BP treatment did not increase p-Tyr expression, GPCRs are another family of receptors where ligand binding causes a similar signaling cascade to BP exposure. Both sweet taste receptors (T1Rs) and bitter taste receptors (T2Rs) are GPCRs that respond to sweet and bitter tastants/odorants. Taste receptors are typically found in the tongue, but have also been reported in other tissue types including the upper and lower airways (50, 63, 223, 253). To try to identify candidate taste receptors that could be targets of flavored e-liquids, we tested the mRNA expression of three T1Rs, 22 T2Rs, and the Gα protein associated with taste reception gustducin (*GNAT3*), in primary whole lung, primary HBECs, CALU3 cells, and HEK293T cells. Since GPCRs are not highly abundant proteins, expression was calculated relative to *CFTR*, an important airway ion channel that is also not highly expressed. HBEC expression data were shown as a bar graph (Fig. 3.9) but data for all tissue/cell types expression were summarized elsewhere (Table 3.2). Generally, almost all taste receptors and gustducin were detected at extremely low levels of expression, if at all. HEK293T cells were the only samples that were normalized to *ORAI1* instead because HEK293T cells do not express *CFTR* (Table 3.2). In HEK293T cells, five T2Rs (*TAS2R3, TAS2R4, TAS2R14, TAS2R31, TAS2R45*) were at similar or greater levels to *ORAI1* expression.

BP autofluorescence imaging reveals e-liquid internalization in CALU3 cells. Previous work from our group has shown that some e-liquids have autofluorescent properties, especially in the UV excitation range (57). BP is one of the least autofluorescent e-liquids tested. However, some fluorescence can be visualized using confocal imaging with a high gain setting. We used this property to test whether BP components could enter cells and potentially stimulate PLC activity independent of extracellular receptor activation. After 3% BP exposure, intracellular autofluorescence was detected (Fig. 3.10*A-B*), suggesting that BP components may directly stimulate PLC activity. Though we know that BP

causes PLC activation to generated IP_3, it is not clear whether this response is triggered by GPCR activation or direct activation of PLC (Fig. 3.10*C*).

Thapsigargin-induced Ca^{2+} response is blunted over time with BP e-liquid exposure. Since we have greatly detailed the acute, dose-dependent effects of BP on cell Ca^{2+} signaling, we next tested whether these effects persisted over time or altered Ca^{2+} homeostasis. Accordingly, we incubated CALU3 cells with 3% BP or PG/VG for 24 h and then measured the thapsigargin-stimulated Ca^{2+} response (Fig. 3.11*A*-*B*). Following exposure to 3% BP, the response to thapsigargin was attenuated. This blunted thapsigargin response was present by 3 h post-BP exposure and persisted over 24 h. Some e-liquids are cytotoxic and decrease the number of cells in culture (211). To check whether prolonged BP exposure was cytotoxic, we stained cell nuclei using DAPI and measured the resultant fluorescence. DAPI fluorescence was not different across groups, indicating that chronic BP exposure had not decreased total cell number (Fig 3.11*E*). We then tested whether the thapsigargin response could be restored following 3 h BP exposure by then performing a 24 h wash out with media. Indeed, the thapsigargin response was rescued with wash out in the BP-exposed cultures (Fig. 3.11*C*-*D*). Again, there was no decrease in DAPI fluorescence with BP or PG/VG treatments compared to 0% BP (Fig. 3.11*F*), suggesting that this inhibited Ca^{2+} response was not due to BP-related cytotoxicity.

The attenuated thapsigargin response following 3 h BP exposure affects both ER Ca^{2+} release and SOCE. To better understand how chronic BP exposure might be inhibiting the thapsigargin-induced Ca^{2+} response, we completed Ca^{2+} replacement studies as before (Fig. 3.5*A*). After 3% BP exposure for 3 h, both ER Ca^{2+} release and SOCE was diminished (Fig. 3.12*A*-*D*). Moreover, cells treated with 3% BP for 1 h only showed a decreased SOCE response ($P = 0.051$), suggesting that the attenuation to thapsigargin starts as early as 1 h and impairs the SOCE response before the ER response. PG/VG treatment did not alter ER/SOCE-dependent thapsigargin responses, as previously shown.

3.5. Discussion

We have previously characterized the effects of over 100 e-liquids on cell viability (211, 216). In these studies, BP was consistently more toxic than the e-liquid base constituents (i.e., PG, VG, nicotine).

We attempted to correlate toxicity versus chemical composition. However, due to the chemical diversity, these studies did not detail how more toxic e-liquids (e.g., BP) exerted their effects. Many cellular pathways regulate proliferation, and Ca^{2+} signaling is a well-known regulator of both cell division and apoptosis (26). Since BP altered cell proliferation, we first focused on its effects on Ca^{2+} homeostasis. Indeed, we found that BP acutely stimulated ER Ca^{2+} release in primary HBECS as well as immortalized CALU3 and HEK293T cells (Fig. 3.1). This response was independent of nicotine, but there was a prolonged plateau compared to baseline with the presence of nicotine (Fig. 3.3). We also saw a similar Ca^{2+} response after both direct e-liquid addition and vaping e-liquid, suggesting that this is a robust, dose-dependent response (Fig. 3.4).

Multiple lines of evidence suggested that BP elicited a classic ER/SOCE-type response. Firstly, pretreatment with BP abolished the effects of the SERCA pump inhibitor thapsigargin (Fig. 3.1) and vice versa (Fig. 3.5*B*). Second, BP still elevated cytoplasmic Ca^{2+} in the absence of extracellular Ca^{2+}, and a second increase in cytosolic Ca^{2+} occurred when extracellular Ca^{2+} was reintroduced (Fig. 3.5*A*). Third, the BP effect was insensitive to the mitochondrial uncoupler CCCP and no change in Ca^{2+} was detected when cells were labeled with the mitochondrial dye rhod-2 (Fig. 3.5*C*-*D*). Finally, BP exposure caused STIM1 and Orai1 to reorganize into puncta (Fig. 3.6*A*-*C*), which is indicative of their activation. Here, these effects reprised those seen with thapsigargin and were independent of nicotine and PG/VG.

Thapsigargin elicits ER Ca^{2+} release by directly inhibiting SERCA pumps (144). However, formation of IP_3 activates IP_3Rs on the ER membrane to physiologically elicit ER Ca^{2+} release (64). Thus, we looked to see whether BP induced IP_3 formation. Indeed, BP induced InsP formation that was (i) PG, VG, and nicotine-independent and (ii) equal in magnitude to the InsP formation induced by UTP addition (Fig. 3.7*A*). Consistent with this observation, the IP_3R antagonist 2-APB abolished both UTP and BP-induced increases in cytosolic Ca^{2+} (Fig. 3.7*B*-*C*). 2-APB can also affect transient receptor potential (TRP) channels (46). However, given that we had established that this was an ER-dependent signal, it is likely that we are not observing inhibition of TRP channels here.

Canonically, GPCR or RTK activation can trigger PLC-mediated IP_3 formation, ER Ca^{2+} release, and SOCE (64, 161, 173, 233). We excluded upstream RTK activation after measuring global tyrosine phosphorylation in BP-treated CALU3 cells (Fig. 3.8). We could not completely exclude the possibility that BP acted upstream of PLC and stimulated a GPCR or its associated G-protein though. We initially hypothesized that taste receptors (GPCRs) might be targets since e-liquids often contain bitter nicotine or sweet flavors. Though taste receptors have been reported in the airways (63, 134, 223), we found little to no expression of several taste receptor isoforms and gustducin (*GNAT3*) in primary and immortalized airway samples as well as HEK293T cells, suggesting that this effect is not taste-mediated. The exceptions were five T2Rs in HEK293T cells that showed similar expression to our *ORAI1* control since HEK293T cells had no *CFTR* expression. Though more experiments are necessary to rule GPCR activation in or out of this mechanism, it seems unlikely that the conserved response to BP would act through a T2R in one cell type and not the others, especially in the absence of gustducin.

PLC is an enzyme that is associated with the inner face of the plasma membrane that cleaves phospholipids (e.g., PIP_2) to form IP_3 (64). Our observation that BP caused InsP formation is good evidence that PLC was being activated by BP however, the mechanism of activation is still unclear. Though we have not completely ruled out a possible GPCR target for BP, we have previously shown that the autofluorescent e-liquid, Pixie Dust, can internalize in HEK293T cells (88). BP is actually one of the least autofluorescent e-liquids and does not interfere with the fluorescent indicators used in this study (57). However, we demonstrated that BP can rapidly enter CALU3 cells (Fig. 3.10*A*-*B*) by imaging autofluorescence at 405 nm with high laser gain settings. The small molecule m-3M3FBS has been reported to acutely activate PLC followed by increases in cytosolic Ca^{2+} signaling in several cell lines, independent of G protein stimulation (14). Of note, Krjukova et al. found that m-3M3FBS may not be a reliable PLC activator in all cell types as they reported that SH-SY5Y cell line had delayed PLC activity, which suggested the Ca^{2+} signal was independent of its activation (125). Yet, it is possible that components in BP e-liquid could similarly move intracellularly and directly access and activate PLC.

IP_3 formation is mediated by PLC activation, usually downstream of cell surface receptor activation. PLC is required for normal physiological function such as G_q-linked GPCR signaling activation (64, 75). However, PLC has also been denoted as a malignancy-linked signal transducing enzyme (270). For instance, PLCγ overexpression increased transformation and tumorigenicity of NIH3T3 cells (231) and altered expression of PLC-β2 promoted mitosis and migration of breast cancer-derived cells (27). Indeed, chronic activation of PLC by inhaling BP or similarly flavored aerosols may have the potential to trigger increased cell proliferation and metastasis, similar to cancer. Moreover, downstream activation of SOCE has also been shown to affect cell proliferation. Chen et al. reported that SOCE responses change with cell cycle, where SOCE is upregulated to transition to the G1/S phase check point and then downregulated to transition from the S to the G2/M phase (44). However, further research is needed to elucidate the long-term effects of vaping PLC-activating e-liquid flavors on cancer risk in the lung.

Indeed, our data shows an acute and robust activation of PLC, resulting in SOCE following BP exposure. Yet, Figures 3.11 and 3.12 suggest that BP e-liquid impairs ER Ca^{2+} release and SOCE with chronic exposure. Knocking down Orai1 and/or STIM1 has been shown to reduce cell proliferation (44), suggesting that impairing SOCE with long-term BP exposure may offset the potential cell proliferation induction caused by increased PLC activity upstream. However, the mechanism by which BP inhibits thapsigargin-dependent ER/SOCE responses is unclear. Furthermore, washing out BP in cultures restores the thapsigargin-dependent Ca^{2+} signal. This suggests that impairment of SOCE from BP or other Ca^{2+}-eliciting flavors would be highly dependent on the amount of e-liquid vaped and time between vaping sessions. Interestingly, STIM1 protein expression was found to be upregulated in HBECs isolated from vapers compared to smokers and non-smokers (88). Moreover, HBEC isolated from mice exposed to PG/VG aerosol showed a similar upregulation of STIM1 compared to air puff controls (88), suggesting that chronic PG/VG exposure alone can alter a key player in Ca^{2+} metabolism. Further studies are needed to understand the long-term effects of vaping PG/VG, as well as Ca^{2+}-eliciting e-liquids on Ca^{2+} metabolism in lung epithelia and other airway cells.

To date, no other study has shown the ability of e-liquids to cause ER Ca^{2+} release. These data could be used to inform FDA regulations regarding e-cig flavorings and potential health effects for users. Specifically, our study provides a detailed look at a BP-flavored e-liquid and its effects on cell Ca^{2+} homeostasis, which could be coupled with *in vivo* human data to find new biomarkers of e-cig exposure and understand alterations of airway cell Ca^{2+} homeostasis in the airways of vapers.

Table 3.1. List of taste receptor mRNA expression in primary and immortalized airway cells. List of the mRNA expression levels of 25 sweet and bitter taste receptors (T1Rs/T2Rs) and associated Gα protein (*GNAT3*) relative to important, low expressed airway ion channels (*CFTR* or *ORAI1*) determined by quantitative RT-PCR in untreated primary whole lung and HBECs, as well as immortalized CALU3 and HEK293T cell lines. Data shown as average gene expression relative to CFTR or Orai1 ± SEM. n = 5 wells per gene and ND = not determined. Primary samples included healthy, non-smoking donors (n = 3-4).

	Whole Lung	**HBEC**	**CALU3**	**HEK293T**
Gene	**AVG ± SEM**	**AVG ± SEM**	**AVG ± SEM**	**AVG ± SEM**
CFTR	1.003 ± 0.024	1.045 ± 0.157	1.015 ± 0.075	0.003 ± 0.003
ADRB2	1.348 ± 0.224	-	-	-
ORAI1	-	-	0.050 ± 0.010	1.004 ± 0.060
GNAT3	ND	0.001 ± 0.001	ND	0.001 ± 0.001
TAS1R1	0.006 ± 0.003	0.001 ± 0.001	0.013 ± 0.010	0.018 ± 0.016
TAS1R2	ND	0.018 ± 0.008	ND	ND
TAS1R3	ND	0.001 ± 0.001	0.015 ± 0.012	0.003 ± 0.003
TAS2R1	0.006 ± 0.002	0.193 ± 0.119	ND	0.069 ± 0.029
TAS2R3	0.027 ± 0.006	0.110 ± 0.067	0.014 ± 0.004	1.835 ± 0.549
TAS2R4	0.031 ± 0.006	0.114 ± 0.069	0.019 ± 0.005	1.423 ± 0.350
TAS2R5	0.035 ± 0.012	0.100 ± 0.063	0.012 ± 0.003	0.438 ± 0.088
TAS2R7	0.001 ± 0.001	0.129 ± 0.091	< 0.001 ± 0.001	0.055 ±0.031
TAS2R8	0.005 ± 0.001	0.052 ± 0.033	< 0.001 ± 0.001	0.196 ± 0.072
TAS2R9	0.019 ± 0.004	0.060 ± 0.038	< 0.001 ± 0.001	0.190 ± 0.095
TAS2R10	0.009 ± 0.002	0.142 ± 0.087	0.002 ± 0.001	0.155 ± 0.035
TAS2R13	0.021 ± 0.005	0.072 ± 0.044	0.001 ± 0.001	0.061 ± 0.006
TAS2R14	0.117 ± 0.019	0.221 ± 0.134	0.010 ± 0.006	1.077 ± 0.367
TAS2R16	0.002 ± 0.001	0.072 ± 0.051	< 0.001 ± 0.001	0.198 ± 0.150
TAS2R19	0.048 ± 0.008	0.388 ± 0.237	0.007 ± 0.003	0.584 ± 0.181
TAS2R20	0.018 ± 0.005	0.201 ± 0.142	0.001 ± 0.001	0.296 ± 0.086
TAS2R30	0.117 ± 0.010	0.062 ± 0.054	0.004 ± 0.003	0.196 ± 0.072
TAS2R31	0.028 ± 0.008	0.046 ± 0.043	0.003 ± 0.002	1.578 ± 0.480
TAS2R38	0.002 ± 0.001	0.062 ± 0.061	< 0.001 ± 0.001	0.139 ± 0.064
TAS2R42	0.006 ± 0.002	0.099 ± 0.097	0.002 ± 0.001	0.319 ± 0.098
TAS2R43	0.023 ± 0.009	0.012 ± 0.011	0.001 ± 0.001	0.197 ± 0.044
TAS2R45	0.032 ± 0.008	0.027 ± 0.025	0.003 ± 0.001	1.679 ± 0.371
TAS2R46	0.024 ± 0.005	0.073 ± 0.061	0.001 ± 0.001	0.385 ± 0.089
TAS2R50	0.010 ± 0.003	0.048 ± 0.048	0.001 ± 0.001	0.148 ± 0.051
TAS2R60	ND	0.037 ± 0.026	0.001 ± 0.001	0.221 ± 0.098

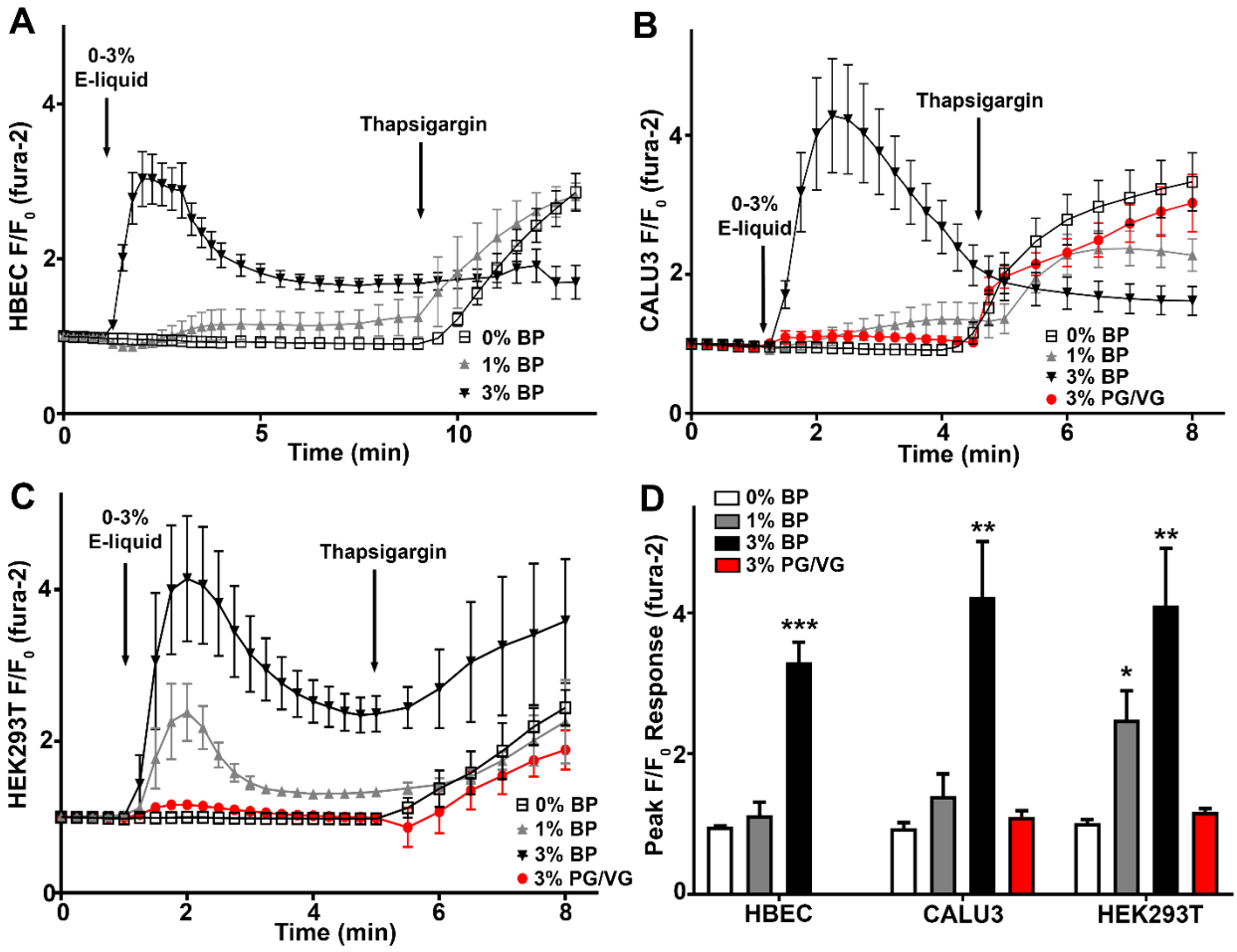

Figure 3.1. Banana Pudding (BP)-flavored e-liquid acutely elevates cytoplasmic Ca^{2+} in primary and immortalized epithelia. Primary human bronchial epithelial cells (HBECs), CALU3 cells, and HEK293T cells were plated on glass coverslips and loaded with a Ca^{2+} indicator (fura-2). Cells were challenged acutely with flavored BP e-liquid + nicotine or PG/VG (e-liquid vehicle) diluted in Ringers solution followed by thapsigargin. *A-C*: Ca^{2+} signals were measured over time and reported as the change in fluorescence (F/F_0). *D*: Peak changes for each cell type in response to the treatments are shown. *A-D*: Symbols and bars represent mean ± SEM. *A-D*: n = 4-11 coverslips per treatment. Statistical differences were shown between all treatments compared to 0% BP control within cell types (*D*) (**P* < 0.05, ***P* < 0.01, ****P* < 0.001).

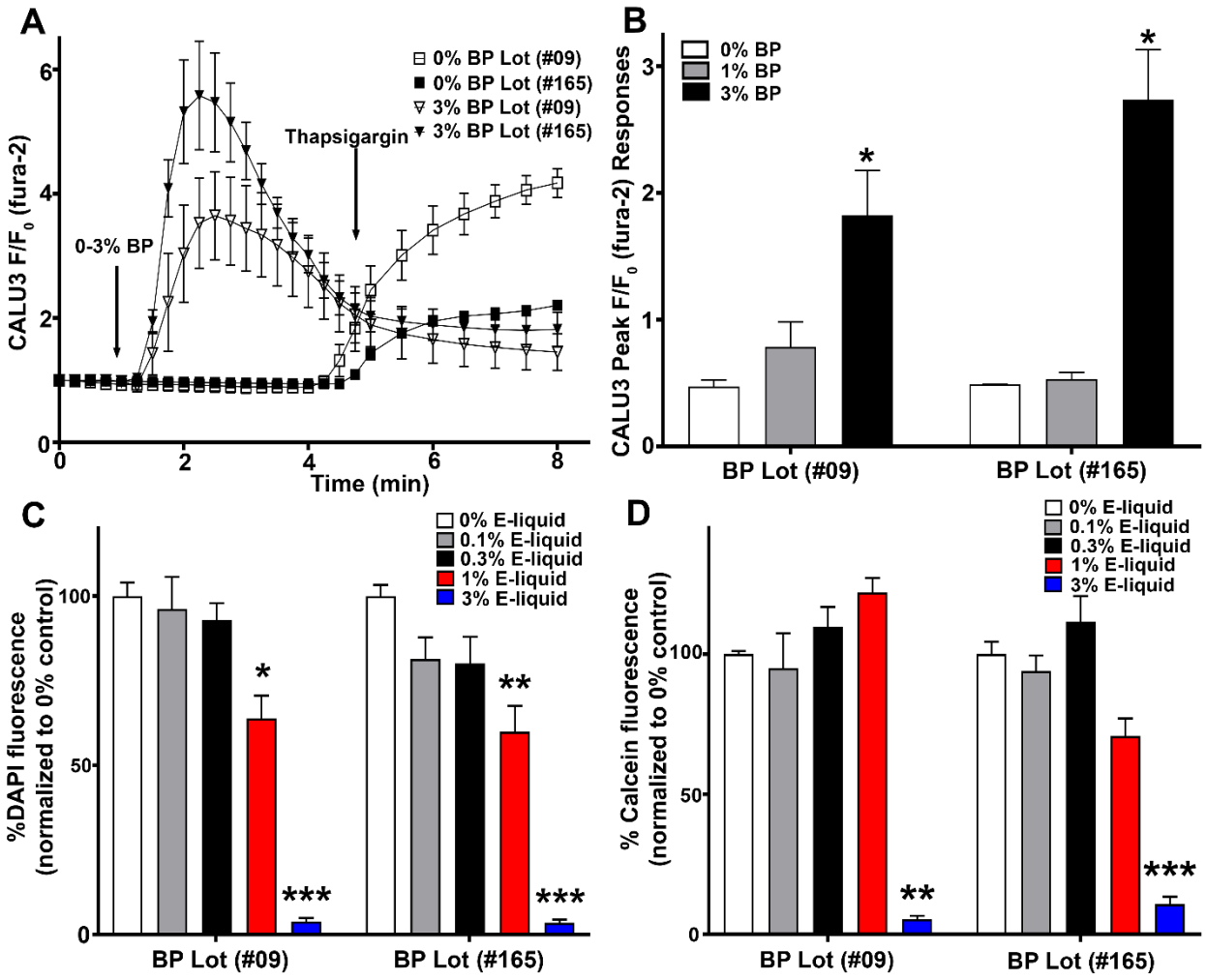

Figure 3.2. BP-flavored e-liquid retains similar cytoplasmic Ca^{2+} and toxicity responses between two purchased lots (batches). CALU3 cells were plated onto glass coverslips glass coverslips and loaded with a Ca^{2+} indicator (fura-2). Cells were challenged acutely with BP e-liquid from two different lots purchased from the same vendor (designated #09 and #165). BP e-liquid was diluted in Ringers solution and followed by thapsigargin. *A*: Ca^{2+} signals were measured over time and reported as the change in fluorescence (F/F_0). *B*: Peak changes per treatment for each BP lot are shown. Additional cells were plated into 96 well plates and treated with BP (%vol/vol) from either lot (#09 and #165) for 24 h. *C*: Cells were fixed and stained with DAPI to measure relative cell number. *D*: Cells were incubated with calcein to measure viability. Symbols represent mean ± SEM. Bars represent peak F/F_0 or %fluorescence normalized to 0% BP control. *A-B*: n = 3-4 coverslips per treatment. *C-D*: n = 9-19 wells per treatment. Statistical differences were shown between all treatments compared to 0% BP control within lot numbers (*B-D*) (*$P < 0.05$, **$P < 0.01$, ***$P < 0.001$).

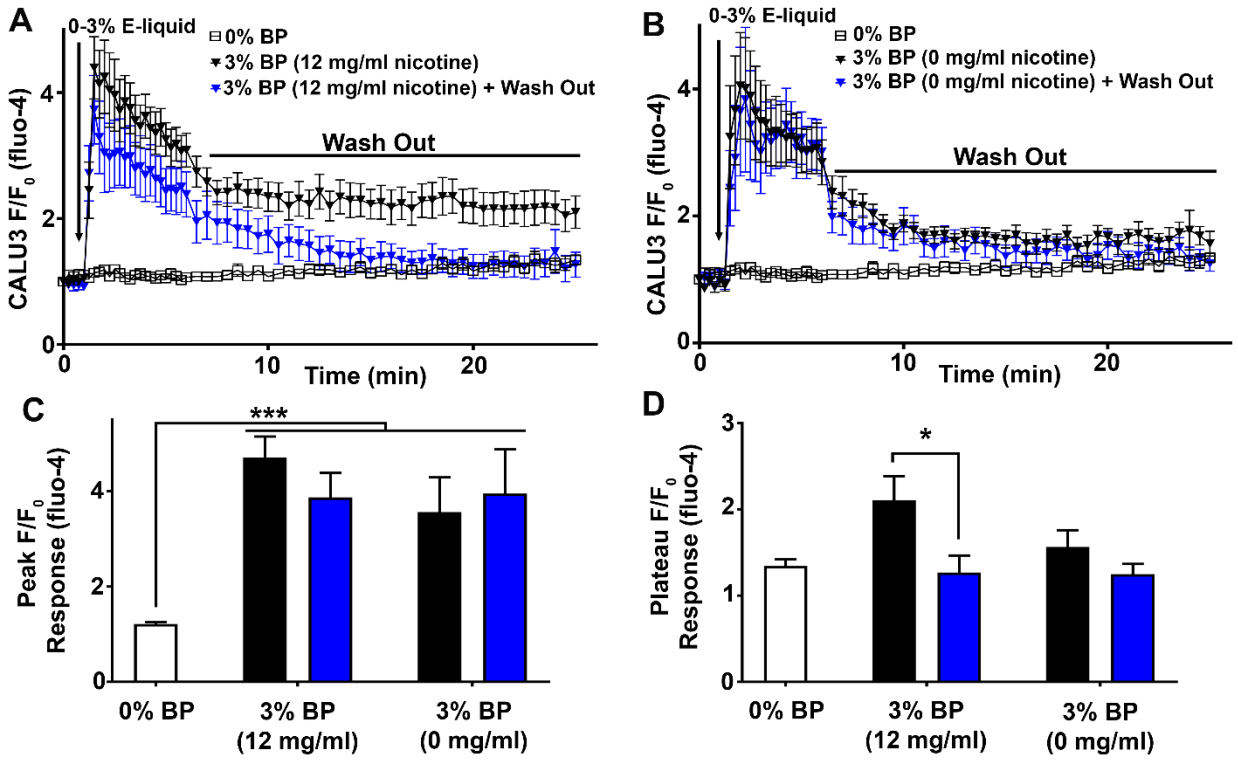

Figure 3.3. BP e-liquid elevates cytoplasmic Ca^{2+} independent of nicotine. CALU3 cells were plated into 12 well plates and loaded with a Ca^{2+} indicator (fluo-4). Cells were challenged acutely with BP e-liquid ± nicotine diluted in Ringers solution. *A-B*: Cells were exposed to the BP e-liquid ± 12 mg/ml nicotine and F/F_0 was measured over time ± treatment wash out. *C-D*: Peak and plateau changes for each treatment were measured at 1.5 and 25 min post-treatment respectively. *A-D*: Symbols and bars represent mean ± SEM. *A-D*: n = 8-13 wells per treatment. Statistical differences were shown between all treatments compared to 0% BP control (*C*) or within treatment ± wash out (*D*) (*$P < 0.05$, ***$P < 0.001$).

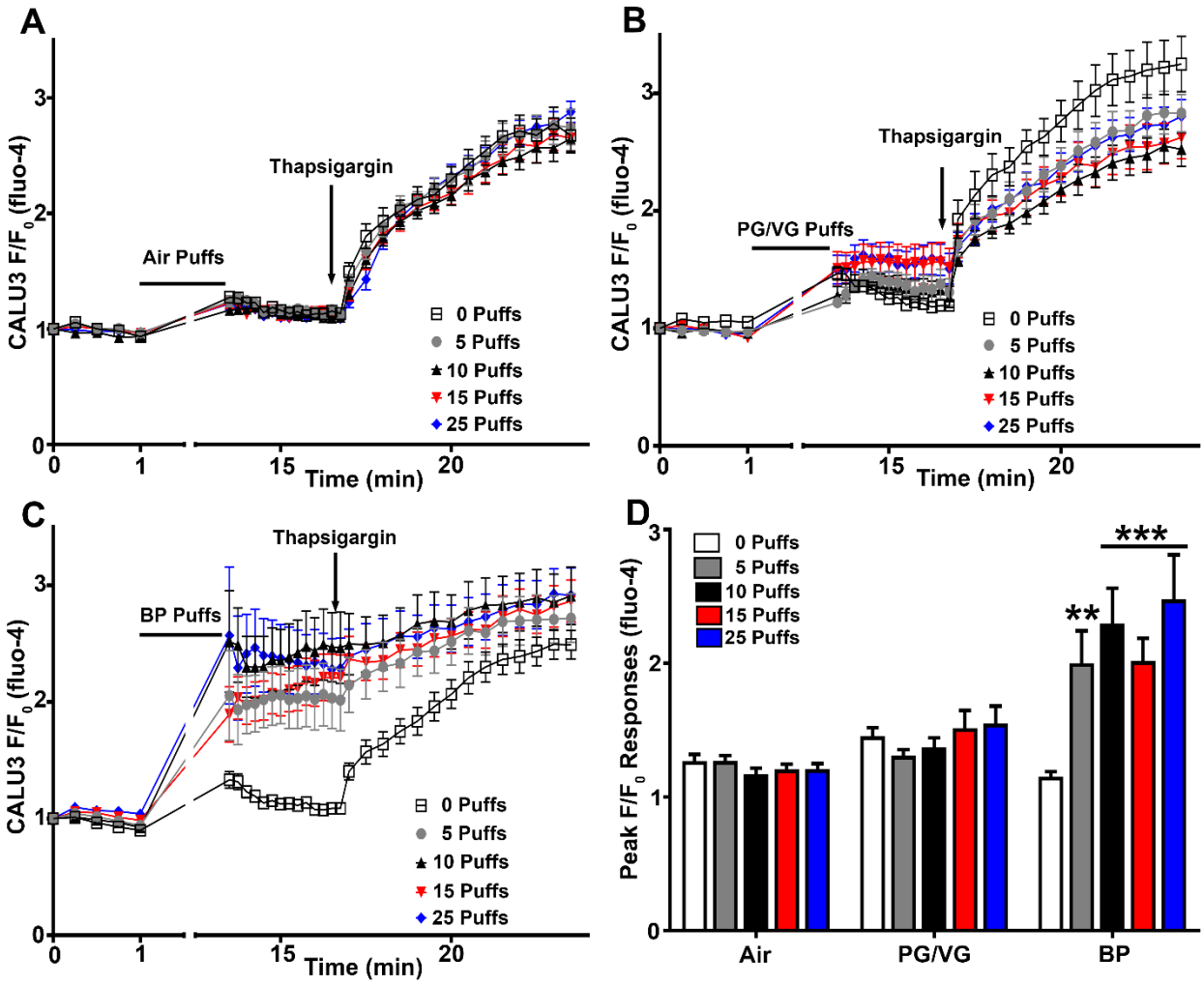

Figure 3.4. BP-flavored aerosol elicits acute dose-dependent increases in cytoplasmic Ca^{2+} in airway epithelia. CALU3 cells were seeded in 96 well plates. Cells were loaded with a Ca^{2+} indicator (fluo-4) and media was replaced with Ringers solution before baseline fluorescence was measured. The cultures were then exposed to puffs of air, PG/VG aerosol, or BP aerosol. After puffs were administered, fluorescence was read at timed intervals following aerosol exposure and thapsigargin addition. Both PG/VG (vehicle) and air puffs were performed as controls. *A-D*: The change in fluorescence (F/F_0) was reported over time and peak changes in fluorescence to exposures were plotted. Symbols and bars represent mean ± SEM. n = 17-30 wells per treatment. Statistical differences were shown between respective doses per treatment compared to their 0 puff control (**$P < 0.01$, ***$P < 0.001$).

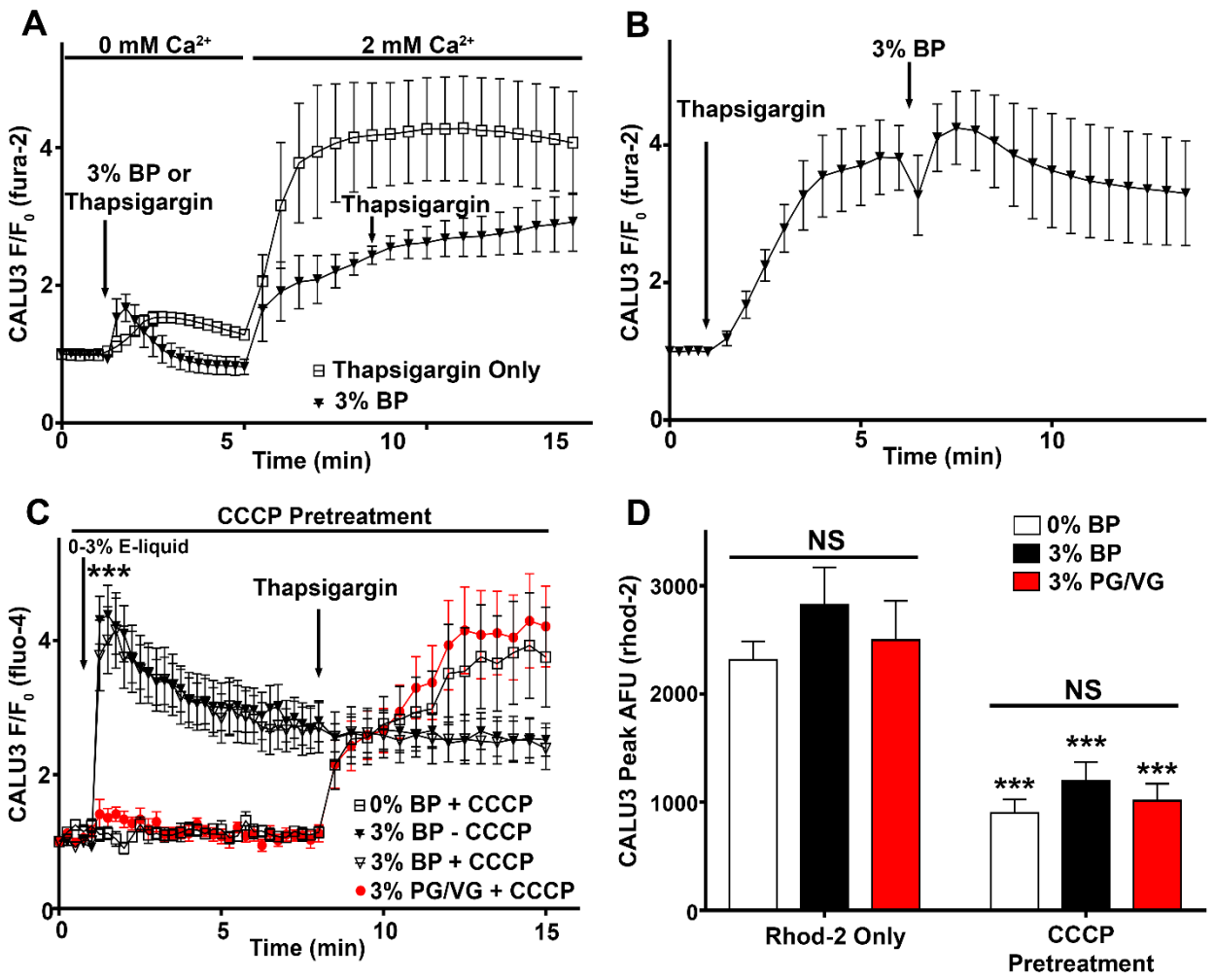

Figure 3.5. BP e-liquid Ca^{2+} responses are ER and SOCE-dependent and do not involve mitochondrial Ca^{2+}. *A-B*: CALU3 cells were seeded onto glass coverslips and loaded with fura-2. *A*: Cells were challenged with BP or PG/VG diluted in Ringers solution either containing nominal (0 mM) or 2 mM Ca^{2+} as indicated. Ca^{2+} signal was measured over time and reported as a trace or the peak fluorescence change in response to treatments. *B*: Cells were challenged with thapsigargin followed by 3% BP. *C*: CALU3 cells were plated into 12 well dishes, loaded with fluo-4, and pretreated ± CCCP before they were exposed to BP or PG/VG diluted in Ringers followed by thapsigargin. *D*: CALU3 cells were plated into 12 well dishes, loaded with a mitochondrial Ca^{2+} indicator (rhod-2), and pretreated ± CCCP before they were exposed to BP or PG/VG diluted in Ringers. Peak changes in mitochondrial Ca^{2+} (AFU) in response to treatments were plotted. Symbols and bars represent mean ± SEM. *A-B*: n = 5-6 coverslips per treatment. *C-D*: n = 7-15 wells per treatment. Statistical differences were reported between treatments and their 0% BP control within groups (*C-D*) (NS = not significant; ***$P < 0.001$) or between respective treatments between rhod-2 only and CCCP pretreatment groups (*D*) (*$P < 0.05$, **$P < 0.01$, ***$P < 0.001$).

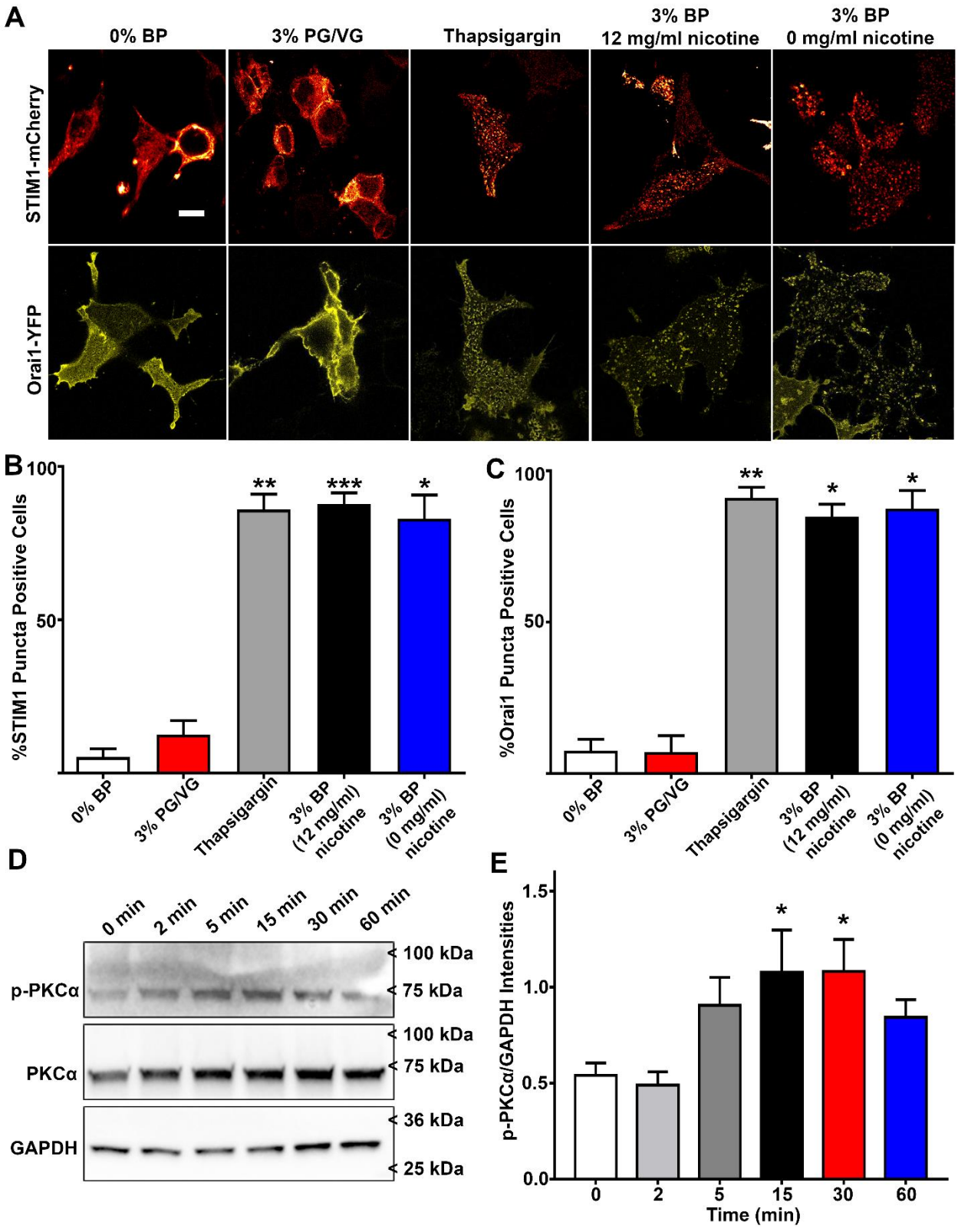

Figure 3.6. BP exposure induces STIM1/Orai1 puncta formation and protein kinase Cα (PKCα) phosphorylation. *A-C*: Transfected HEK293T cells were exposed to either 0% BP (media only), 3%

PG/VG, thapsigargin, or 3% BP ± 12 mg/ml nicotine, for 5-10 min. Cells were fixed and imaged and the percentage of puncta-positive cells were measured for both STIM1-mCherry and Orai1-YFP respectively. Scale bar represents 25 μm. *D-E*: CALU3 cells were seeded into 60 mm dishes and treated with 3% BP diluted in media for 0-60 min, as indicated. Protein lysates were collected and immunoblots were performed for phosphorylated PKCα (p-PKCα), total PKCα, and GAPDH (loading control). Representative blots of all proteins with treatment were shown. Band intensities were measured and the ratio of p-PKCα/GAPDH intensities were plotted. Bars represent mean + SEM. *A-C*: n = 4-9 coverslips per treatment. *D-E*: n = 6 blots per time point. *B-E*: Statistical differences were calculated between all groups compared to their 0% BP control or 0 min time point (*$P < 0.05$, **$P < 0.01$, ***$P < 0.001$).

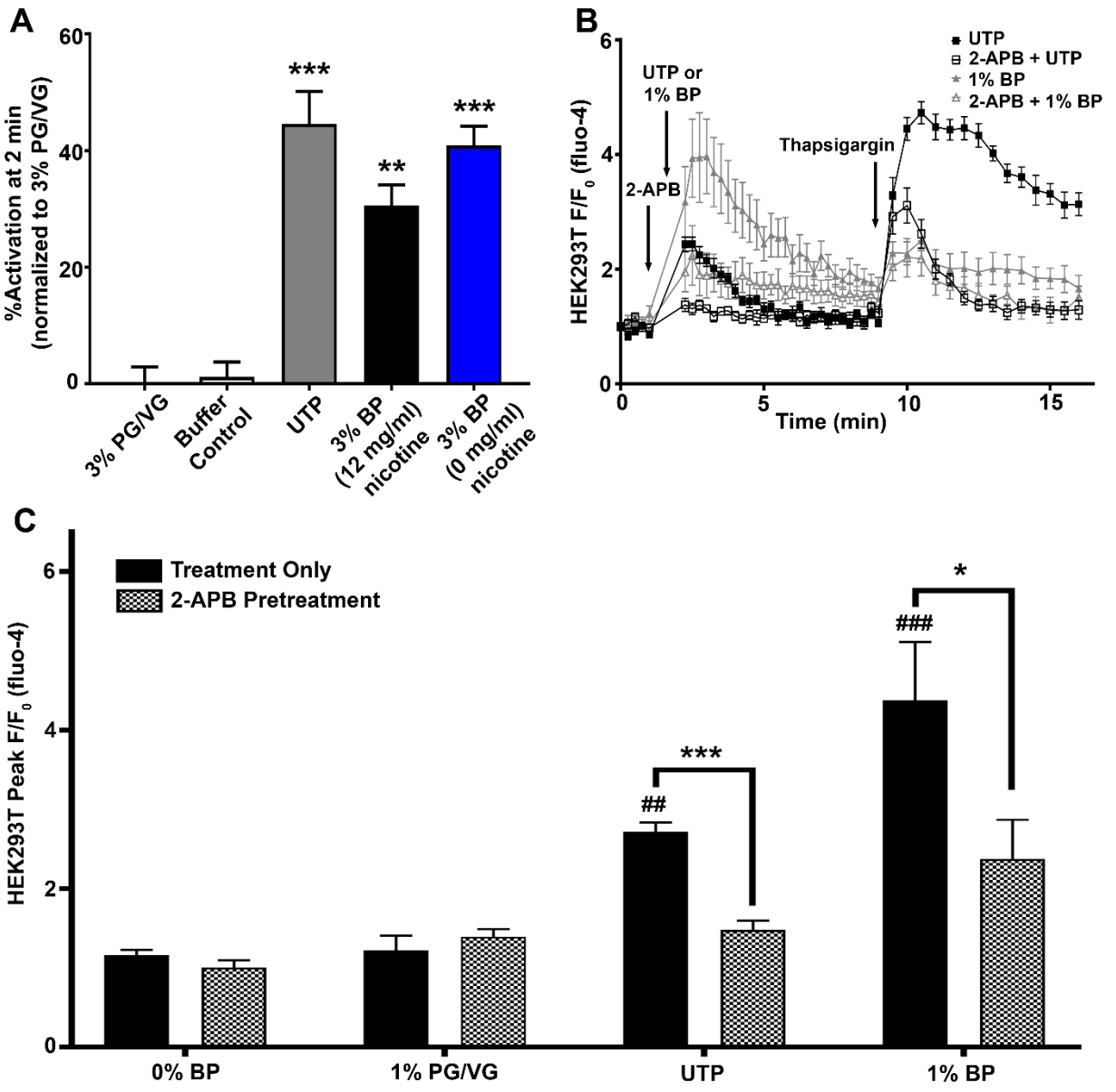

Figure 3.7. BP stimulates inositol phosphate accumulation and the BP response is sensitive to IP_3R antagonist 2-APB. *A*: HEK293T cells were seeded in 24 well plates and incubated with [^{3}H]inositol phosphate. Cells were exposed to 200 µM UTP or 0-3% BP or PG/VG for 2 min and total intracellular inositol phosphate was collected, measured, and plotted as percent activation normalized to 3% PG/VG. *B*-*C*: HEK293T cells were seeded in 12 well plates and loaded with a Ca^{2+} indicator (fluo-4). Cells were treated with 100 µM UTP or e-liquids ± 2-APB, which was added for 1 min prior to the treatment, followed by thapsigargin. Responses were measured as change in fluorescence (F/F_0) and peak changes were also plotted. Symbols and bars represent mean ± SEM. *A*: n = 9-12 replicates per treatment with doses compared to 3% PG/VG control (***P* < 0.01, ****P* < 0.001). *C*: n = 8-12 wells per treatment with doses compared to 0% BP only (##*P* < 0.01, ###*P* < 0.001). Additional differences shown between treatments and their respective 2-APB treatments (**P* < 0.05, ****P* < 0.001).

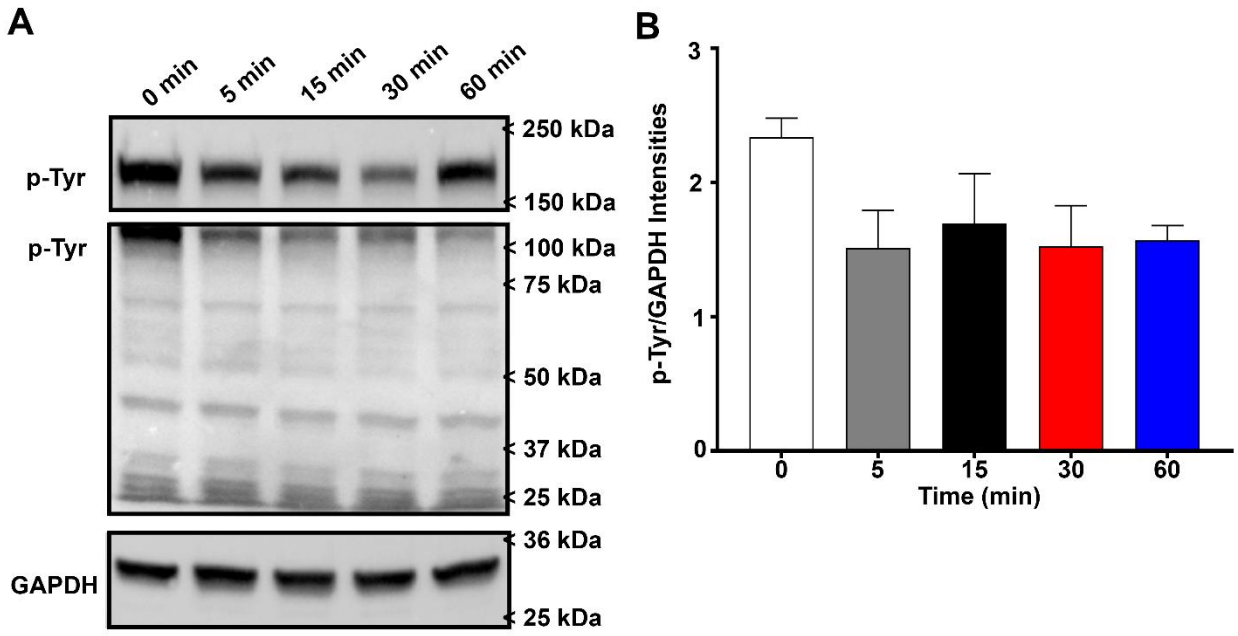

Figure 3.8. IP_3 formation-independent of receptor tyrosine kinase (RTK) activation. CALU3 cells were seeded into 60 mm culture dishes and treated with 3% BP diluted in media for 0-60 min. Protein lysates were collected and immunoblots were performed for phosphorylated tyrosine residues (p-Tyr) and GAPDH (loading control). *A:* Representative blots with indicated treatments were shown. p-Tyr blots were cut to avoid overexposure of more intense bands (≥ 100 kDa). *B*: Relative treatment intensities were measured as a ratio of p-Tyr lane intensities/GAPDH bands and were plotted. Bars represent mean + SEM. n = 3-4 blots per time point.

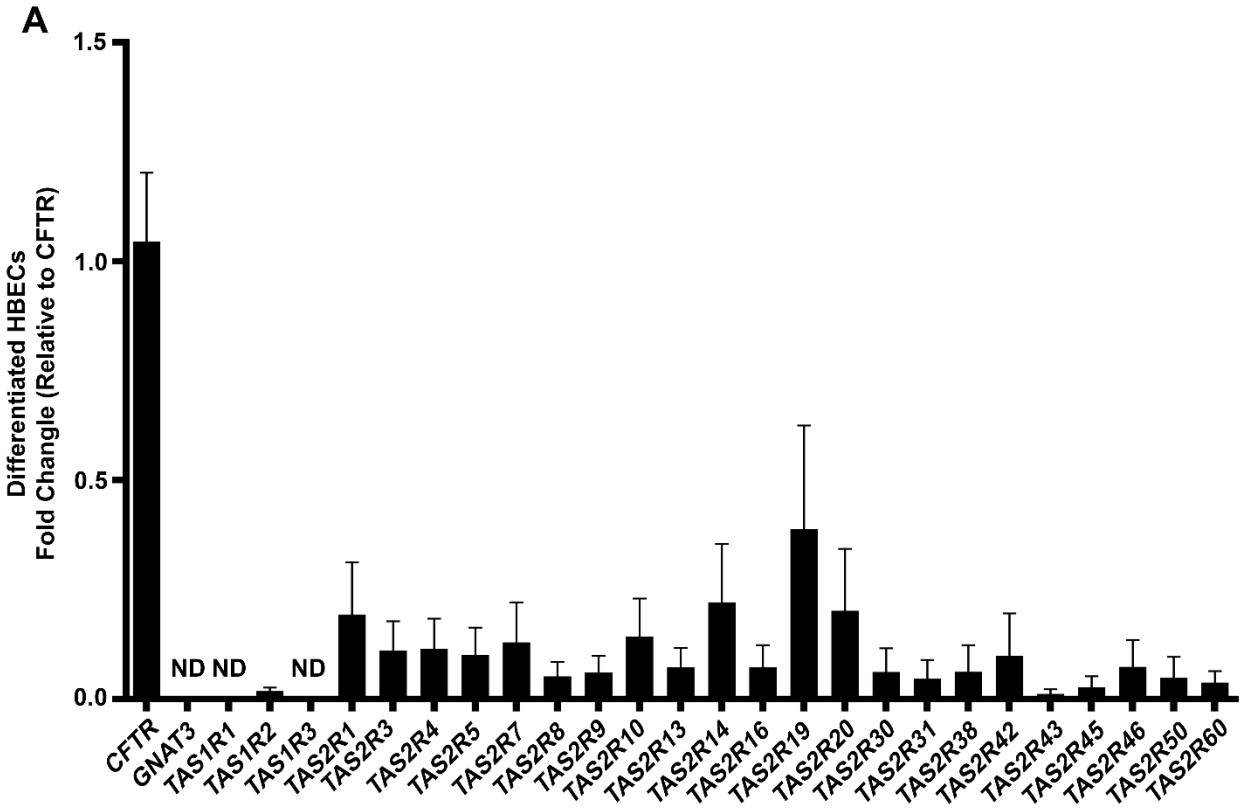

Figure 3.9. Endogenous taste receptor mRNA expression very low or not detected in primary HBECs. *A*: RNA was isolated from untreated primary HBECs and endogenous mRNA expression of gustducin (Gα) and sweet and bitter taste receptors (T1Rs/T2Rs) were measured relative to *CFTR* expression. Results are summarized in Table 3.2 along with endogenous whole lung, CALU3 cell, and HEK293T cell taste receptor expression. Bars represent mean + SEM. n = 5 wells per gene. ND = not detected.

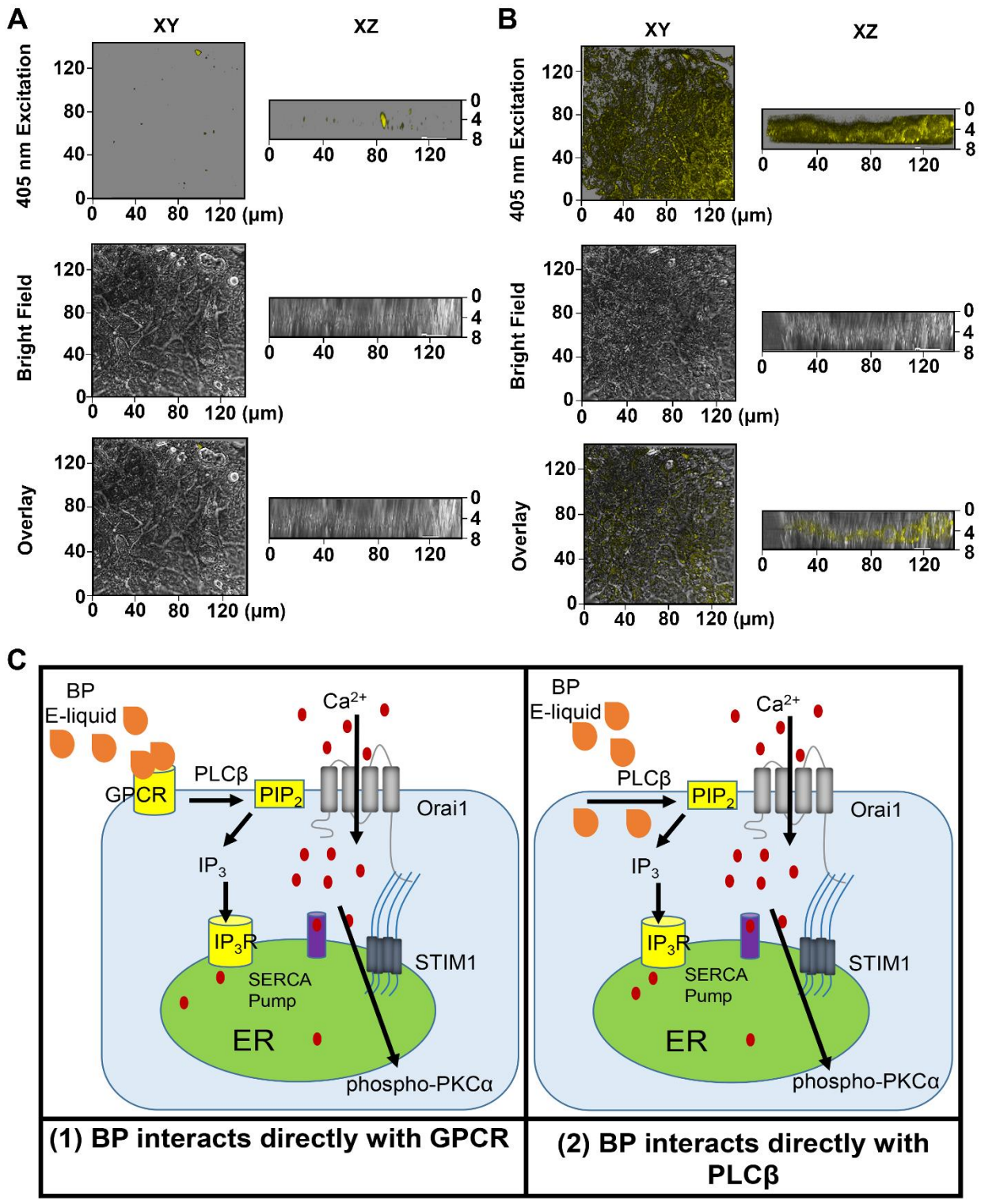

Figure 3.10. BP autofluorescence imaging shows e-liquid internalization in lung epithelia. CALU3 cells were plated onto glass coverslips and imaged pre- and post-3% BP, diluted in Ringer's solution. *A*: Representative fluorescence, bright field, and overlay images of CALU3 cells pre-BP exposure. *B*: Representative fluorescence, bright field, and overlay images 2 min post-BP exposure. n = 3 coverslips

per treatment. *C*: Diagrams predict likely targets of BP e-liquid upstream of IP_3 formation. (1) BP e-liquid components activate ligand binding with plasma membrane localized GPCR, stimulating PLCβ to cleave PIP_2, forming IP_3 which acts on ER IP_3Rs to empty ER Ca^{2+}, elicit SOCE, and increase PKCα phosphorylation. (2) BP e-liquid forms direct adduct to plasma membrane-bound PLCβ and triggers similar IP_3-dependent ER Ca^{2+}/SOCE response and PKCα phosphorylation independent of plasma membrane receptor activation.

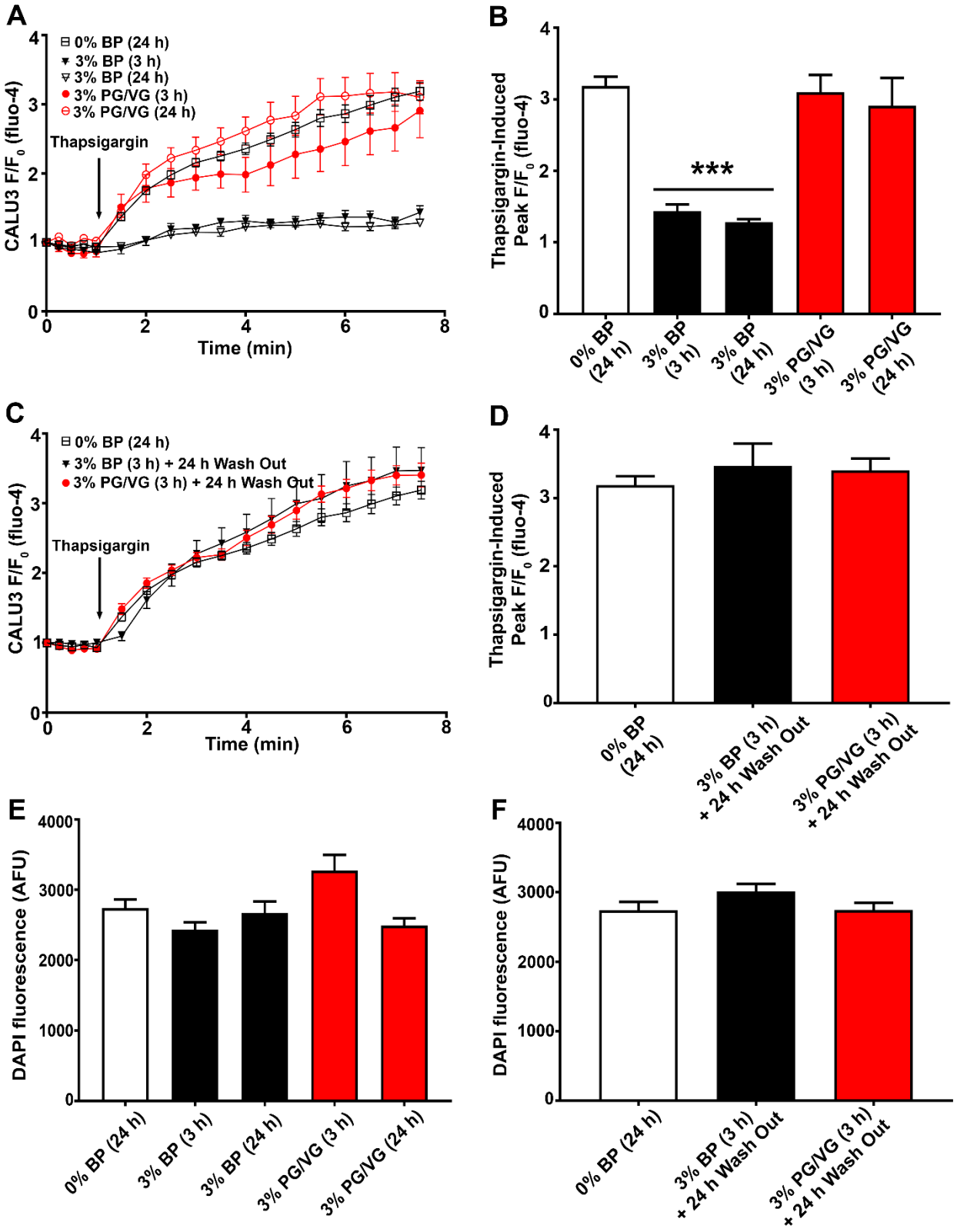

Figure 3.11. Pre-treatment with BP e-liquid attenuates thapsigargin-induced Ca^{2+} release. CALU3 cells were seeded into 96 well plates and then exposed to 0-3% BP or PG/VG for 3-24 h incubations ±

wash out with media, as labeled. Cells were loaded with a Ca^{2+} indicator (fluo-4) and media was replaced with Ringers solution before the cytosolic Ca^{2+} response to thapsigargin was measured. *A*,*C*: Results were reported as a change in fluorescence (F/F_0) over time. *B*,*D*: Peak responses to thapsigargin were measured per treatment. *E*-*F*: Following Ca^{2+} measurements, cells were fixed and stained with DAPI to measure relative total cell number fluorescence. *A*-*F*: Symbols and bars represent mean ± SEM. n = 13-33 wells per treatment. *A*-*F*: Statistical differences were shown between all treatments and their respective 0% BP control (***$P < 0.001$). Overall interactions were detected at ($P < 0.05$) in *E*-*F*, but no differences were found between groups compared to 0% BP.

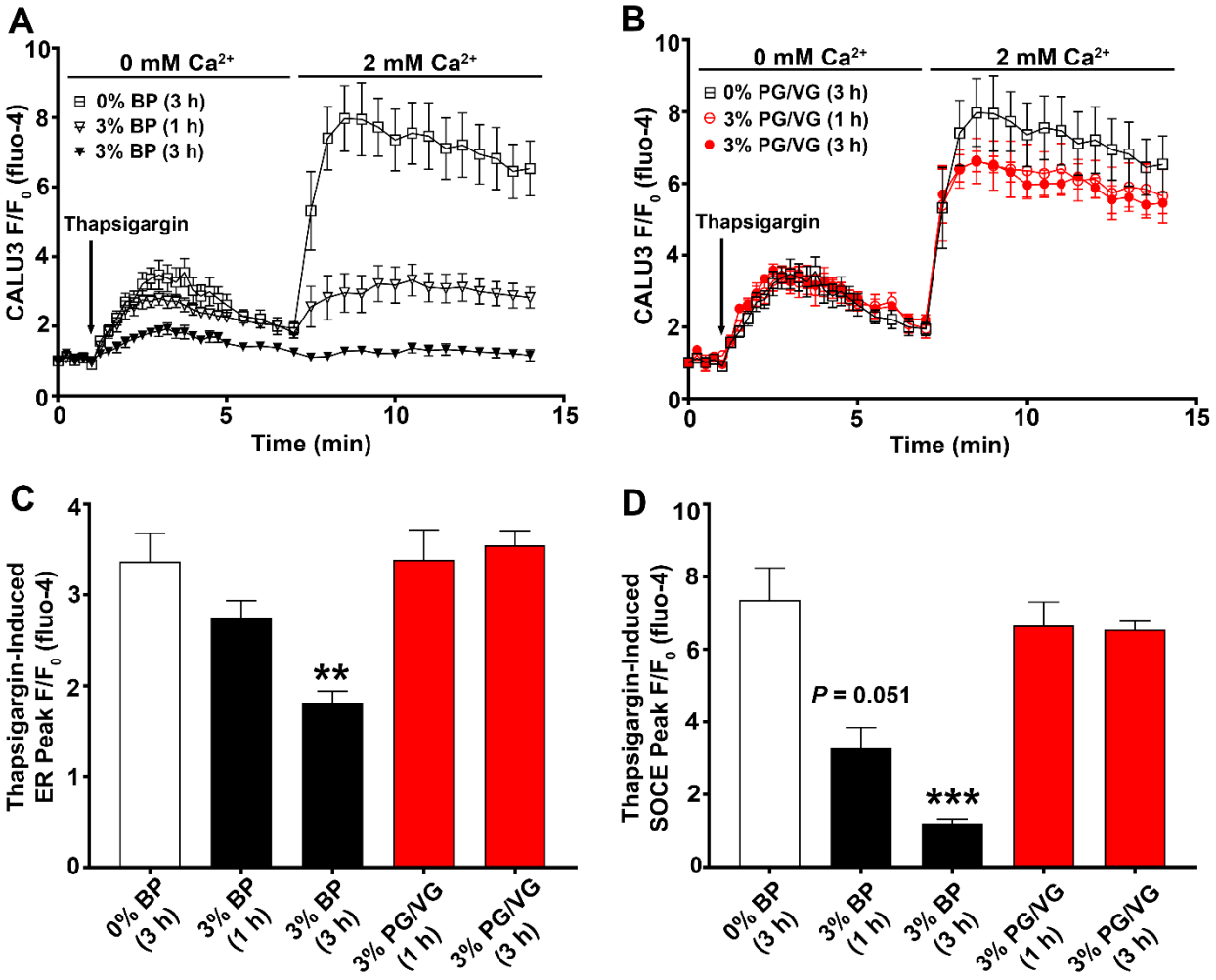

Figure 3.12. 3 h BP pre-treatment inhibits both ER and SOCE thapsigargin-induced Ca^{2+} release. CALU3 cells were seeded into 12 well plates and then exposed to 0-3% BP or PG/VG for 1 or 3 h incubations. Cells were loaded with a Ca^{2+} indicator (fluo-4) and media was replaced with Ringers solution before the cytosolic Ca^{2+} response to thapsigargin was measured ± extracellular Ca^{2+}. *A-B*: Results were reported as a change in fluorescence (F/F_0) over time. *C*: Peak F/F_0 ER (intracellular) thapsigargin responses were measured. *D*: Peak F/F_0 SOCE thapsigargin responses were measured. *A-D*: Symbols and bars represent mean ± SEM. n = 6-10 wells per treatment. *C-D*: Statistical differences were shown between all treatments and respective 0% BP controls (**$P < 0.01$; ***$P < 0.001$).

Chapter 4: Flavoring Chemicals Identified in E-liquids Elicit Dose-Dependent Cytosolic and Store Operated-Ca^{2+} Entry in Lung Epithelia

4.1. Overview

Commercially available flavored e-liquids often contain a mixture of individual flavoring chemicals at varying concentrations. The chemistry and biology of inhaling these complex mixtures through vaping is not well understood. Calcium (Ca^{2+}) is an important second messenger that regulates cell signaling, innate defenses, and proliferation in many cell types (e.g., pulmonary epithelia). We have previously shown that a Banana Pudding (BP)-flavored e-liquid induced phospholipase C (PLC)-mediated Ca^{2+} signaling. To better understand how widespread this effect might be, we screened 100 e-liquids and determined that 42 were able to acutely alter cytosolic Ca^{2+} levels. When we analyzed the Ca^{2+} responses with qualitative chemical constituent data, we found several flavoring chemicals correlated with a cytosolic Ca^{2+} response. We characterized six of the flavoring chemicals and found that four dose-dependently elevated cytosolic Ca^{2+} responses with the following potency: menthol > ethyl vanillin > vanillin > ethyl maltol. We then performed additional experiments with vanillin and ethyl vanillin. Ethyl vanillin acutely initiated store-operated Ca^{2+} entry, suggesting that it is not working through transient receptor potential channels. Treating cells with a combination of vanillin and ethyl vanillin, also elicited a cytosolic Ca^{2+} response. Lastly, long-term exposure of pulmonary epithelia to vanillin and ethyl vanillin inhibited cell viability/proliferation. Thus, flavoring chemicals commonly used in e-liquids should be tested further for long-term health effects from inhalation exposure due to vaping.

---

[4]Contributing authors: Temperance R Rowell, Bryan T Zorn, James E Keating, Gary L Glish, and Robert Tarran.

4.2. Introduction

Most flavoring chemicals are commonly used in food products and 'generally recognized as safe' (GRAS) for ingestion [http://www.accessdata.fda.gov/scripts/fdcc/?set_SCOGS]. The best case for testing these flavorants for inhalation toxicity is the development of bronchiolitis obliterans (i.e., 'Popcorn Lung') in workers exposed to diacetyl (butter flavor) inhalation in manufacturing plants (124). Though it is known that diacetyl inhalation can cause fibrotic lung disease, diacetyl and similar chemicals have still been detected in commercial e-liquids (5). Though the scientific e-cigarette (e-cig) field is attempting to fill gaps in knowledge, there is still much that remains to be understood regarding the role of vaping flavoring chemicals in long-term airway health.

Humans sense flavors primarily through olfactory cells located in the mouth and nose. While salty flavors are detected by the activation of ion channels (e.g., epithelial sodium channel), sweet, umami (glutamate), and bitter flavors typically stimulate taste receptors. Taste receptors are G protein-coupled receptors (GPCRs) recognized as T1Rs (sweet/umami type receptors) and T2Rs (bitter type receptors) (121). Ligand binding causes activation of PLCβ2 to generate inositol 1,4,5-triphosphate (IP_3) via gustducin, a G_α protein. IP_3 triggers a release of ER Ca^{2+} to continue the signal cascade, typically leading to store operated Ca^{2+} entry (SOCE) to prolong the Ca^{2+} signal and refill the ER Ca^{2+}supply (Fig. 4.1). Taste receptors are low affinity, meaning that most ligand binding affinities occur in the high μM to mM range, often mirroring flavoring concentrations found in foods (121). Beyond the tongue, taste receptor expression has been reported in the brain (201), pancreas (170), and the upper and lower airways (63, 134, 223, 253). Airway T2Rs have been shown to promote innate defenses in the respiratory tract, suggesting that they are a protective mechanism against inhaled noxious pollutants/toxicants which are generally perceived as bitter. For example, activating T2Rs in ciliated lung epithelia increased ciliary beat frequency, an important mechanism in mucociliary clearance (223). T2Rs in nasal epithelia have also demonstrated the ability to induce antimicrobial peptide secretion via Ca^{2+} signaling. However, activation of T1Rs in those same nasal epithelia suppressed T2R-dependent antimicrobial peptide secretion and increased susceptibility of infection (134).

Apart from taste receptors, many flavoring chemicals (e.g., menthol, cinnamaldehyde, vanillin) are known ligands of transient receptor potential (TRP) channels (190). TRP channels are generally permeable to Ca^{2+} ions, thereby increasing cytosolic [Ca^{2+}]. However, TRP channels are not associated with IP_3 formation or ER Ca^{2+} release (41), which was demonstrated with exposure to a BP-flavored e-liquid. It is important to understand how these e-liquids, and individual flavorings, may be triggering Ca^{2+} responses. Interestingly, some flavoring chemicals are reactive aldehydes which have the potential to react with macromolecules (i.e., protein, DNA) and form adducts. Protein and DNA adduct formation has been well-documented with exposure to reactive aldehydes in tobacco smoke (e.g., acrolein) and have biological consequences. For instance, acrolein has formed adducts with cysteine residues in neutrophil nicotinamide adenine dinucleotide phosphate oxidase components, impairing neutrophil respiratory burst activation (174). Similarly, cinnamaldehyde has inhibited other immune cell functions through adduct formation with protein kinases (120). Thus, individual flavorings that have the ability to trigger cytosolic Ca^{2+} responses should be investigated for their ability to form adducts with upstream pathway components to better understand their mechanism of action. We previously characterized the ability of a BP-flavored e-liquid to activate PLC-dependent ER Ca^{2+} release and SOCE. Given this novel physiological role of an e-liquid to alter cell Ca^{2+} homeostasis, we aimed to conduct a screen of 100 e-liquids to understand the scope of these commercially available products to elicit cytosolic Ca^{2+} responses in pulmonary epithelia. We then sought to analyze the Ca^{2+} responses with corresponding chemical constituent data to predict flavoring chemicals that may be contributing to the response and then characterize the flavorings' roles in Ca^{2+} signaling and inhalation toxicity.

4.3. Methods

Flavored e-liquids. E-liquids were purchased from The Vapor Girl (www.thevaporgirl.com) and NJOY (www.njoy.com/e-juice), as designated in Table 4.1. Nicotine concentrations for each flavored e-liquid can also be found in Table 4.1. A vehicle control of 55/45 propylene glycol (PG)/vegetable glycerin (VG) was prepared in our laboratory.

Chemicals and reagents. PG, VG, DMSO, probenecid, thapsigargin, triacetin, isoamyl acetate, vanillin, ethyl vanillin, ethyl maltol, and menthol were purchased from Sigma-Aldrich. Fluo-4 (AM), lipofectamine 2000, and the Vybrant MTT Cell Proliferation Assay Kit were purchased from ThermoFisher. Paraformaldehyde (PFA) was purchased from Affymetrix. Thapsigargin and fluo-4 (AM) were reconstituted using DMSO and applied to cells in experiments where the final DMSO concentration was $\leq 0.1\%$. STIM1 tagged with mCherry on the C-terminus was kindly provided by Dr. Ricardo Dolmetsch (181).

Cell culture and transfections. CALU3 cells were cultured in Minimum Essential Media (MEM) alpha with 10% FBS and penicillin/streptomycin (Gibco) with 5% CO_2 at 37°C. CALU3 cells were seeded into 12 or 96 well plastic dishes (Corning) for fluo-4 experiments. HEK293T cells were cultured in D-MEM (high glucose) with 10% FBS and penicillin/streptomycin (Gibco) with 5% CO_2 at 37°C. HEK293T cells were plated onto glass coverslips for STIM1 puncta imaging experiments.

Ca^{2+} signaling. Changes in cytosolic [Ca^{2+}] were measured using fluo-4 dye. CALU3 cells were loaded with 8 μM fluo-4 in the presence of 1 mM probenecid for 40 min at 37°C prior to experiments. Cultures were then rinsed with PBS and replaced with a standard Ringer's solution as described (211). Fluorescence intensities were measured every 15 or 30 sec using a Tecan Infinite Pro plate reader (ex: 490 ± 10 nm, em: 516 ± 5 nm) at room temperature. Changes in fluo-4 fluorescence were normalized to the baseline (F/F_0) after subtracting background light levels. Traces were plotted to show F/F_0 over time and the peak change in F/F_0 was measured for each dose. Thapsigargin was added to cultures for a final concentration of 2 μM. Individual chemical flavorings were prepared in either 100% ethanol or PG/VG, diluted in Ringer's solution, and exposed to cells at the final concentration (mM). Nonlinear regression curves were fit to each flavoring's dose response in the fluo-4 assays using GraphPad Prism to calculate EC_{50} values, where appropriate.

Heatmap of peak cytosolic Ca^{2+} screen. Peak cytosolic Ca^{2+} responses of 100 flavored e-liquids were measured and compared to the 0% e-liquid control. Statistically significant responses ($P < 0.05$) were $\log_2$-transformed and a heatmap was generated using Morpheus software (Broad Institute).

E-liquid chemical constituent analysis from cytosolic Ca^{2+} screen. A random forest classification model using the statistical software R version 3.4.1 was used to predict whether significant cytosolic Ca^{2+} responses in cell cultures could be determined using qualitative gas chromatography-mass spectrometry (GC-MS) chemical constituent presence/absence data, as well as the sum of all chemicals within each e-liquid as input features (138, 249). The model (n = 100) used a randomly sampled training set (70%) in which the remaining data were used as a test set using 10001 decision trees. The mtry parameter was determined by using the lowest out-of-bag error rate resulting from tuneRF with stepFactor = 0.85, ntreeTry = 10001, improve = 0.005. The random forest models were repeated using 10 seeds (1, 2, 3…10).

STIM1 puncta quantification. HEK293T cells were plated onto glass coverslips and transfected with STIM1-mCh using lipofectamine 2000 per manufacturer's protocol as described (198). Cells expressing STIM1-mCherry were treated with 0-30 mM ethyl vanillin or 2 µM thapsigargin for 5-10 min. Cells were fixed with 4% PFA for 10 min at room temperature following treatment, and rinsed with PBS before imaging. All puncta imaging was conducted on a Leica SP8 confocal microscope with a 63 x 1.4 NA oil immersion objective. Multiple images were taken per coverslip from different parts of the coverslip and ≥ 12 transfected cells were visually analyzed for the percentage of puncta positive cells per coverslip.

Cell proliferation. The MTT assays were performed with CALU3 cells as instructed by the manufacturer following a 24 h exposure with 0-30 mM vanillin or ethyl vanillin. Cells were allowed to proliferate for 4 h after removal of the treatments. Data were calculated as percent absorbance of each treatment compared with the average of their respective 0 mM control treatments in each plate. Nonlinear regression curves were fit to each flavoring's dose response in the MTT assays using GraphPad Prism to calculate IC_{50} values, where appropriate.

Quantitative GC-MS. Flavor concentrations were determined by standard addition (216). E-liquids were diluted in methanol and quantitative standards. Selected ion monitoring mass spectra were

acquired for each of the quantified flavors. Peak areas of quantitative ions were integrated for quantification of each of the flavors.

Statistical analyses. All statistics were run using Prism Graphpad (San Diego) software. Data were analyzed using the Kruskal-Wallis test with Dunn's multiple comparisons test or the Mann-Whitney test where appropriate. *P*-values ≤ 0.05 were found to be significant and reported ($*P \leq 0.05$, $**P \leq 0.01$, $***P \leq 0.001$).

4.4. Results

Numerous commercially available e-liquids elicit cytosolic Ca^{2+} responses and analysis of chemical constituents reveals vanillin, ethyl vanillin, and ethyl maltol may contribute. Since we discovered the novel action of a BP-flavored e-liquid on cytosolic Ca^{2+} signaling in lung epithelia from one brand of e-liquid, we decided to screen a number of flavored e-liquids from local and national vendors. We found that 42 of 100 flavored e-liquids screened elicited a cytosolic Ca^{2+} signal compared to the 0% e-liquid control ($P < 0.05$) (Fig. 4.2*A*). We previously analyzed over 200 e-liquids by GC-MS, which are accessible in an online database (www.eliquidinfo.org) (216). To better understand why a number of e-liquids might be able to elicit a cytosolic Ca^{2+} response, these data were used to compare e-liquids for chemical composition relative to their cytosolic Ca^{2+} response.

The average accuracy of correctly classified e-liquids using random forest models was 75%, suggesting that qualitative constituent data may be able to predict cytosolic Ca^{2+} signaling (Fig. 4.2*B*). The total number of chemicals in each e-liquid was consistently found to be the most important variable in classification. However, the presence of ethyl vanillin (CAS: 121-32-4), vanillin (CAS: 121-33-5), and ethyl maltol (CAS: 4940-11-8) were also considered to be major variables in classification (Fig. 4.2*B*). It is worth noting that GC-MS analysis of BP revealed the presence of all three of these chemicals (www.eliquidinfo.org).

Several common flavoring chemicals previously identified in Ca^{2+}-eliciting e-liquids cause dose-dependent cytosolic Ca^{2+} responses. We chose to follow up with six chemicals identified as major variables associated with the Ca^{2+} response and common to commercial e-liquids (112). We loaded

CALU3 cells with fluo-4 (cytosolic Ca^{2+} indicator) and then exposed cells to triacetin, isoamyl acetate (banana), vanillin, ethyl vanillin, ethyl maltol (caramel), or menthol and measured cytosolic Ca^{2+} responses. We found that four of six chemicals were able to dose-dependently elicit a response in CALU3 cells above respective 0 mM and vehicle controls (Fig. 4.3*A*-*C*). We calculated EC_{50}s for those four chemicals, whose potency are summarized here: menthol > ethyl vanillin > vanillin > ethyl maltol (Table 4.2). Menthol was not found in the BP-flavored e-liquid however, it was found in our top two screening hits (e.g., Arctic Tobacco, Menthol). These common flavoring chemicals have the potential to dose-dependently alter important Ca^{2+} signaling responses in the lung with e-cig use.

Ethyl vanillin recruits STIM1 puncta formation (SOCE). Cytosolic Ca^{2+} influx is governed by plasma membrane receptors, pumps, and channels. Generally, Ca^{2+} can either flow through membrane ion channels (e.g., TRP channels) or it can trigger a coordinated Ca^{2+} release from the ER, followed by an influx of Ca^{2+} through a membrane pore known as SOCE. SOCE involves the aggregation of stromal interaction molecule 1 (STIM1), an ER transmembrane protein, into discrete puncta at the ER-plasma membrane junction. STIM1 aggregation activates Orai1, a plasma membrane Ca^{2+} channel which is required for the subsequent Ca^{2+} influx (141, 189). We transfected HEK293T cells with STIM1-mCherry and looked for the puncta formation of these proteins following exposure. Transfected cells were treated with 0-30 mM ethyl vanillin or 2 μM thapsigargin for 5-10 min and were imaged by confocal microscopy (Fig. 4.4*A*). Cells treated with ≥ 10 mM ethyl vanillin increased STIM1 puncta formation to a similar degree as thapsigargin (Fig. 4.4*B*). Ethyl vanillin dose-dependently caused downstream activation of STIM1, suggesting that the cytosolic Ca^{2+} response is likely ER/SOCE-dependent.

Vanillin and ethyl vanillin reduce cell viability/proliferation following 24 h exposure. Ca^{2+} signaling orchestrates many important cellular functions including cell viability/proliferation, and SOCE is important for these functions. Since ethyl vanillin elicited an ER/SOCE-dependent Ca^{2+} response in lung epithelia, we used the MTT assay to indirectly assess cell viability and proliferative ability following chronic exposure to vanillin or ethyl vanillin. 24 h exposure to either vanillin or ethyl vanillin dose-dependently decreased CALU3 cell viability/proliferation (Fig. 4.5*A*). An IC_{50} of 11.37 mM was

calculated for ethyl vanillin, but an IC_{50} for vanillin could not be determined in this dosing range (Table 4.2). While vanillin and ethyl vanillin elicited ER/SOCE-dependent Ca^{2+} responses in CALU3 cells with acute exposures, longer exposures decreased cell viability/proliferation.

Ca^{2+}-eliciting e-liquids contain millimolar levels of vanillin and ethyl vanillin. GC-MS was used previously to identify the presence/absence of chemical constituents in over 200 flavored e-liquids (www.eliquidinfo.org). In this study, vanillin and ethyl vanillin were quantified using GC-MS and standard curves for each constituent. Both vanillin and ethyl vanillin were quantified in two lots (designated #09 and #165) of BP-flavored e-liquids, which were both characterized to elicit an ER/SOCE-dependent Ca^{2+} responses in CALU3 cells. Vanillin was also quantified in Chocolate Banana, another Ca^{2+}-eliciting flavor. Vanillin was present at 22.58 ± 2.22 and 18.56 ± 4.47 mM, while ethyl vanillin was present at 15.19 ± 1.81 and 11.22 ± 3.74 mM in respective lots of BP (Fig. 4.6). Vanillin was also present at 125.80 ± 1.80 mM in Chocolate Banana-flavored e-liquid. These data show that some Ca^{2+}-eliciting e-liquids contain millimolar levels of vanillin and ethyl vanillin. Moreover, vanillin concentrations ranged from 18.56 ± 4.47 to 125.80 ± 1.80 mM between two different Ca^{2+}-eliciting e-liquids, suggesting that concentrations of each flavoring can vary greatly between e-liquids and toxicity information should cover a wide range of concentrations.

Combining vanillin and ethyl vanillin produce increases in cytosolic Ca^{2+} responses, suggesting additive effects. Since vanillin and ethyl vanillin were both present in millimolar concentrations and independently able to induce Ca^{2+} signaling, we tested the potential for additive effects of vanillin and ethyl vanillin in CALU3 cells. We loaded cells with fluo-4 and acutely exposed them to increasing doses with equal parts of vanillin and ethyl vanillin as indicated (Fig. 4.7*A*-*B*). We found that exposing cells to solutions containing 5 mM vanillin + 5 mM ethyl vanillin elicited a Ca^{2+} response. Since 5 mM of either vanillin or ethyl vanillin alone was below the EC_{50} for Ca^{2+} signaling, these data suggest that additive effects of individual flavoring chemicals could play a role in lung epithelial Ca^{2+} responses.

4.5. Discussion

To understand the breadth of commercially available e-liquids and their ability to induce Ca^{2+} signaling, we screened 100 flavored e-liquids and found 42 of 100 increased cytosolic Ca^{2+} (Fig. 4.1*A*; Table 4.1). Some e-cig studies have already identified chemical constituents in e-liquids and/or tested select flavoring chemicals on many different parameters in airway cell types (47, 85, 211, 216, 226, 252). However, our study is one of the first to try to systematically identify and predict flavoring chemicals affecting cytosolic Ca^{2+} responses from a large dataset. Figure 4.2*B* highlights the top 27 chemicals that are correlated with cytosolic Ca^{2+} responses in lung epithelia. It is worth noting that our model only correctly classified 75% of the dataset, which may not generally be considered robust. However, there are other factors that may contribute to this value. For instance, the GC-MS dataset incorporated into our model is strictly qualitative. These data only provide presence or absence of a detected chemical in the model, not dose. The model would likely be improved in the future with quantitative chemical datasets as well. For example, Sassano et al. found that the concentrations of a single constituent present in seven different flavored-e-liquids varied greatly (216).

Interestingly, the model identified the number of chemicals detected in an e-liquid to be the top predictive variable correlated to Ca^{2+} responses (Fig. 4.2*B*), indicating that the more chemicals detected in a flavor, the more likely it was to elicit a cytosolic Ca^{2+} signal. Reinikovaite et al., reported that e-cig cytotoxicity in their study was correlated with both the number and concentration of chemicals used in e-liquids (200). It is possible that more complex e-liquid mixtures (i.e., number of chemical constituents) can impact their effects on cells (e.g., Ca^{2+} responses), but would need to be tested. The top three chemicals associated with a cytosolic Ca^{2+} responses from our analysis were ethyl vanillin, vanillin, and ethyl maltol (Fig. 4.2*B*). All three chemicals have been commonly found in e-liquids and have the potential to affect cell function (15, 85, 112, 211, 216, 226, 252). Therefore, we characterized the dose-dependent Ca^{2+} responses of six chemicals from our list.

We found that four of six chemicals dose-dependently elicited a cytosolic Ca^{2+} signal above their 0 mM and vehicle control (menthol > ethyl vanillin > vanillin > ethyl maltol) (Fig. 4.3). Ethyl maltol has

not previously been shown to alter Ca^{2+} homeostasis and more work needs to be done to fully understand the impact of these findings. However, many common flavoring chemicals have been reported to activate TRP channels. For example, menthol is a known TRPM8 agonist with an EC_{50} of 80 μM (160). Menthol also appeared in the top two flavored e-liquid hits (e.g., Arctic Tobacco, Menthol) from our Ca^{2+} screen. Vanillin and ethyl vanillin have been shown to activate TRPV1, TRPV3, and TRPA1 (143, 268, 269). Xu et al., reported that both vanillin and ethyl vanillin activated TRPV3-mediated Ca^{2+} signaling with 10 mM (269), which was similar to our EC_{50} concentrations (Fig. 4.3*C*; Table 4.2). However, we also showed that ethyl vanillin was capable of forming STIM1 puncta, suggesting that it activates SOCE, which is not associated with TRP channels (Fig. 4.4). Ethyl vanillin was also found to cause IP_3 formation in odorant cilia, though a receptor or channel target was not reported (33). We previously showed that acute exposure to BP e-liquid also generates IP_3 formation and ER/SOCE-dependent responses in lung epithelia, suggesting that it is not acting through TRP channels despite containing both vanillin and ethyl vanillin. More work is needed to characterize the Ca^{2+} signaling pathway that these vanillin species are working through to elucidate whether these chemicals may contribute to or be responsible for our BP e-liquid Ca^{2+} mechanism.

Ca^{2+} is a ubiquitous second messenger signaling system that cells use to regulate important processes (e.g., cell growth and proliferation, apoptosis) (26). Indeed, vanillin, ethyl vanillin, and ethyl maltol are commonly detected in e-liquids and have been investigated for toxicity and other properties relevant to airway health (15, 85, 211, 216, 226). We treated CALU3 cells with vanillin or ethyl vanillin for 24 h and measured cell viability/proliferation using the MTT assay and demonstrated dose-dependent decreases in cell viability/proliferation with both chemicals (Fig. 4.5). This is in accordance with Sassano et al. where a positive correlation was demonstrated between vanillin, but not triacetin concentrations, and toxicity in commercial e-liquids (216). They also reported a positive correlation between cinnamaldehyde concentrations and toxicity, though we did not include cinnamaldehyde in this study.

Interestingly, vanillin has been studied as an anti-cancer compound and demonstrated to reduce the proliferation and metastasis of some cancer cell lines (105, 142, 171). Specifically, micromolar

concentrations of vanillin were shown to bind directly to calcium/calmodulin-dependent protein kinase IV (CAMKIV) in hepatic carcinoma and neuroblastoma cells, inducing apoptosis (171). CAMKIV is involved in the regulation of apoptosis and cell cycle via Ca^{2+} signaling, and overexpression has been found in lung and hepatocellular carcinomas (113, 266). Though we have not looked at the role of CAMKIV and vanillin, we have demonstrated that prolonged exposure to vanillin and the vanillin-containing BP e-liquid reduce cell viability/proliferation in CALU3 cells (Fig. 4.5) (211). Since vanillin is a reactive aldehyde, it has the potential to react with nucleophilic protein residues (e.g., cysteine) to form protein adducts similar to cinnamaldehdye or acrolein (120, 174). In the case of CAMKIV, vanillin is covalently bound to lysine and aspartic acid residues (171). It is unclear whether vanillin and ethyl vanillin are individually inhibiting cell proliferation in CALU3 cells through CAMKIV binding. Both chemicals are also found in BP e-liquid, which altered Ca^{2+} homeostasis acutely (i.e., PLC-dependent IP_3 formation) and chronically (i.e., attenuated ER Ca^{2+}/SOCE thapsigargin response, reduced cell viability/proliferation). It is unclear if/how vanillin and ethyl vanillin may be involved in these outcomes, but future experiments should investigate the ability of these flavorings to interact with important proteins involved in PLC- and ER/SOCE-dependent Ca^{2+} signaling.

Current e-cig literature has also characterized roles for vanillin, maltol, and ethyl maltol in other airway cell functions. For instance, Sherwood and Boitano tested vanillin (%vol/vol) and found that their dose range did not induce cytotoxicity on 16HBE14o- lung epithelia, while ethyl maltol did (226). Meanwhile, Gerloff et al. found that ortho-vanillin and maltol induced proinflammatory IL-8 secretion in Beas2B and HFL-1, but not H292 cells (85). These data suggest that the individual flavorings may have the capacity to alter airway cells, dependent upon the cell type and dose. Our results could be used to inform FDA regulations regarding the presence and concentrations of individual flavoring chemicals allowed in commercially available e-liquids. Specifically, our data predicted flavorings from a large data set that may contribute to Ca^{2+} signaling and further characterized dose-dependent effects of six chemicals on Ca^{2+} homeostasis in lung epithelia. Specifically, vanillin and ethyl vanillin were identified in a PLC-dependent Ca^{2+}-eliciting BP e-liquid but also highly correlated with toxicity (216). This study

also reported their dose-dependent outcomes in cytosolic Ca^{2+} signaling, SOCE activation, and cell viability/proliferation in lung epithelia. We also demonstrated that there may be additive effects of flavoring concentration on cytosolic Ca^{2+} signaling (Fig. 4.6-7). More studies are required to investigate the role of the presence of these chemicals, their concentrations, and possible additive effects in cell Ca^{2+} signaling and the effects of their aerosolized products on lung health.

Table 4.1. List of flavored e-liquids used in 3% cytosolic Ca^{2+} screen in Fig. 4.2. List of 100 e-liquids used in the fluo-4 screen with their respective flavor, mean peak Ca^{2+} responses, SEM, *P*-value, vendor source, and advertised nicotine concentration.

E-liquid Flavor	Mean Peak Ca^{2+} Response	SEM	*P*-value	Vendor	Nicotine (mg/ml)
0% E-liquid (control)	1.080	0.06	N/A	N/A	0
3% PG/VG (vehicle)	1.372	0.07	> 0.9999	Sigma	0
Arctic Tobacco	10.832	0.52	< 0.0001	The Vapor Girl	12
Menthol	8.703	0.46	< 0.0001	NJOY	10
Hot Cinnamon Candies	6.780	0.69	< 0.0001	The Vapor Girl	12
Peach Tea	6.124	0.87	< 0.0001	NJOY	10
Cool Mint	3.927	0.36	< 0.0001	The Vapor Girl	12
Banana Pudding	3.216	0.37	< 0.0001	The Vapor Girl	12
Banana Pudding	3.193	0.22	< 0.0001	The Vapor Girl	0
Valkyrie	3.002	0.46	< 0.0001	The Vapor Girl	12
Black Coffee	2.710	0.29	< 0.0001	The Vapor Girl	12
Biscotti	2.605	0.25	< 0.0001	The Vapor Girl	12
Caramel Corn Crunch	2.525	0.14	< 0.0001	The Vapor Girl	12
Chocolate Tobacco Heaven	2.350	0.18	< 0.0001	The Vapor Girl	12
Candy Corn	2.282	0.12	< 0.0001	The Vapor Girl	12
Key Lime Pie	2.182	0.11	< 0.0001	The Vapor Girl	12
Caramel Apple	2.172	0.08	< 0.0001	The Vapor Girl	12
Captain Suckle	1.994	0.08	0.0003	The Vapor Girl	12
Cheesecake with Graham Cracker	2.086	0.10	0.0004	The Vapor Girl	12
Cinnamon Roll	2.098	0.15	0.0006	The Vapor Girl	12
Strawberry Mango Smoothie	2.180	0.20	0.0007	The Vapor Girl	12
Missed Her Cookie	2.132	0.15	0.0007	The Vapor Girl	12
Chocolate Pecan Fudge	2.118	0.15	0.0007	The Vapor Girl	12
Apple Pie	2.082	0.12	0.0007	The Vapor Girl	12
Candy Cane	1.994	0.03	0.0007	The Vapor Girl	12
Circus Guava	2.128	0.21	0.0008	The Vapor Girl	12
Chocolate Banana	2.074	0.13	0.0009	The Vapor Girl	12
Angel Lust	1.989	0.09	0.0009	The Vapor Girl	12
Tiramisu	1.996	0.10	0.0015	The Vapor Girl	12
Dulce de Leche	1.971	0.11	0.0019	The Vapor Girl	12
Kola	3.226	0.82	0.0027	The Vapor Girl	12
RY4 Doubler	1.960	0.16	0.0048	The Vapor Girl	12
Pumpkin Pie	2.270	0.28	0.0056	The Vapor Girl	12
Chocolate Dipt Raspberry	1.891	0.11	0.0089	The Vapor Girl	12
Double Espresso	1.891	0.17	0.0096	NJOY	10

E-liquid Flavor	**Mean Peak Ca^{2+} Response**	**SEM**	***P*-value**	**Vendor**	**Nicotine (mg/ml)**
Honey Vanilla Tobacco	1.854	0.10	0.0155	The Vapor Girl	12
DB's Dessert	1.818	0.08	0.0180	The Vapor Girl	12
Chocolate Moo	1.949	0.19	0.0184	The Vapor Girl	12
Bavarian Crème Donut	1.801	0.11	0.0336	The Vapor Girl	12
Sweet Potato Pie	1.784	0.08	0.0339	The Vapor Girl	12
Lemon Meringue Pie	1.853	0.15	0.0350	The Vapor Girl	12
Sugar Cookie	1.787	0.10	0.0398	The Vapor Girl	12
Butterscotch	1.784	0.11	0.0461	The Vapor Girl	12
Black Cherry	1.765	0.08	0.0461	The Vapor Girl	12
Marshmallow	1.729	0.07	0.0781	The Vapor Girl	12
Crispy Melon	1.742	0.09	0.0785	The Vapor Girl	12
Strawberry Pop O'Tarts	1.701	0.08	0.1204	The Vapor Girl	12
Vanilla Custard	1.696	0.05	0.1251	The Vapor Girl	12
Chocolate Fudge	1.675	0.07	0.1322	The Vapor Girl	12
Buttery Nipple	1.718	0.12	0.1420	The Vapor Girl	12
Menthol Tobacco	1.911	0.32	0.1727	The Vapor Girl	12
Chai Latte	1.669	0.12	0.2911	The Vapor Girl	12
Bubble Gum	1.691	0.15	0.3984	The Vapor Girl	12
Arctic Raspberry	1.652	0.12	0.4539	The Vapor Girl	12
Blueberry Cinnamon Streusel Muffin	1.647	0.13	0.4544	The Vapor Girl	12
Slug Juice	1.610	0.09	0.5847	The Vapor Girl	12
Pillow Fight	1.596	0.07	0.6791	The Vapor Girl	12
Peach Piano	1.597	0.04	0.6970	The Vapor Girl	12
Root Beer	1.560	0.07	0.9216	The Vapor Girl	12
Cuba Libre	1.564	0.09	> 0.9999	The Vapor Girl	12
Black Dragon	1.563	0.09	> 0.9999	The Vapor Girl	12
Black Thorn	1.562	0.09	> 0.9999	The Vapor Girl	12
Orphan Tears	1.562	0.08	> 0.9999	The Vapor Girl	12
Coconut Rum	1.552	0.08	> 0.9999	The Vapor Girl	12
Banana	1.527	0.05	> 0.9999	The Vapor Girl	12
Chai	1.525	0.10	> 0.9999	The Vapor Girl	12
Coconut Water	1.501	0.08	> 0.9999	The Vapor Girl	12
Desert Cow	1.500	0.18	> 0.9999	The Vapor Girl	12
Cherry Kola	1.499	0.06	> 0.9999	The Vapor Girl	12
RY4 Classic	1.498	0.07	> 0.9999	The Vapor Girl	12
Cat Nip	1.477	0.09	> 0.9999	The Vapor Girl	12
Clove Cigar	1.470	0.13	> 0.9999	The Vapor Girl	12
Bubbly Berry	1.470	0.07	> 0.9999	The Vapor Girl	12
Butter Crunch	1.455	0.10	> 0.9999	NJOY	10
Alchemy	1.444	0.08	> 0.9999	The Vapor Girl	12
Cotton Berry	1.429	0.06	> 0.9999	The Vapor Girl	12

E-liquid Flavor	**Mean Peak Ca^{2+} Response**	**SEM**	***P*-value**	**Vendor**	**Nicotine (mg/ml)**
French Vanilla Hazelnut Espresso	1.418	0.10	> 0.9999	The Vapor Girl	12
Mt. DUDE	1.412	0.04	> 0.9999	The Vapor Girl	12
Black and Blue Berries	1.408	0.09	> 0.9999	NJOY	10
Kiwi Blast	1.402	0.12	> 0.9999	The Vapor Girl	12
Icy Blast	1.397	0.06	> 0.9999	The Vapor Girl	12
Strawberries and Champagne	1.389	0.08	> 0.9999	The Vapor Girl	12
Single Malt Scotch	1.313	0.06	> 0.9999	NJOY	10
Blue Pom	1.279	0.06	> 0.9999	The Vapor Girl	12
Watermelon	1.268	0.06	> 0.9999	The Vapor Girl	12
Pomegranate	1.266	0.11	> 0.9999	NJOY	10
Pixie Dust	1.256	0.08	> 0.9999	The Vapor Girl	12
Blue Moo	1.249	0.03	> 0.9999	The Vapor Girl	12
Blood Orange	1.247	0.04	> 0.9999	NJOY	10
Vanilla Bean	1.238	0.08	> 0.9999	NJOY	10
Arctic Strawberry	1.237	0.04	> 0.9999	The Vapor Girl	12
Bartlett Pear	1.207	0.03	> 0.9999	The Vapor Girl	12
Grape Soda	1.201	0.09	> 0.9999	The Vapor Girl	12
Raspberry	1.195	0.05	> 0.9999	The Vapor Girl	12
Classic Tobacco	1.192	0.05	> 0.9999	NJOY	10
Grape!	1.190	0.03	> 0.9999	The Vapor Girl	12
Bahama Mama	1.174	0.04	> 0.9999	The Vapor Girl	12
Sour Fruit Punch	1.149	0.05	> 0.9999	The Vapor Girl	12
Black Peppercorn	1.134	0.05	> 0.9999	The Vapor Girl	12
Captain Zach Cigar	1.098	0.06	> 0.9999	The Vapor Girl	0
Cranberry Crunch	1.074	0.04	> 0.9999	The Vapor Girl	12
Cranberry Delight	1.058	0.03	> 0.9999	The Vapor Girl	12

Table 4.2. List of EC_{50} and IC_{50} values for flavoring chemicals dose response curves in Figures 4.3*C* and 4.5. Nonlinear regression curves were fit to the mean peak cytosolic Ca^{2+} response (Fig. 4.3*C*) or mean percent absorbance results (Fig. 4.5). ND represents 'not determined' where curves could not be fit in the range of doses tested. The EC_{50} and IC_{50} values were reported where appropriate (mM).

Treatment	**EC_{50} (mM)**
Triacetin	ND
Isoamyl Acetate	ND
Vanillin	15.88
Ethyl Vanillin	9.52
Ethyl Maltol	21.14
Menthol	3.02
Treatment	**IC_{50} (mM)**
Vanillin	ND
Ethyl Vanillin	11.37

A

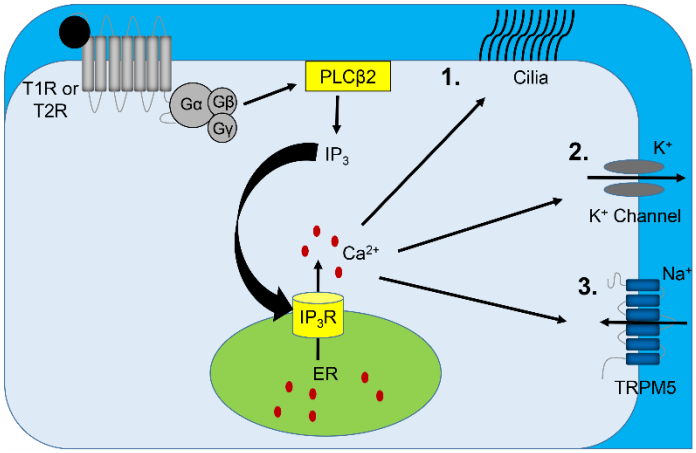

Sweet (T1R) and Bitter (T2R) Taste Receptor Cell Signal Transduction

Figure 4.1. Similar signal transduction pathway of sweet and bitter taste receptors with different downstream effects in (1) airway epithelia, (2) airway smooth muscle, (3) airway solitary chemosensory, and gustatory cell types. Sweet (T1R) and bitter (T2R) taste receptors are GPCRs that activate PLCβ2 to generate IP_3 and induce ER Ca^{2+} release. (1) In airway epithelial cells, increases in cytosolic Ca^{2+} stimulate downstream activation of cilia beat frequency. (2) In airway smooth muscle cells, K^+ channel activation is triggered downstream of cytosolic Ca^{2+} signaling that results in smooth muscle relaxation. (3) In solitary chemosensory airway cells and gustatory cells of the tongue, direct activation of TRPM5 by Ca^{2+} is necessary to confer sweet and bitter taste reception.

Figure 4.2. Multiple flavored e-liquids elevate cytosolic Ca^{2+} levels. 100 different flavored e-liquids were screened for their ability to elicit a cytosolic Ca^{2+} signal. CALU3 cells were seeded into 96 well plates and loaded with fluo-4. Cells were challenged with 3% flavored e-liquids and peak Ca^{2+} responses were compared. Peak Ca^{2+} responses were reported in Table 4.1. *A*: All significant responses (42) were

log_2-transformed and plotted on a heat map. *B*: Heatmap showing the top 28 factors/chemicals' mean decrease in Gini index average across 10 random forest classifiers (n = 100). Ordering of chemicals are hierarchically clustered. *A*: n = 7-12 wells per treatment. Doses were compared to the 0% e-liquid control.

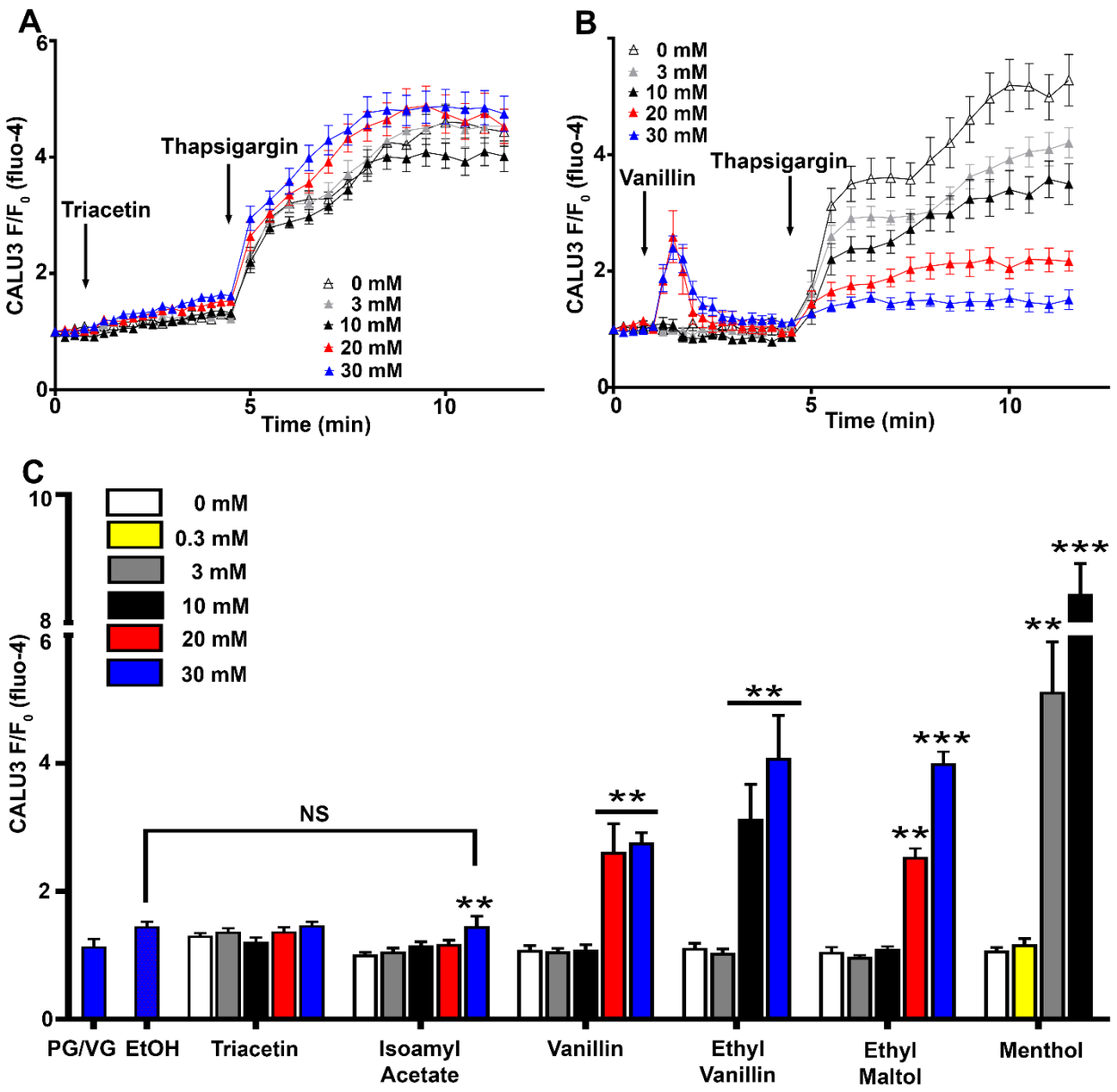

Figure 4.3. Common chemical constituents found in Ca^{2+}-eliciting e-liquids dose-dependently elevate cytosolic Ca^{2+}. Cells were challenged acutely with triacetin, isoamyl acetate (banana), vanillin, ethyl vanillin, ethyl maltol (caramel), or menthol. Vehicle controls for PG/VG and ethanol (EtOH) were also measured. *A-B*: Representative traces of a non-Ca^{2+}-eliciting and Ca^{2+}-eliciting flavoring chemicals reported as the change in fluorescence (F/F_0). *C*: Peak changes in dose-dependent response from all flavoring chemicals and vehicles tested. *A-C*: Symbols and bars represent mean ± SEM. *A-C*: n = 7-15 wells per treatment. Statistical differences were shown between all treatments compared to their respective 0 mM control (**$P < 0.01$, ***$P < 0.001$). NS represents not significant between dose and respective vehicle control.

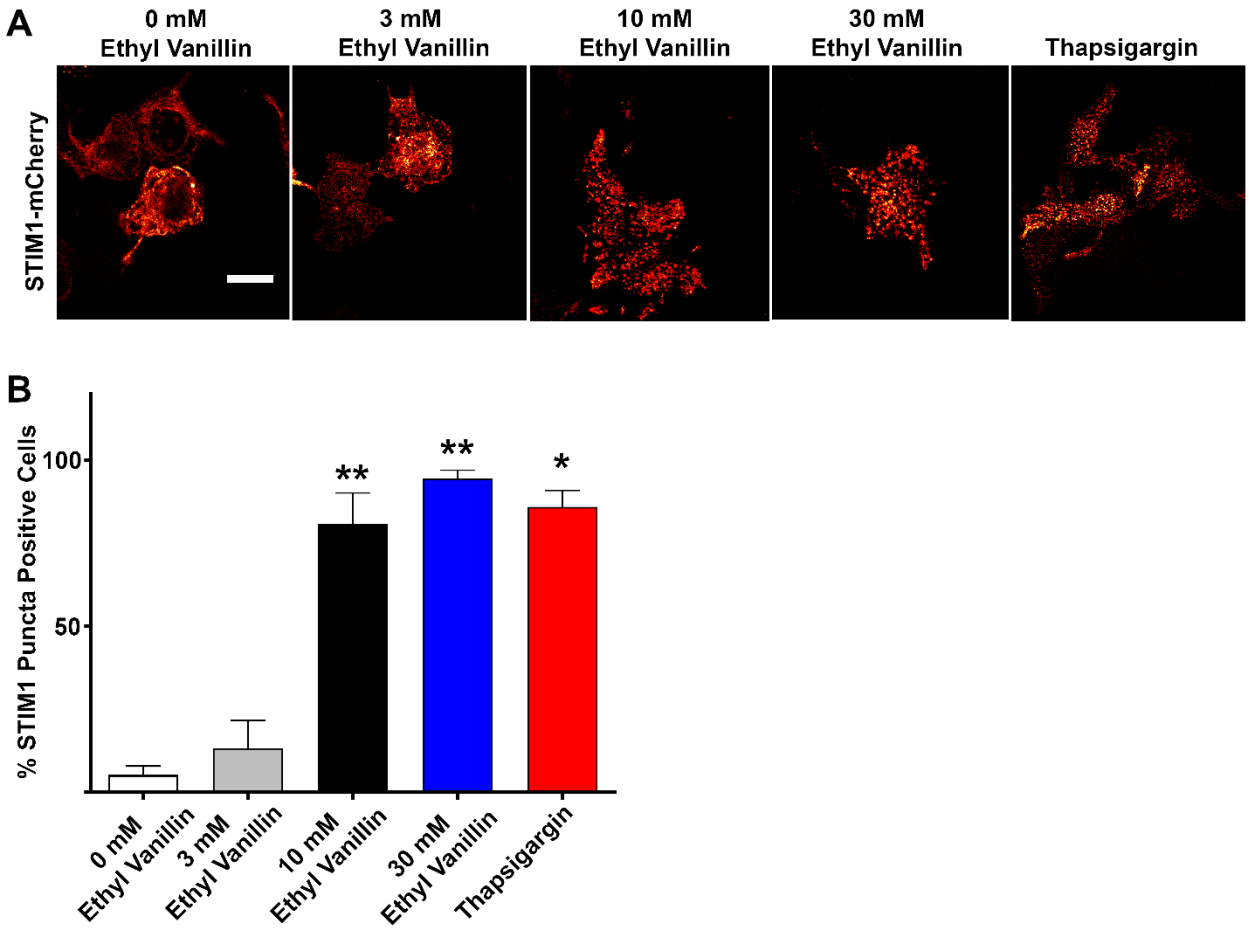

Figure 4.4. Ethyl vanillin stimulates STIM1 puncta formation, activating SOCE. HEK293T cells were plated on glass coverslips and transfected with STIM1-mCherry. Transfected cells were treated with 0-30 mM ethyl vanillin or thapsigargin for 5-10 min. *A*: Cells were fixed and imaged. Scale bar represents 25 μm. *B*: The percentage of puncta-positive cells were measured. Bars represent mean + SEM. n = 4-9 coverslips per treatment. Statistical differences were calculated between all groups compared to the 0 mM control (*$P < 0.05$, **$P < 0.01$).

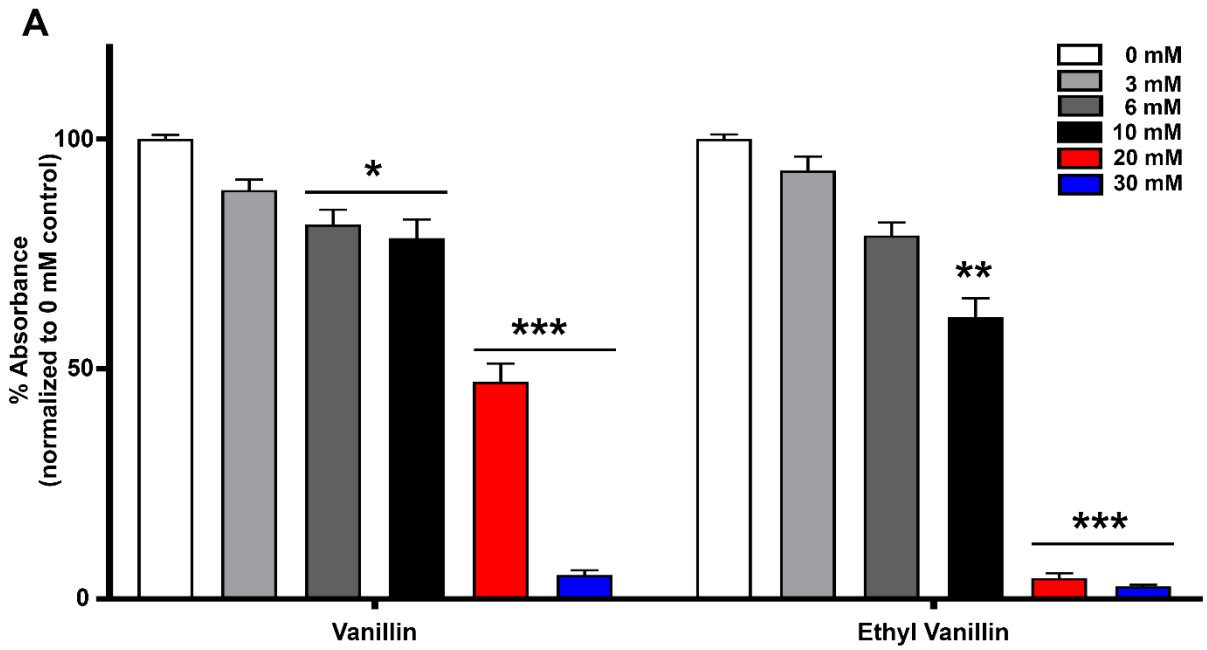

Figure 4.5. 24 h exposure to vanillin and ethyl vanillin dose-dependently decreases cell viability/proliferation. CALU3 cells were seeded into 96 well plates and then exposed to 0-30 mM vanillin or ethyl vanillin for 24 h. Media was changed and cells were treated with MTT and allowed to proliferate for 4 h. *A*: MTT absorbance was measured at the end of the 24 h treatment and plotted as percent absorbance compared to each treatment's 0 mM control. Bars represent mean + SEM. n = 11-19 wells per treatment. Statistical differences were calculated between all doses and their respective 0 mM control (*$P < 0.05$, **$P < 0.01$, ***$P < 0.001$).

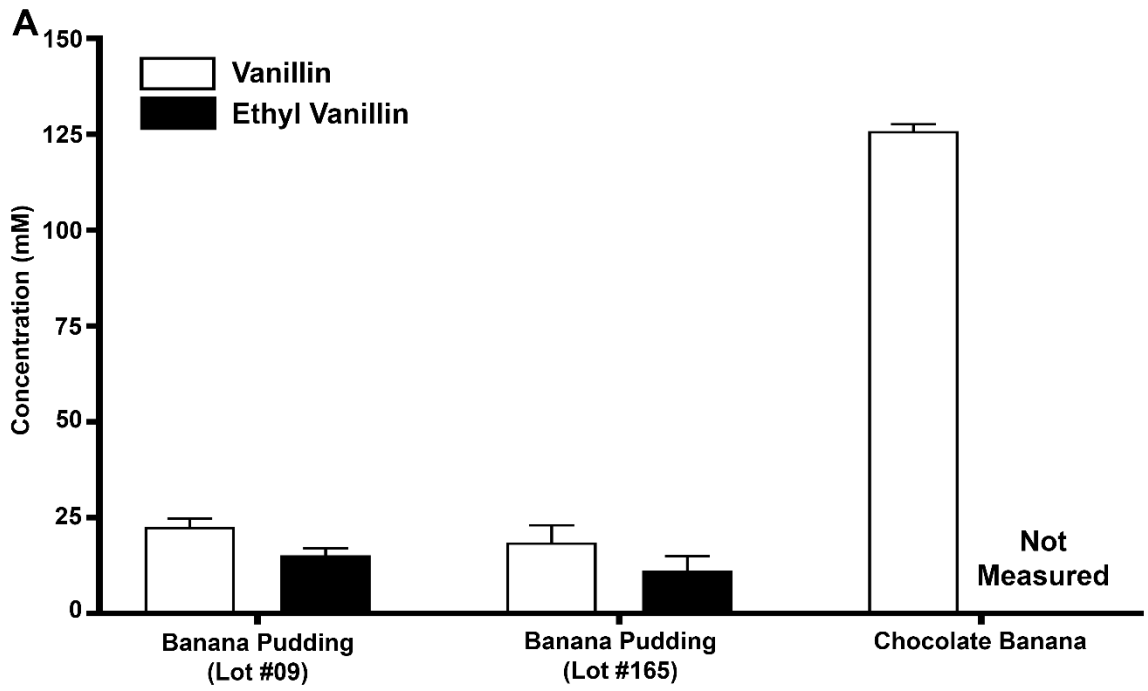

Figure 4.6. Vanillin and ethyl vanillin quantified in Ca^{2+}-eliciting banana-flavored e-liquids. *A*: The presence of vanillin and ethyl vanillin were quantified in two different lots of Banana Pudding e-liquid purchased and used in previous Ca^{2+} signaling experiments. Vanillin was also quantified in Chocolate Banana, another Ca^{2+}-eliciting flavored e-liquid. Quantifications were performed using GC-MS with vanillin or ethyl vanillin standard curves to measure respective amounts of each chemical per e-liquid.

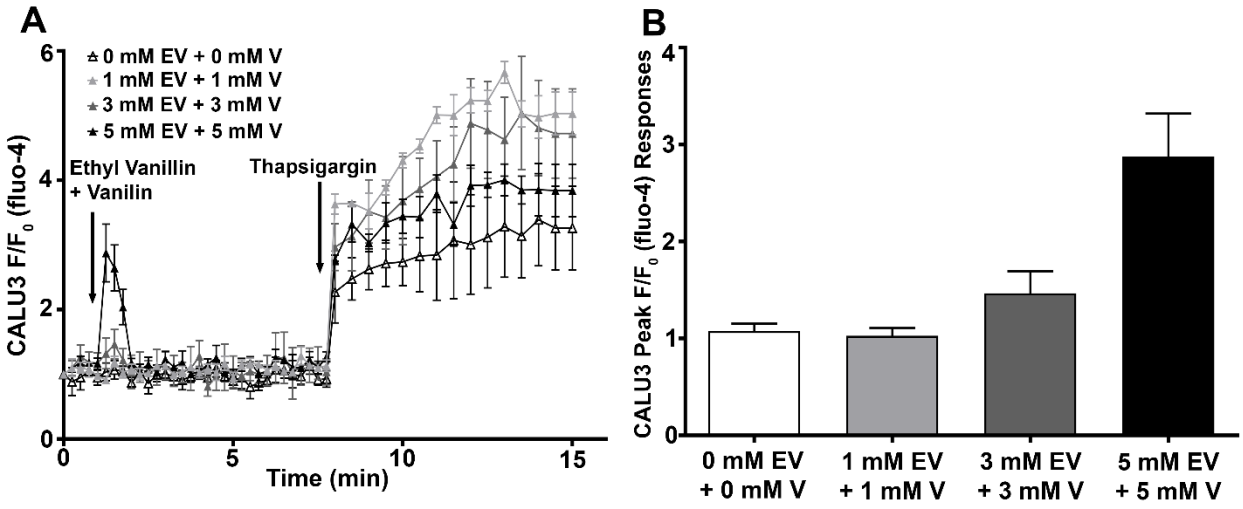

Figure 4.7. Additive effects of ethyl vanillin (EV) and vanillin (V) elicit cytosolic Ca^{2+} signal in CALU3 cells. Cells were plated into 96 well plates and loaded with fluo-4 before acute exposure to combinations of EV and V. *A*: Changes in fluorescence were measured over time with varying concentrations of EV and V. *B*: Peak changes in fluorescence were reported. Symbols and bars represent mean ± SEM. n = 3 wells per treatment.

Chapter 5: Conclusions and Future Directions

5.1. Overview

The overall goal of this dissertation was to better understand the biological effects of commercially available flavored e-cigarette (e-cig) products on pulmonary epithelial cells. Since these products have only been available for the past 10 years as a 'safer' smoking alternative, there was very little known about their toxicological profiles or subsequent physiological effects when we began this research. Instead of focusing our work on the rapidly changing design of e-cig devices, we specifically chose to tackle the issue of e-liquids and their chemical constituents (i.e., nicotine, PG/VG, flavors). Nicotine has been well studied and its presence in e-liquids presented the potential for nicotine addiction, which drives tobacco cravings, and physiological changes that nicotine can exert change on the body, especially in the brain during adolescent development (24, 59). Both PG and VG are 'generally recognized as safe' (GRAS) for ingestion. However, one study reported that short term controlled occupational exposures to aerosolized PG caused ocular and upper airway irritation in nonasthmatic adults (265). Before the advent of e-cigs, most flavoring chemicals were used primarily in foods and were GRAS. However, inhalation safety with regard to flavoring chemicals in e-cigs were questioned when diacetyl was detected in commercially available e-liquids (5). Diacetyl (butter flavor) has caused the fibrotic lung disease bronchiolitis obliterans ('Popcorn Lung') in some manufacturing workers after inhalation exposure (124). Therefore, we focused on characterizing the dose- and time-dependent toxicological and physiological effects of nicotine, PG/VG, flavored e-liquids, and individual flavoring chemicals on pulmonary epithelial cells to inform human health and e-cig regulations.

5.2. Flavor-Dependent E-liquid Toxicity

To establish whether a lung epithelial cell line showed variable toxicity responses to nicotine, PG/VG, or different flavored e-liquids, we first developed a set of screening assays to compare these responses. We found that of the 13 different e-liquid flavors that we tested, 4 of the 13 had more toxic responses compared to the other flavors or the PG/VG control. These exposures were performed with unheated e-liquids diluted in culture media and cells were treated for 24 h, which are not directly translatable to e-cig users' vaping exposure. However, this approach allowed us to precisely control dose and exposure time. These data demonstrate that (1) PG/VG can potentially be toxic to lung epithelia and (2) there are flavor-dependent effects of commercially available e-liquids on lung epithelial toxicity. At the time, there were few studies that investigated flavor-dependent toxicity categories for e-liquids in a variety of cell types (15, 21, 226). Our group has since expanded e-liquid toxicity screening and found that from an additional 148 flavored e-liquids, cytotoxicity results ranged between flavors and could be classified as having 'normal growth', 'reduced growth', 'no growth' or 'toxic' effects on a variety of airway cells (216).

In Chapter 2, we additionally found that trends in toxicity were recapitulated when we exposed cells to heated e-liquid aerosol. These findings were also confirmed by Sassano et al. (216). The work from Chapter 2 also explored nicotine-dependent effects and found that nicotine could exert physiological responses on a lung epithelial cell line, but appeared to be non-specific in the e-liquid dilution concentrations exposed to cells. Lastly, our data showed that of the four most toxic flavors which we identified, two appeared to be cytotoxic (i.e., apoptotic, necrotic) while two others likely inhibited cell proliferation. While the mechanisms of action are unclear, additional identification of their chemical constituents and comparison between these toxic flavors showed that they shared only nicotine and PG/VG, suggesting that the heterogeneous e-liquid mixtures likely possessed a number of flavoring chemicals that contributed to their measured toxicity, instead of just one or two.

5.3. Flavor-Dependent E-liquid Ca^{2+} Signaling

We followed up the observation that one of the more toxic flavored e-liquids (e.g., Banana Pudding or BP) inhibited cell proliferation by characterizing its acute and chronic effects on cell Ca^{2+} signaling, since Ca^{2+} can play a role in cell proliferation. We found that BP acutely activated phospholipase C (PLC)-dependent generation of inositol 1,4,5-triphosphate (IP_3) with downstream activation of ER/SOCE-dependent Ca^{2+} responses, which has not been previously reported. This is the first study to characterize the role of flavored e-liquids in IP_3 formation and cell Ca^{2+} dynamics. Activation of this signaling pathway is common in numerous cell functions and usually occurs downstream of G protein-coupled receptors (GPCRs) or receptor tyrosine kinases (RTKs) (64, 161, 173, 233). We demonstrated that these signaling events were independent of RTK activation, but have not yet isolated a specific upstream target (i.e., GPCR, PLC). While we do not understand the long-term health outcomes of vaping Ca^{2+}-eliciting flavors, we have demonstrated that longer exposures to BP caused the ER Ca^{2+} release and store-operated Ca^{2+} entry (SOCE) responses to diminish. These data suggest that pulmonary epithelial functions requiring these signaling components could be altered with chronic exposure (i.e., regulation of exocytosis, enzyme activity, transcription, cell cycle, apoptosis). It is therefore imperative Ca^{2+}-eliciting e-liquids be further tested for effects of the vaped products on pulmonary morphology and function.

5.4. Role of Individual Flavoring Chemicals in Ca^{2+} Signaling and Toxicity

We performed a cytosolic Ca^{2+} screen on 100 commercially available flavored e-liquids and demonstrated that 42 elicited significant cytosolic Ca^{2+} responses in lung epithelia. We followed this up with an analysis of chemicals present in each e-liquid that identified the mere presence of certain flavoring chemicals highly correlated with a cytosolic Ca^{2+} signal. We chose six chemicals to further characterize and demonstrated that four were capable of eliciting dose-dependent cytosolic Ca^{2+} responses in lung epithelia. We further investigated vanillin and ethyl vanillin because they were found in BP e-liquid and were top hits from our Ca^{2+} screen analysis. Sassano et al. also reported that 63 of 148 screened e-liquids contained vanillin and there was a positive correlation between vanillin concentration

and toxicity (216). Sherwood and Boitano previously published effects of vanillin on airway epithelial viability as well (226). While vanillin and ethyl vanillin are known transient receptor potential vanilloid (TRPV) channel ligands (143, 269), we showed that ethyl vanillin activated SOCE, similar to BP e-liquid and not TRPV activation. Longer exposures of vanillin and ethyl vanillin also dose-dependently reduced cell viability/proliferation similar to BP. Vanillin previously has been reported as a natural cancer therapeutic that has some ability to inhibit cell proliferation (105, 142, 171). In addition to the anti-proliferative effects seen with vanillin, we found that ethyl maltol also induced cytosolic Ca^{2+} signaling but we did not find reports of this caramel flavor associated with Ca^{2+} signaling in the literature. Since vanillin, ethyl vanillin, and ethyl maltol are such common flavorings and GRAS for ingestion, more research is necessary to understand the biological consequences of their dose-dependent exposures on airway cells as well as their potential additive roles in complex flavored e-liquid mixtures.

5.5. Future Directions

This dissertation sought to enhance our knowledge regarding flavor-dependent effects of commercially available e-liquids on pulmonary epithelia in an effort to inform the public of potential changes in lung physiology associated with chronic vaping. Given that there were over 7,000 unique flavored e-liquids in the United States of America (276), we chose to broadly screen a number of flavored e-liquids for dose-dependent cytotoxicity. We also characterized the flavor-dependent effects of e-liquids and their constituents to alter cell Ca^{2+} signaling following an observation from our toxicity screen. We further coupled toxicity and Ca^{2+} screening outcomes with qualitative chemical constituent data to pinpoint common flavoring chemicals that could be contributing to our findings. The overall goal of the studies were to use cell assays to identify the most biologically relevant components of e-liquids (i.e., nicotine, PG/VG, flavorings) to closely examine in follow up experiments with chronic e-cig exposure (i.e., primary lung cell models, mouse models). In this way, we could better understand what cellular markers of exposure to measure and characterize dose- and time-dependent effects of these constituents on the lungs to target for regulation or validate for new biomarkers of e-cig exposure.

Upstream initiator of PLC-mediated IP_3/Ca^{2+} response to BP e-liquid and the potential role of Ca^{2+}-eliciting flavoring chemicals. We detailed the effects of flavored e-liquids and their chemical constituents on Ca^{2+} homeostasis (Chapters 3-4). While we characterized some of these effects in great detail, there are still many aspects that we have yet to understand. For example, while we identified the novel ability of BP e-liquid to generate IP_3 and ER-SOCE-dependent Ca^{2+} signaling, we have yet to identify (1) the upstream target of activation and (2) the roles of vanillin, ethyl vanillin, and ethyl maltol in this mechanism. Understanding the upstream mechanism of action that allows flavored e-liquids and their constituents to alter a PLC-mediated signaling pathway is important to understanding how they will affect Ca^{2+} homeostasis and the oscillatory nature of Ca^{2+} regulation. These are physiologically important processes that protect cells from toxic levels of cytosolic Ca^{2+} and deliver different cellular signals to various locations at optimal times (242). In pulmonary epithelia, Ca^{2+} is also necessary to regulate innate defenses that are part of mucociliary clearance (e.g., mucin secretion, ciliary beat frequency, ion regulation of airway surface liquid height) (97, 129, 139, 153).

We currently posit that upstream targets of IP_3 formation might be ligand-binding to GPCRs or direct PLC activation via protein-adduct formation. We had previously submitted BP and PG/VG stocks for primary screening of GPCR activation using competitive radioligand binding assays (28). These results are summarized in Table 5.1 where > 50% indicates potential receptor binding. Only 1 of 27 screened receptors reported > 50% inhibition (i.e., histamine receptor 2 or H2). H2 receptor is a G_s-coupled receptor that stimulates cyclic adenosine monophosphate (cAMP) production and protein kinase A (PKA) activation, not IP_3 formation (271). Since the %inhibition was higher in PG/VG than BP, these data suggest that the potential binding of this GPCR is likely mediated by the vehicle (PG/VG) and is not specific to flavorings found in BP (Table 5.1). In this dissertation, we did not investigate the ability of flavored e-liquids to regulate cAMP production, which is another important cell 2^{nd} messenger. Future studies should include characterizing cAMP production by e-liquids, and especially by PG/VG. Of note, the experimental doses for the GPCR screen did not achieve the 3% threshold for experiment-specific reasons, suggesting that if the dosing were increased in a subsequent e-liquid screen, there could possibly

be more hits. BP along with vanillin, ethyl vanillin, and ethyl maltol should tested for GPCR activation to rule in or out a single, shared GPCR target present in all of the cell types that we tested for IP_3 formation and Ca^{2+} signaling.

Vanillin and ethyl vanillin are small reactive aldehydes with the potential for binding to proteins and forming adducts, altering protein activity. For instance, vanillin has been shown to bind to calcium/calmodulin-dependent protein kinase type IV (CAMKIV) and inhibit cell proliferation in tumor cells (171), while cinnamaldehyde has been shown to inhibit immune cell function following thiolation of cysteine residues in certain kinases (120). Since we demonstrated that vanillin and ethyl vanillin were present in BP e-liquid and were also able to activate Ca^{2+} signaling, we intend to explore whether BP, vanillin, and/or ethyl vanillin have the ability to form adducts with PLC, causing receptor-independent PLC activation.

Inhibition of ER/SOCE-dependent Ca^{2+} responses following prolonged exposure to BP e-liquid and the potential role of flavoring chemicals. While the upstream mechanism (i.e., GPCR and/or direct PLC activation) is important to understand e-liquid/flavor-induced changes in Ca^{2+} homeostasis, our finding that prolonged BP exposure caused inhibition of the thapsigargin-induced Ca^{2+} responses was also novel. Inhibiting this response may be an indicator of potential harm since these Ca^{2+} responses play a role in many important cellular functions (e.g., cell proliferation, gene/protein expression, innate defense) (97, 139, 153). Specifically, SOCE activation has been identified to alter growth factor and local inflammatory responses via transcription factors in airway epithelia (215). We also found from our screen in Chapter 2 that a Kola-flavored e-liquid had a similar effect on thapsigargin-induced Ca^{2+} responses following prolonged exposure (Fig. 5.1*A*). Thus, it is likely that these effects are not restricted to one or two unique e-liquids and we should conduct a larger, more comprehensive screen along with similar chemical constituent analyses to predict the potential contributions of flavoring chemicals.

Interestingly, our GPCR screen included the sigma (σ) 1 receptor, which is an ER chaperone that has been shown to inhibit SOCE responses in cells by attenuating stromal interaction molecule 1 (STIM1) coupling to Orai1 (236). The σ1 receptor results were not > 50% inhibition (BP ~31%; ~15% PG/VG)

however, it was one of the only receptors that showed any preference for BP over PG/VG at the dose tested (< 3%). Generally, σ1 receptors are endogenously expressed throughout the body and when activated, can move within the ER membrane to interact with plasma membrane signaling proteins (e.g., ion channels) (239). Therefore, it would be pertinent to look into a potential role for ER σ1 receptors in ER/SOCE-dependent regulation in Ca^{2+} signaling, especially with the attenuated Ca^{2+} response to thapsigargin. Future experiments are necessary to ascertain whether 3% BP exposure can specifically bind to and activate the σ1 receptor.

Role of altered kinase phosphorylation in response to Ca^{2+}-eliciting e-liquids. Lastly, we showed that BP-induced Ca^{2+} signaling can differentially regulate kinase phosphorylation in lung epithelia. For example, we showed that BP caused transient increases in Ca^{2+}-dependent protein kinase C (PKC) phosphorylation but did not increase total protein tyrosine phosphorylation. Protein kinases are important cellular regulators of complex processes (e.g., cell cycle) and are grouped into distinct families (i.e. tyrosine kinases, AGC kinases, or calcium/calmodulin-dependent protein kinases) (12, 168, 207). For example, tyrosine kinases phosphorylate protein tyrosine residues while other kinases may phosphorylate serine/threonine residues. While total tyrosine phosphorylation in BP-treated cells did not statistically change over time, the responses trended toward decreased phosphorylation, with some individual bands in the western blot showing visual variability in protein expression over time. Interestingly, we performed a kinase array (45 kinases/phosphorylation sites included) with lung epithelia following BP e-liquid exposure and found that protein phosphorylation was varied, but several kinases were dephosphorylated compared to the control group (Table 5.2; Fig. 5.2*A*). Of course the array is only a snapshot of phosphorylation states at one time point post-exposure (10 min) and the transient changes of each kinase might change over time. For example, our blots showed that changes in PKCα phosphorylation peaked at 15-30 min post-exposure while total tyrosine phosphorylation did not change over 60 min. We also exposed lung epithelia to heated BP aerosol (10x 70 ml puffs/culture) (Table 5.2; Fig. 5.2*B*). Again we found that kinase phosphorylation was either unchanged or decreased compared with the control. However, few responses overlapped and included cAMP response element binding (CREB) protein and

β–catenin. CREB is an important transcription factor whose downregulation is an indicator of neurological diseases, while β–catenin is responsible for regulating cell-cell adhesion, as well as transcription, and has been implicated in cancer (45, 104). Though it is not clear exactly how BP e-liquid altered kinase phosphorylation, understanding this process will likely assist in assessing any disease risk associated with chronic vaping of a Ca^{2+}-eliciting flavor.

Of note, we used a 2nd generation e-cig device and only 10 puffs, which may not have been enough to elicit a Ca^{2+} response following aerosol exposure similar to our data in Chapter 3 using a 3rd generation device at 100 W setting. More detailed studies using parameters shown to elicit Ca^{2+} responses should be conducted using a 3rd generation device for comparison. Interestingly, Schweitzer et al. found that exposing lung microvascular endothelia to condensed e-cig vapor containing nicotine increased p38 mitogen-activated protein kinase and myosin light chain phosphorylation (222). In turn, these responses did not cause necrosis but did inhibit cell proliferation, suggesting nicotine was a contributing factor. Therefore, it is likely that e-liquids are capable of altering a number of important cellular pathways through the regulation of kinase phosphorylation. Future studies are needed to understand what kinases may be involved in exposure to common flavoring chemicals, how transient or permanent these changes to phosphorylation are, and the resulting effects on important airway cell functions (e.g., mucociliary clearance, innate defenses) in order to more accurately predict potential disease or identify new biomarkers of e-cig exposure.

Overall, the long-term effects of chronic e-cig use in the airways are not known and there are many variables that could play a role in potential pathogenesis (i.e., nicotine, PG/VG, flavoring chemicals, user topography, device style, device settings). In this dissertation, we focused on trying to determine whether or not e-liquids were safe for inhalation. We did this by investigating how flavored e-liquids and their constituent chemicals affect lung epithelial toxicity and function. Specifically, our results demonstrated that there were flavor-dependent differences in e-liquid toxicity and cell Ca^{2+} signaling. We currently know that e-cig use is associated with biological changes in pulmonary cells and chronic bronchitis respiratory symptoms in current vapers (88, 157, 199, 259), so it is important to

understand how flavor-dependent changes might be contributing to these changes to predict risk of potential disease with long-term use. For instance, altering SOCE activity or the expression of its requisite components (i.e., STIM1/Orai1) has been demonstrated to play a role in cancer and immune diseases. Since many of the individual flavoring chemicals that we focused on in our studies are GRAS for ingestion, it is vital that we elucidate how and why pulmonary cells are affected in a different fashion than those in the digestive tract. For instance, some users reported inhaling over 200 puffs/day (6-30 ml of e-liquid/day) (88). With e-cig aerosol deposition reported up to 45% in the lung (232), pulmonary cells may be exposed to a higher concentration of chemicals in the liquid lining fluid of the lung than their digestive tract counterparts. It is also important to note that many of the e-liquid flavors and constituent chemicals we investigated are appealing to adolescent users (98). Therefore, it is imperative that the dose-dependent effects of popular flavorings be further investigated to inform FDA regulations in an effort to fully communicate their potential health risks to e-cig users.

Table 5.1. List of % inhibition values of Banana Pudding (BP) or PG/VG e-liquid per receptor subtype. Primary screening results of dilutions of either BP-flavored e-liquid (0 mg/ml nicotine) or 55PG/45VG vehicle from starting stocks of 10 or 30% e-liquid in DMSO. Screening performed with competitive radioligand binding assays. Significant inhibition is considered > 50% and negative inhibition representation binding stimulation, which can happen non-specifically with high concentrations of compounds. n = 4 determinations per receptor subtype for each treatment. NT = not tested. Receptor families included in the screen were GABA (GABAA), serotonin (5-HT1-7), histamine (H1-4), adrenergic (α1A-2C, β1-3), dopamine (D1-4), and sigma (1-2) receptors.

Receptor	**10% BP Stock**	**30% BP Stock**	**30% PG/VG Stock**
5-HT1A	0.4	0.6	-2.4
5-HT1D	-10.3	-5.0	-0.1
5-htle	5.4	NT	NT
5-HT2A	16.3	15.5	18.5
5-HT2B	23.1	39.4	31.4
5-HT2C	0.8	-0.2	11.9
5-HT3	-14.3	-12.2	8.0
5-ht5a	-14.2	-14.9	7.4
5-HT6	-22	-20.7	7.3
5-HT7	-12.3	-19.5	5.9
α1A	13.4	-10.0	-11.8
α1B	-7.7	3.6	3.9
α2B	-18.7	-13.9	-12.9
α2C	-17.6	-12.6	4.3
β1	13.9	19.0	14.1
β3	20.2	29.6	34.5
D1	17.2	19.6	17.4
D2	-1.4	10.9	3.6
D3	-7.4	3.3	10.1
D4	19.3	17.1	22.7
GABAA	19.8	14.7	28.7
H1	25.0	24.1	31.5
H2	**43.6**	**56.5**	**65.5**
H3	20.0	19.4	24.6
H4	28.9	31.3	32.7
Sigma 1 GP	**31.2**	**32.4**	**14.7**
Sigma 2	-15.2	10.3	22.1

Table 5.2. List of kinase phosphorylation responses in pulmonary epithelial cultures following BP e-liquid or aerosol exposures. Kinase arrays were run on pooled samples of lysates from (1) CALU3 cells exposed to 0 or 3% BP e-liquid for 10 min or (2) human bronchial epithelial cells (HBECs) exposed to 10x 70 ml puffs of air or BP aerosol. Samples were pooled from at least three different cultures and run in duplicate per treatment. Values represent average (AU) ± SD.

	0% BP E-liquid	**3% BP E-liquid**	**Air Puffs (10x)**	**BP Puffs (10x)**
Kinase	AVG ± SD	AVG ± SD	AVG ± SD	AVG ± SD
Reference 1	213390 ± 2700	211753 ± 518	257040 ± 1	257030 ± 8
P38a	13036 ± 2885	13639 ± 2923	132896 ± 13113	104816 ± 8994
ERK1/2	74334 ± 590	46279 ± 1220	151765 ± 8657	165019 ± 6668
JNK1/2/3	16811 ± 4	14673 ± 1297	120197 ± 9209	105711 ± 662
GSK-3α/β	53277 ± 171	46606 ± 1338	121858 ± 909	109629 ± 178
p53	161068 ± 489	154411 ± 1665	125854 ± 3837	119667 ± 5701
Reference 2	183388 ± 1047	182074 ± 3205	257033 ± 11	257029 ± 16
EGFR	79721 ± 4786	67863 ± 444	140317 ± 2876	99628 ± 35052
MSK1/2	28546 ± 3267	26659 ± 75	182134 ± 445	161893 ± 4880
AMPKα1	15697 ± 1749	11115 ± 2167	103279 ± 523	94329 ± 880
Akt 1/2/3	154799 ± 4477	158877 ± 2197	119546 ± 3170	103671 ± 4605
Akt 1/2/3	25134 ± 1354	19614 ± 2342	105313 ± 3299	106218 ± 679
p53	142982 ± 382	127785 ± 459	181105 ± 2940	180480 ± 6766
TOR	15297 ± 1259	13545 ± 1117	179462 ± 2452	152911 ± 2753
CREB	136143 ± 2584	115320 ± 2688	191992 ± 1918	156111 ± 4909
HSP27	22708 ± 1791	19210 ± 2713	135449 ± 802	116948 ± 8984
AMPKα2	14243 ± 2739	11388 ± 186	178966 ± 4690	140790 ± 2810
β-catenin	40878 ± 3297	27349 ± 1129	202297 ± 660	180160 ± 3859
P70 S6 Kinase	10297 ± 1068	21616 ± 2084	96753 ± 2636	102824 ± 1197
p53	86987 ± 5228	58810 ± 2886	81460 ± 878	84282 ± 2363
c-Jun	56200 ± 3331	34186 ± 4335	96887 ± 2063	98966 ± 774
Src	14702 ± 1037	9321 ± 257	117231 ± 7133	105595 ± 991
Lyn	12752 ± 238	11374 ± 170	154924 ± 2679	130297 ± 200
Lck	7456 ± 33	6042 ± 21	108142 ± 1488	86199 ± 57
STAT2	17931 ± 72	17160 ± 139	207733 ± 2433	172146 ± 8896
STAT5a	13816 ± 402	12088 ± 238	183657 ± 2127	166111 ± 218
P70 S6 Kinase	21616 ± 2084	13403 ± 1911	113507 ± 4511	112995 ± 3998
RSK1/2/3	7957 ± 800	4505 ± 1050	99936 ± 4163	103566 ± 69
eNOS	369 ± 50	-1740 ± 318	78946 ± 4004	82737 ± 6432
Fyn	13784 ± 432	9989 ± 674	136147 ± 2529	146555 ± 4378
Yes	15818 ± 1148	7984 ± 30	144449 ± 888	119622 ± 1152
Fgr	1059 ± 824	-899 ± 549	98695 ± 2668	96942 ± 787
STAT6	13721 ± 518	11317 ± 290	179657 ± 2259	142167 ± 1536
STAT5b	11269 ± 270	9534 ± 325	192960 ± 2676	175556 ± 4839
STAT3	7502 ± 197	3288 ± 796	137152 ± 546	134359 ± 3544

Kinase	0% BP E-liquid	3% BP E-liquid	Air Puffs (10x)	BP Puffs (10x)
p27	5407 ± 289	-908 ± 216	86790 ± 3764	89393 ± 485
PLC-γ1	3149 ± 773	-792 ± 218	82741 ± 4964	88530 ± 4226
Hck	36089 ± 134	26428 ± 2116	162538 ± 2240	150474 ± 4108
Chk-2	37575 ± 2470	28168 ± 583	139497 ± 5027	119386 ± 5833
FAK	21449 ± 1327	10234 ± 118	118687 ± 2031	103120 ± 4465
PDGF Rβ	5292 ± 364	4066 ± 122	115853 ± 2473	98807 ±948
STAT5a/b	7536 ± 542	6462 ± 216	150974 ± 943	131712 ± 5407
STAT3	37689 ± 42	22016 ± 400	83194 ± 870	88903 ± 2015
WNK1	136811 ± 1037	117692 ± 569	210277 ± 1088	209765 ± 3774
PYK2	8332 ± 1941	1952 ± 602	88150 ± 3603	95472 ± 585
Reference 3	211303 ± 2674	203782 ± 1807	257038 ± 4	257033 ± 9
PRAS40	20718 ± 1078	20226 ± 945	162820 ± 9591	142599 ± 290
HSP60	153054 ± 399	156458 ± 1025	252706 ±5976	248353 ± 11073

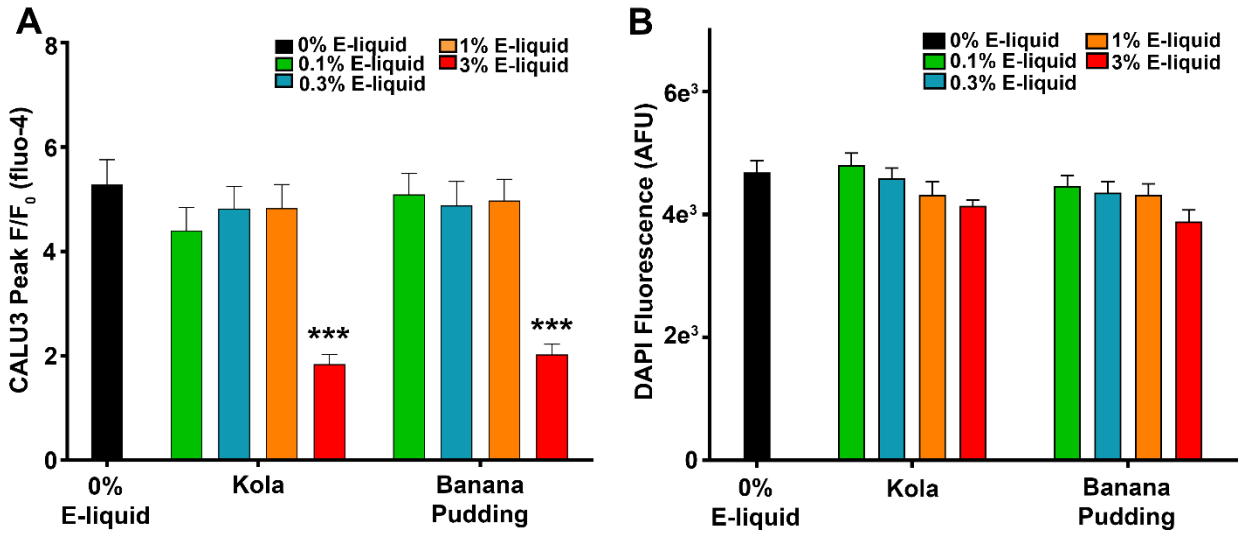

Figure 5.1. Chronic exposure to Kola-flavored e-liquid found to inhibit thapsigargin-induced Ca^{2+} response, similar to BP. CALU3 cells were exposed to Kola or BP-flavored e-liquids diluted in culture media for 24 h. *A*: Cells were loaded with fluo-4 dye and peak Ca^{2+} responses to thapsigargin were measured. *B*: Cells were fixed following Ca^{2+} assays and stained with DAPI for relative cell number per culture. Bars represent mean + SEM. n = 9-18 wells per treatment from 3 independent experiments. Statistical differences compared between all treatments and the 0% e-liquid control (***$P < 0.001$).

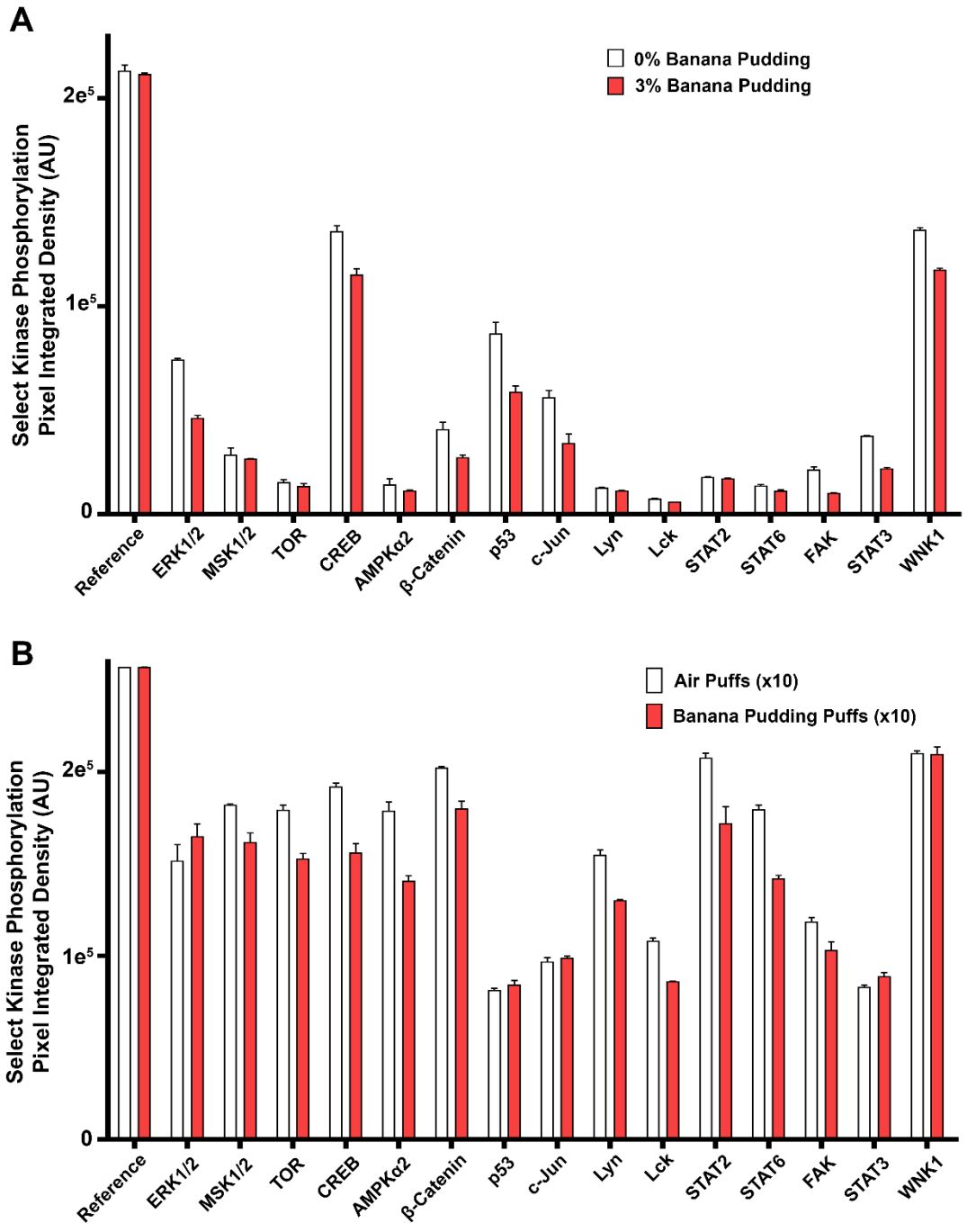

Figure 5.2. Select kinases show decreased phosphorylation with exposure to either BP e-liquid or aerosol in airway cultures. CALU3 cells were exposed to 0 or 3% BP (12 mg/ml nicotine) e-liquid for 10 min and HBECs were exposed to 10x 70 ml puffs of air or heated BP e-liquid (aerosol). Protein lysates were collected from the airway epithelial cultures and ran on kinase arrays. A full list of the phosphorylation results are found in Table 5.2. *A-B*: Select kinase results were plotted as the mean of pooled samples + SD for both e-liquid and aerosol exposures. Samples were pooled from at least three cultures and run in duplicate per treatment.

REFERENCES

1. **Abbott LC, and Winzer-Serhan UH**. Smoking during pregnancy: lessons learned from epidemiological studies and experimental studies using animal models. *Critical reviews in toxicology* 42: 279-303, 2012.

2. **Adriani W, Macrì S, Pacifici R, and Laviola G**. Peculiar vulnerability to nicotine oral self-administration in mice during early adolescence. *Neuropsychopharmacology* 27: 212-224, 2002.

3. **Albuquerque EX, Pereira EF, Alkondon M, and Rogers SW**. Mammalian nicotinic acetylcholine receptors: from structure to function. *Physiological Reviews* 89: 73-120, 2009.

4. **Alexander NS, Blount A, Zhang S, Skinner D, Hicks SB, Chestnut M, Kebbel FA, Sorscher EJ, and Woodworth BA**. Cystic fibrosis transmembrane conductance regulator modulation by the tobacco smoke toxin acrolein. *The Laryngoscope* 122: 1193-1197, 2012.

5. **Allen JG, Flanigan SS, LeBlanc M, Vallarino J, MacNaughton P, Stewart JH, and Christiani DC**. Flavoring chemicals in e-cigarettes: diacetyl, 2, 3-pentanedione, and acetoin in a sample of 51 products, including fruit-, candy-, and cocktail-flavored e-cigarettes. *Environmental Health Perspectives (Online)* 124: 733-739, 2016.

6. **Ambrose BK, Rostron BL, Johnson SE, Portnoy DB, Apelberg BJ, Kaufman AR, and Choiniere CJ**. Perceptions of the relative harm of cigarettes and e-cigarettes among US youth. *American Journal of Preventive Medicine* 47: S53-S60, 2014.

7. **Anand V, McGinty KL, O'Brien K, Guenthner G, Hahn E, and Martin CA**. E-cigarette use and beliefs among urban public high school students in north carolina. *Journal of Adolescent Health* 57: 46-51, 2015.

8. **Anderson SJ, and Ling PM**. "And they told two friends… and so on": RJ Reynolds' viral marketing of Eclipse and its potential to mislead the public. *Tobacco control* 17: 222-229, 2008.

9. **Andrè E, Campi B, Materazzi S, Trevisani M, Amadesi S, Massi D, Creminon C, Vaksman N, Nassini R, and Civelli M**. Cigarette smoke–induced neurogenic inflammation is mediated by α, β-unsaturated aldehydes and the TRPA1 receptor in rodents. *The Journal of clinical investigation* 118: 2574-2582, 2008.

10. **Aoki M, Takao T, Takao K, Koike F, and Suganuma N**. Lower expressions of the human bitter taste receptor TAS2R in smokers: reverse transcriptase-polymerase chain reaction analysis. *Tobacco induced diseases* 12: 1, 2014.

11. **Aoshiba K, Nagai A, Yasui S, and Konno K**. Nicotine prolongs neutrophil survival by suppressing apoptosis. *Journal of Laboratory and Clinical Medicine* 127: 186-194, 1996.

12. **Arencibia JM, Pastor-Flores D, Bauer AF, Schulze JO, and Biondi RM**. AGC protein kinases: from structural mechanism of regulation to allosteric drug development for the treatment of human diseases. *Biochimica Et Biophysica Acta (BBA)-Proteins and Proteomics* 1834: 1302-1321, 2013.

13. **Arrazola RA, Singh T, Corey CG, Husten CG, Neff LJ, Apelberg BJ, Bunnell RE, Choiniere CJ, King BA, and Cox S**. Tobacco use among middle and high school students-United States, 2011-2014. *MMWR Morbidity and mortality weekly report* 64: 381-385, 2015.

14. **Bae Y-S, Lee TG, Park JC, Hur JH, Kim Y, Heo K, Kwak J-Y, Suh P-G, and Ryu SH**. Identification of a compound that directly stimulates phospholipase C activity. *Molecular pharmacology* 63: 1043-1050, 2003.

15. **Bahl V, Lin S, Xu N, Davis B, Wang Y-h, and Talbot P**. Comparison of electronic cigarette refill fluid cytotoxicity using embryonic and adult models. *Reproductive Toxicology* 34: 529-537, 2012.

16. **Bandell M, Story GM, Hwang SW, Viswanath V, Eid SR, Petrus MJ, Earley TJ, and Patapoutian A**. Noxious cold ion channel TRPA1 is activated by pungent compounds and bradykinin. *Neuron* 41: 849-857, 2004.

17. **Barker AF, Bergeron A, Rom WN, and Hertz MI**. Obliterative bronchiolitis. *New England Journal of Medicine* 370: 1820-1828, 2014.

18. **Barnes PJ**. Cellular and molecular mechanisms of chronic obstructive pulmonary disease. *Clinics in chest medicine* 35: 71-86, 2014.

19. **Barrington-Trimis JL, Samet JM, and McConnell R**. Flavorings in Electronic Cigarettes An Unrecognized Respiratory Health Hazard? *JAMA* 312: 2493-2494, 2014.

20. **Bastos LCS, and Pereira PAdP**. Influence of heating time and metal ions on the amount of free fatty acids and formation rates of selected carbonyl compounds during the thermal oxidation of canola oil. *Journal of agricultural and food chemistry* 58: 12777-12783, 2010.

21. **Behar R, Davis B, Wang Y, Bahl V, Lin S, and Talbot P**. Identification of toxicants in cinnamon-flavored electronic cigarette refill fluids. *Toxicology in vitro* 28: 198-208, 2014.

22. **Behar RZ, and Talbot P**. Puffing topography and nicotine intake of electronic cigarette users. *PloS one* 10: e0117222, 2015.

23. **Bennett WD, Brown JS, Zeman KL, Hu S-C, Scheuch G, and Sommerer K**. Targeting delivery of aerosols to different lung regions. *Journal of aerosol medicine* 15: 179-188, 2002.

24. **Benowitz NL**. Nicotine Addiction. *The New England Journal of Medicine* 362: 2295-2303, 2010.

25. **Benowitz NL, Hukkanen J, and Jacob III P**. Nicotine chemistry, metabolism, kinetics and biomarkers. In: *Nicotine psychopharmacology*Springer, 2009, p. 29-60.

26. **Berridge MJ, Bootman MD, and Roderick HL**. Calcium signalling: dynamics, homeostasis and remodelling. *Nature reviews Molecular cell biology* 4: 517-529, 2003.

27. **Bertagnolo V, Benedusi M, Brugnoli F, Lanuti P, Marchisio M, Querzoli P, and Capitani S**. Phospholipase C-β2 promotes mitosis and migration of human breast cancer-derived cells. *Carcinogenesis* 28: 1638-1645, 2007.

28. **Besnard J, Ruda GF, Setola V, Abecassis K, Rodriguiz RM, Huang X-P, Norval S, Sassano MF, Shin AI, and Webster LA**. Automated design of ligands to polypharmacological profiles. *Nature* 492: 215, 2012.

29. **Bessac BF, and Jordt S-E**. Breathtaking TRP channels: TRPA1 and TRPV1 in airway chemosensation and reflex control. *Physiology* 23: 360-370, 2008.

30. **Bhalla DK, Hirata F, Rishi AK, and Gairola CG**. Cigarette smoke, inflammation, and lung injury: a mechanistic perspective. *Journal of Toxicology and Environmental Health, Part B* 12: 45-64, 2009.

31. **Bove PF, and van der Vliet A**. Nitric oxide and reactive nitrogen species in airway epithelial signaling and inflammation. *Free Radical Biology and Medicine* 41: 515-527, 2006.

32. **Bozinovski S, Vlahos R, Anthony D, McQualter J, Anderson G, Irving L, and Steinfort D**. COPD and squamous cell lung cancer: aberrant inflammation and immunity is the common link. *British journal of pharmacology* 2015.

33. **Breer H, and Boekhoff I**. Odorants of the same odor class activate different second messenger pathways. *Chemical Senses* 16: 19-29, 1991.

34. **Brown CJ, and Cheng JM**. Electronic cigarettes: product characterisation and design considerations. *Tobacco control* 23: ii4-ii10, 2014.

35. **Cannon DS, Baker TB, Piper ME, Scholand MB, Lawrence DL, Drayna DT, McMahon WM, Villegas GM, Caton TC, and Coon H**. Associations between phenylthiocarbamide gene polymorphisms and cigarette smoking. *Nicotine & Tobacco Research* 7: 853-858, 2005.

36. **Cantin AM, Hanrahan JW, Bilodeau G, Ellis L, Dupuis A, Liao J, Zielenski J, and Durie P**. Cystic fibrosis transmembrane conductance regulator function is suppressed in cigarette smokers. *American journal of respiratory and critical care medicine* 173: 1139-1144, 2006.

37. **Caporaso N, Gu F, Chatterjee N, Sheng-Chih J, Yu K, Yeager M, Chen C, Jacobs K, Wheeler W, and Landi MT**. Genome-wide and candidate gene association study of cigarette smoking behaviors. *PloS one* 4: e4653, 2009.

38. **Caramori G, Casolari P, Cavallesco GN, Giuffrè S, Adcock I, and Papi A**. Mechanisms involved in lung cancer development in COPD. *The international journal of biochemistry & cell biology* 43: 1030-1044, 2011.

39. **Carmines E, and Gaworski C**. Toxicological evaluation of glycerin as a cigarette ingredient. *Food and chemical toxicology* 43: 1521-1539, 2005.

40. **Casella IG, and Contursi M**. Quantitative analysis of acrolein in heated vegetable oils by liquid chromatography with pulsed electrochemical detection. *Journal of agricultural and food chemistry* 52: 5816-5821, 2004.

41. **Caterina MJ, Schumacher MA, Tominaga M, Rosen TA, Levine JD, and Julius D**. The capsaicin receptor: a heat-activated ion channel in the pain pathway. *Nature* 389: 816, 1997.

42. **Cervellati F, Muresan X, Sticozzi C, Gambari R, Montagner G, Forman H, Torricelli C, Maioli E, and Valacchi G**. Comparative effects between electronic and cigarette smoke in human keratinocytes and epithelial lung cells. *Toxicology in vitro* 28: 999-1005, 2014.

43. **Chen K-M, Sacks PG, Spratt TE, Lin J-M, Boyiri T, Schwartz J, Richie JP, Calcagnotto A, Das A, and Bortner J**. Modulations of benzo [a] pyrene-induced DNA adduct, cyclin D1 and PCNA in oral tissue by 1, 4-phenylenebis (methylene) selenocyanate. *Biochemical and biophysical research communications* 383: 151-155, 2009.

44. **Chen Y-W, Chen Y-F, Chen Y-T, Chiu W-T, and Shen M-R**. The STIM1-Orai1 pathway of store-operated Ca 2+ entry controls the checkpoint in cell cycle G1/S transition. *Scientific reports* 6: 22142, 2016.

45. **Chrivia JC, Kwok RP, Lamb N, Hagiwara M, Montminy MR, and Goodman RH**. Phosphorylated CREB binds specifically to the nuclear protein CBP. *Nature* 365: 855, 1993.

46. **Chung M-K, Lee H, Mizuno A, Suzuki M, and Caterina MJ**. 2-aminoethoxydiphenyl borate activates and sensitizes the heat-gated ion channel TRPV3. *Journal of Neuroscience* 24: 5177-5182, 2004.

47. **Clapp PW, Pawlak EA, Lackey JT, Keating JE, Reeber SL, Glish GL, and Jaspers I**. Flavored e-cigarette liquids and cinnamaldehyde impair respiratory innate immune cell function. *American Journal of Physiology-Lung Cellular and Molecular Physiology* 313: L278-L292, 2017.

48. **Clarke P, and Reuben M**. Release of [3H]-noradrenaline from rat hippocampal synaptosomes by nicotine: mediation by different nicotinic receptor subtypes from striatal [3H]-dopamine release. *British Journal of Pharmacology* 117: 595-606, 1996.

49. **Clunes LA, Davies CM, Coakley RD, Aleksandrov AA, Henderson AG, Zeman KL, Worthington EN, Gentzsch M, Kreda SM, and Cholon D**. Cigarette smoke exposure induces CFTR internalization and insolubility, leading to airway surface liquid dehydration. *The FASEB Journal* 26: 533-545, 2012.

50. **Cohen SP, Buckley BK, Kosloff M, Garland AL, Bosch DE, Cheng G, Radhakrishna H, Brown MD, Willard FS, and Arshavsky VY**. Regulator of G-protein signaling-21 (RGS21) is an inhibitor of bitter gustatory signaling found in lingual and airway epithelia. *Journal of Biological Chemistry* 287: 41706-41719, 2012.

51. **Collawn JF, and Matalon S**. CFTR and lung homeostasis. *American Journal of Physiology-Lung Cellular and Molecular Physiology* 307: L917-L923, 2014.

52. **Conti-Fine BM, Navaneetham D, Lei S, and Maus AD**. Neuronal nicotinic receptors in non-neuronal cells: new mediators of tobacco toxicity? *European Journal of Pharmacology* 393: 279-294, 2000.

53. **Corcoran T, Niven R, Verret W, Dilly S, and Johnson B**. Lung deposition and pharmacokinetics of nebulized cyclosporine in lung transplant patients. *Journal of Aerosol Medicine and Pulmonary Drug Delivery* 27: 178-184, 2014.

54. **Cormier A, Paas Y, Zini R, Tillement J-P, Lagrue G, Changeux J-P, and Grailhe R**. Long-term exposure to nicotine modulates the level and activity of acetylcholine receptors in white blood cells of smokers and model mice. *Molecular pharmacology* 66: 1712-1718, 2004.

55. **Davis B, Dang M, Kim J, and Talbot P**. Nicotine concentrations in electronic cigarette refill and do-it-yourself fluids. *Nicotine & Tobacco Research* 17: 134-141, 2015.

56. **Davis B, Razo A, Nothnagel E, Chen M, and Talbot P**. Unexpected nicotine in Do-it-Yourself electronic cigarette flavourings. *Tobacco control* tobaccocontrol-2015-052468, 2015.

57. **Davis ES, Sassano MF, Goodell H, and Tarran R**. E-Liquid Autofluorescence can be used as a Marker of Vaping Deposition and Third-Hand Vape Exposure. *Scientific reports* 7: 7459, 2017.

58. **Dawkins L, Turner J, Roberts A, and Soar K**. 'Vaping'profiles and preferences: an online survey of electronic cigarette users. *Addiction* 108: 1115-1125, 2013.

59. **de la Peña JB, Ahsan HM, Tampus R, Botanas CJ, dela Peña IJ, Kim HJ, Sohn A, dela Peña I, Shin CY, and Ryu JH**. Cigarette smoke exposure during adolescence enhances sensitivity to the rewarding effects of nicotine in adulthood, even after a long period of abstinence. *Neuropharmacology* 99: 9-14, 2015.

60. **Dehkordi O, Millis RM, Dennis GC, Jazini E, Williams C, Hussain D, and Jayam-Trouth A**. Expression of alpha-7 and alpha-4 nicotinic acetylcholine receptors by GABAergic neurons of rostral ventral medulla and caudal pons. *Brain research* 1185: 95-102, 2007.

61. **DeMarini DM**. Genotoxicity of tobacco smoke and tobacco smoke condensate: a review. *Mutation Research/Reviews in Mutation Research* 567: 447-474, 2004.

62. **Derfus AM, Chan WC, and Bhatia SN**. Intracellular delivery of quantum dots for live cell labeling and organelle tracking. *Advanced Materials* 16: 961-966, 2004.

63. **Deshpande DA, Wang WC, McIlmoyle EL, Robinett KS, Schillinger RM, An SS, Sham JS, and Liggett SB**. Bitter taste receptors on airway smooth muscle bronchodilate by localized calcium signaling and reverse obstruction. *Nature medicine* 16: 1299-1304, 2010.

64. **Dickson EJ, Falkenburger BH, and Hille B**. Quantitative properties and receptor reserve of the IP3 and calcium branch of Gq-coupled receptor signaling. *The Journal of general physiology* 141: 521-535, 2013.

65. **Dolmetsch RE, Xu K, and Lewis RS**. Calcium oscillations increase the efficiency and specificity of gene expression. *Nature* 392: 933, 1998.

66. **Domej W, Oettl K, and Renner W**. Oxidative stress and free radicals in COPD–implications and relevance for treatment. *International journal of chronic obstructive pulmonary disease* 9: 1207, 2014.

67. **Doolittle D, Lee C, Ivett J, Mirsalis J, Riccio E, Rudd C, Burger G, and Hayes A**. Comparative studies on the genotoxic activity of mainstream smoke condensate from cigarettes which burn or only heat tobacco. *Environmental and molecular mutagenesis* 15: 93-105, 1990.

68. **Doyle I, Ratcliffe M, Walding A, Bon EV, Dymond M, Tomlinson W, Tilley D, Shelton P, and Dougall I**. Differential gene expression analysis in human monocyte-derived macrophages: impact of cigarette smoke on host defence. *Molecular immunology* 47: 1058-1065, 2010.

69. **Egleton RD, Brown KC, and Dasgupta P**. Nicotinic acetylcholine receptors in cancer: multiple roles in proliferation and inhibition of apoptosis. *Trends in pharmacological sciences* 29: 151-158, 2008.

70. **Eisner MD, Anthonisen N, Coultas D, Kuenzli N, Perez-Padilla R, Postma D, Romieu I, Silverman EK, and Balmes JR**. An official American Thoracic Society public policy statement: Novel risk factors and the global burden of chronic obstructive pulmonary disease. *American journal of respiratory and critical care medicine* 182: 693-718, 2010.

71. **England LJ, Bunnell RE, Pechacek TF, Tong VT, and McAfee TA**. Nicotine and the developing human: a neglected element in the electronic cigarette debate. *American journal of preventive medicine* 49: 286-293, 2015.

72. **Enoch M-A, Harris CR, and Goldman D**. Does a reduced sensitivity to bitter taste increase the risk of becoming nicotine addicted? *Addictive behaviors* 26: 399-404, 2001.

73. **Enslen H, Tokumitsu H, Stork P, Davis RJ, and Soderling TR**. Regulation of mitogen-activated protein kinases by a calcium/calmodulin-dependent protein kinase cascade. *Proceedings of the National Academy of Sciences* 93: 10803-10808, 1996.

74. **Etter JF, and Bullen C**. Electronic cigarette: users profile, utilization, satisfaction and perceived efficacy. *Addiction* 106: 2017-2028, 2011.

75. **Falkenburger BH, Dickson EJ, and Hille B**. Quantitative properties and receptor reserve of the DAG and PKC branch of Gq-coupled receptor signaling. *The Journal of general physiology* 141: 537-555, 2013.

76. **Fallin A, and Glantz SA**. Tobacco-Control Policies in Tobacco-Growing States: Where Tobacco Was King. *Milbank Quarterly* 93: 319-358, 2015.

77. **Farsalinos KE, Kistler KA, Gillman G, and Voudris V**. Evaluation of electronic cigarette liquids and aerosol for the presence of selected inhalation toxins. *Nicotine & Tobacco Research* 17: 168-174, 2014.

78. **Farsalinos KE, Romagna G, Tsiapras D, Kyrzopoulos S, and Voudris V**. Evaluation of electronic cigarette use (vaping) topography and estimation of liquid consumption: implications for research protocol standards definition and for public health authorities' regulation. *International Journal of Environmental Research and Public Health* 10: 2500-2514, 2013.

79. **Farsalinos KE, Spyrou A, Stefopoulos C, Tsimopoulou K, Kourkoveli P, Tsiapras D, Kyrzopoulos S, Poulas K, and Voudris V**. Nicotine absorption from electronic cigarette use: comparison between experienced consumers (vapers) and naïve users (smokers). *Scientific Reports* 5: 1-8, 2015.

80. **Farsalinos KE, Voudris V, and Poulas K**. E-cigarettes generate high levels of aldehydes only in 'dry puff'conditions. *Addiction* 110: 1352-1356, 2015.

81. **Fenech M, Kirsch-Volders M, Natarajan A, Surralles J, Crott J, Parry J, Norppa H, Eastmond D, Tucker J, and Thomas P**. Molecular mechanisms of micronucleus, nucleoplasmic bridge and nuclear bud formation in mammalian and human cells. *Mutagenesis* 26: 125-132, 2011.

82. **Fowles J, and Dybing E**. Application of toxicological risk assessment principles to the chemical constituents of cigarette smoke. *Tobacco Control* 12: 424-430, 2003.

83. **Garcia-Arcos I, Geraghty P, Baumlin N, Campos M, Dabo AJ, Jundi B, Cummins N, Eden E, Grosche A, and Salathe M**. Chronic electronic cigarette exposure in mice induces features of COPD in a nicotine-dependent manner. *Thorax* 71: 1119-1129, 2016.

84. **Garmendia J, Morey P, and Bengoechea JA**. Impact of cigarette smoke exposure on host–bacterial pathogen interactions. *European Respiratory Journal* 39: 467-477, 2012.

85. **Gerloff J, Sundar IK, Freter R, Sekera ER, Friedman AE, Robinson R, Pagano T, and Rahman I**. Inflammatory response and barrier dysfunction by different e-cigarette flavoring chemicals identified by gas chromatography–mass spectrometry in e-liquids and e-vapors on human lung epithelial cells and fibroblasts. *Applied in vitro toxicology* 3: 28-40, 2017.

86. **Gerzanich V, Wang F, Kuryatov A, and Lindstrom J**. α5 subunit alters desensitization, pharmacology, Ca++ permeability and Ca++ modulation of human neuronal α3 nicotinic receptors. *Journal of Pharmacology and Experimental Therapeutics* 286: 311-320, 1998.

87. **Ghosh A, Boucher R, and Tarran R**. Airway hydration and COPD. *Cellular and Molecular Life Sciences* 72: 3637-3652, 2015.

88. **Ghosh A, Coakley RC, Mascenik T, Rowell TR, Davis ES, Rogers K, Webster MJ, Dang H, Herring LE, and Sassano MF**. Chronic E-cigarette Exposure Alters the Human Bronchial Epithelial Proteome. *American journal of respiratory and critical care medicine* 2018.

89. **Giovenco DP, Lewis MJ, and Delnevo CD**. Factors associated with e-cigarette use: a national population survey of current and former smokers. *American journal of preventive medicine* 47: 476-480, 2014.

90. **Goksör E, Åmark M, Alm B, Gustafsson PM, and Wennergren G**. The impact of pre-and post-natal smoke exposure on future asthma and bronchial hyper-responsiveness. *Acta Paediatrica* 96: 1030-1035, 2007.

91. **Goniewicz ML, Gupta R, Lee YH, Reinhardt S, Kim S, Kim B, Kosmider L, and Sobczak A**. Nicotine levels in electronic cigarette refill solutions: A comparative analysis of products from the US, Korea, and Poland. *International Journal of Drug Policy* 26: 583-588, 2015.

92. **Gopalakrishnan M, Monteggia LM, Anderson DJ, Molinari EJ, Piattoni-Kaplan M, Donnelly-Roberts D, Arneric SP, and Sullivan JP**. Stable expression, pharmacologic properties and regulation of the human neuronal nicotinic acetylcholine alpha 4 beta 2 receptor. *Journal of Pharmacology and Experimental Therapeutics* 276: 289-297, 1996.

93. **Gwilt CR, Donnelly LE, and Rogers DF**. The non-neuronal cholinergic system in the airways: an unappreciated regulatory role in pulmonary inflammation? *Pharmacology & therapeutics* 115: 208-222, 2007.

94. **Hahn J, Monakhova YB, Hengen J, Kohl-Himmelseher M, Schüssler J, Hahn H, Kuballa T, and Lachenmeier DW**. Electronic cigarettes: overview of chemical composition and exposure estimation. *Tobacco induced diseases* 12: 1-12, 2014.

95. **Hallstrand TS, Hackett TL, Altemeier WA, Matute-Bello G, Hansbro PM, and Knight DA**. Airway epithelial regulation of pulmonary immune homeostasis and inflammation. *Clinical Immunology* 151: 1-15, 2014.

96. **Hammond D, Collishaw NE, and Callard C**. Secret science: tobacco industry research on smoking behaviour and cigarette toxicity. *The Lancet* 367: 781-787, 2006.

97. **Hansen M, Boitano S, Dirksen ER, and Sanderson MJ**. Intercellular calcium signaling induced by extracellular adenosine 5′-triphosphate and mechanical stimulation in airway epithelial cells. *Journal of Cell Science* 106: 995-1004, 1993.

98. **Harrell M, Weaver S, Loukas A, Creamer M, Marti C, Jackson C, Heath J, Nayak P, Perry C, and Pechacek T**. Flavored e-cigarette use: Characterizing youth, young adult, and adult users. *Preventive medicine reports* 5: 33-40, 2017.

99. **Harvey B-G, Strulovici-Barel Y, Vincent TL, Mezey JG, Raviram R, Gordon C, Salit J, Tilley AE, Chung A, and Sanders A**. High correlation of the response of upper and lower lobe small airway epithelium to smoking. *PloS one* 8: 2013.

100. **Hassan F, Xu X, Nuovo G, Killilea DW, Tyrrell J, Da Tan C, Tarran R, Diaz P, Jee J, and Knoell D**. Accumulation of metals in GOLD4 COPD lungs is associated with decreased CFTR levels. *Respiratory research* 15: 69, 2014.

101. **Hatsukami DK, Ebbert JO, Feuer RM, Stepanov I, and Hecht SS**. Changing smokeless tobacco products: new tobacco-delivery systems. *American journal of preventive medicine* 33: S368-S378, 2007.

102. **Haugland RP, MacCoubrey IC, and Moore PL**. Dual-fluorescence cell viability assay using ethidium homodimer and calcein AM. Google Patents; US Patent and Trademark Office, 1994.

103. **Heck GL, Mierson S, and DeSimone JA**. Salt taste transduction occurs through an amiloride-sensitive sodium transport pathway. *Science* 223: 403-405, 1984.

104. **Hinck L, Nelson WJ, and Papkoff J**. Wnt-1 modulates cell-cell adhesion in mammalian cells by stabilizing beta-catenin binding to the cell adhesion protein cadherin. *The Journal of cell biology* 124: 729-741, 1994.

105. **Ho K, Yazan LS, Ismail N, and Ismail M**. Apoptosis and cell cycle arrest of human colorectal cancer cell line HT-29 induced by vanillin. *Cancer epidemiology* 33: 155-160, 2009.

106. **Hogg JC, and Timens W**. The pathology of chronic obstructive pulmonary disease. *Annual Review of Pathological Mechanical Disease* 4: 435-459, 2009.

107. **Houghton AM**. Mechanistic links between COPD and lung cancer. *Nature Reviews Cancer* 13: 233-245, 2013.

108. **Huang MF, Lin WL, and Ma YC**. A study of reactive oxygen species in mainstream of cigarette. *Indoor air* 15: 135-140, 2005.

109. **Hung RJ, McKay JD, Gaborieau V, Boffetta P, Hashibe M, Zaridze D, Mukeria A, Szeszenia-Dabrowska N, Lissowska J, and Rudnai P**. A susceptibility locus for lung cancer maps to nicotinic acetylcholine receptor subunit genes on 15q25. *Nature* 452: 633-637, 2008.

110. **Hurt RD, Murphy JG, and Dunn WF**. Did We Finally Slay the Evil Dragon of Cigarette Smoking in the Late 20th Century?: Unfortunately, the Answer Is No—the Dragon Is Still Alive and Well in the 21st Century and Living in the Third World. Shame on Us! *Chest* 146: 1438-1443, 2014.

111. **Husari A, Shihadeh A, Talih S, Hashem Y, El Sabban M, and Zaatari G**. Acute Exposure to Electronic and Combustible Cigarette Aerosols: Effects in an Animal Model and in Human Alveolar Cells. *Nicotine Tob Res* 18: 613-619, 2016.

112. **Hutzler C, Paschke M, Kruschinski S, Henkler F, Hahn J, and Luch A**. Chemical hazards present in liquids and vapors of electronic cigarettes. *Archives of Toxicology* 88: 1295-1308, 2014.

113. **Ichinose K, Rauen T, Juang Y-T, Kis-Toth K, Mizui M, Koga T, and Tsokos GC**. Cutting edge: calcium/calmodulin-dependent protein kinase type IV is essential for mesangial cell proliferation and lupus nephritis. *The Journal of Immunology* 187: 5500-5504, 2011.

114. **Jensen RP, Luo W, Pankow JF, Strongin RM, and Peyton DH**. Hidden formaldehyde in e-cigarette aerosols. *New England Journal of Medicine* 372: 392-394, 2015.

115. **Johnson MD, Schilz J, Djordjevic MV, Rice JR, and Shields PG**. Evaluation of in vitro assays for assessing the toxicity of cigarette smoke and smokeless tobacco. *Cancer Epidemiology Biomarkers & Prevention* 18: 3263-3304, 2009.

116. **Jones WJ, and Silvestri GA**. The Master Settlement Agreement and its impact on tobacco use 10 years later: lessons for physicians about health policy making. *Chest Journal* 137: 692-700, 2010.

117. **Jordt S-E, Bautista DM, Chuang H-h, McKemy DD, Zygmunt PM, Högestätt ED, Meng ID, and Julius D**. Mustard oils and cannabinoids excite sensory nerve fibres through the TRP channel ANKTM1. *Nature* 427: 260, 2004.

118. **Keller M, Liu X, Wohland T, Rohde K, Gast M-T, Stumvoll M, Kovacs P, Tönjes A, and Böttcher Y**. TAS2R38 and its influence on smoking behavior and glucose homeostasis in the German Sorbs. *PloS one* 8: e80512, 2013.

119. **Kesarwala A, Krishna M, and Mitchell J**. Oxidative stress in oral diseases. *Oral diseases* 22: 9-18, 2016.

120. **Kim BH, Lee YG, Lee J, Lee JY, and Cho JY**. Regulatory effect of cinnamaldehyde on monocyte/macrophage-mediated inflammatory responses. *Mediators of inflammation* 2010: 2010.

121. **Kinnamon SC**. Taste receptor signalling–from tongues to lungs. *Acta physiologica* 204: 158-168, 2012.

122. **Kishimoto A, Takai Y, Mori T, Kikkawa U, and Nishizuka Y**. Activation of calcium and phospholipid-dependent protein kinase by diacylglycerol, its possible relation to phosphatidylinositol turnover. *Journal of Biological Chemistry* 255: 2273-2276, 1980.

123. **Kleinstreuer C, and Feng Y**. Lung deposition analyses of inhaled toxic aerosols in conventional and less harmful cigarette smoke: a review. *International journal of environmental research and public health* 10: 4454-4485, 2013.

124. **Kreiss K, Gomaa A, Kullman G, Fedan K, Simoes EJ, and Enright PL**. Clinical bronchiolitis obliterans in workers at a microwave-popcorn plant. *New England Journal of Medicine* 347: 330-338, 2002.

125. **Krjukova J, Holmqvist T, Danis AS, Åkerman KE, and Kukkonen JP**. Phospholipase C activator m-3M3FBS affects Ca2+ homeostasis independently of phospholipase C activation. *British journal of pharmacology* 143: 3-7, 2004.

126. **Kuebler WM**. Inflammatory pathways and microvascular responses in the lung. *Pharmacological Reports* 57: 196, 2005.

127. **Kuschner W, D'Alessandro A, Wong H, and Blanc P**. Dose-dependent cigarette smoking-related inflammatory responses in healthy adults. *European Respiratory Journal* 9: 1989-1994, 1996.

128. **Lam DC-l, Girard L, Ramirez R, Chau W-s, Suen W-s, Sheridan S, Tin VP, Chung L-p, Wong MP, and Shay JW**. Expression of nicotinic acetylcholine receptor subunit genes in non–small-cell lung cancer reveals differences between smokers and nonsmokers. *Cancer Research* 67: 4638-4647, 2007.

129. **Lazarowski ER, Tarran R, Grubb BR, van Heusden CA, Okada S, and Boucher RC**. Nucleotide release provides a mechanism for airway surface liquid homeostasis. *Journal of Biological Chemistry* 279: 36855-36864, 2004.

130. **Lee CK, Doolittle DJ, Burger GT, and Hayes AW**. Comparative genotoxicity testing of mainstream whole smoke from cigarettes which burn or heat tobacco. *Mutation Research/Genetic Toxicology* 242: 37-45, 1990.

131. **Lee J, Taneja V, and Vassallo R**. Cigarette smoking and inflammation cellular and molecular mechanisms. *Journal of dental research* 91: 142-149, 2012.

132. **Lee L-Y, Burki N, Gerhardstein D, Gu Q, Kou Y, and Xu J**. Airway irritation and cough evoked by inhaled cigarette smoke: role of neuronal nicotinic acetylcholine receptors. *Pulmonary pharmacology & therapeutics* 20: 355-364, 2007.

133. **Lee RJ, and Cohen NA**. Bitter and sweet taste receptors in the respiratory epithelium in health and disease. *Journal of Molecular Medicine* 92: 1235-1244, 2014.

134. **Lee RJ, Kofonow JM, Rosen PL, Siebert AP, Chen B, Doghramji L, Xiong G, Adappa ND, Palmer JN, and Kennedy DW**. Bitter and sweet taste receptors regulate human upper respiratory innate immunity. *The Journal of clinical investigation* 124: 1393-1405, 2014.

135. **Lee RJ, Xiong G, Kofonow JM, Chen B, Lysenko A, Jiang P, Abraham V, Doghramji L, Adappa ND, and Palmer JN**. T2R38 taste receptor polymorphisms underlie susceptibility to upper respiratory infection. *The Journal of clinical investigation* 122: 4145-4159, 2012.

136. **Lee YH, Gawron M, and Goniewicz ML**. Changes in puffing behavior among smokers who switched from tobacco to electronic cigarettes. *Addictive behaviors* 48: 1-4, 2015.

137. **Lerner CA, Sundar IK, Yao H, Gerloff J, Ossip DJ, McIntosh S, Robinson R, and Rahman I**. Vapors produced by electronic cigarettes and e-juices with flavorings induce toxicity, oxidative stress, and inflammatory response in lung epithelial cells and in mouse lung. *PloS one* 10: e0116732, 2015.

138. **Liaw A, and Wiener M**. Classification and regression by randomForest. *R news* 2: 18-22, 2002.

139. **Lieb T, Frei CW, Frohock JI, Bookman RJ, and Salathe M**. Prolonged increase in ciliary beat frequency after short-term purinergic stimulation in human airway epithelial cells. *The Journal of physiology* 538: 633-646, 2002.

140. **Lim HB, and Kim SH**. Inhallation of e-cigarette cartridge solution aggravates allergen-induced airway inflammation and hyper-responsiveness in mice. *Toxicological research* 30: 13, 2014.

141. **Liou J, Fivaz M, Inoue T, and Meyer T**. Live-cell imaging reveals sequential oligomerization and local plasma membrane targeting of stromal interaction molecule 1 after Ca2+ store depletion. *Proceedings of the National Academy of Sciences* 104: 9301-9306, 2007.

142. **Lirdprapamongkol K, Sakurai H, Kawasaki N, Choo M-K, Saitoh Y, Aozuka Y, Singhirunnusorn P, Ruchirawat S, Svasti J, and Saiki I**. Vanillin suppresses in vitro invasion and in vivo metastasis of mouse breast cancer cells. *European journal of pharmaceutical sciences* 25: 57-65, 2005.

143. **Lübbert M, Kyereme J, Schöbel N, Beltrán L, Wetzel CH, and Hatt H**. Transient receptor potential channels encode volatile chemicals sensed by rat trigeminal ganglion neurons. *PloS one* 8: e77998, 2013.

144. **Lytton J, Westlin M, and Hanley MR**. Thapsigargin inhibits the sarcoplasmic or endoplasmic reticulum Ca-ATPase family of calcium pumps. *Journal of Biological Chemistry* 266: 17067-17071, 1991.

145. **Macklin KD, Maus AD, Pereira EF, Albuquerque EX, and Conti-Fine BM**. Human vascular endothelial cells express functional nicotinic acetylcholine receptors. *Journal of Pharmacology and Experimental Therapeutics* 287: 435-439, 1998.

146. **Mandil R, Ashkenazi E, Blass M, Kronfeld I, Kazimirsky G, Rosenthal G, Umansky F, Lorenzo PS, Blumberg PM, and Brodie C**. Protein kinase Cα and protein kinase Cδ play opposite roles in the proliferation and apoptosis of glioma cells. *Cancer Research* 61: 4612-4619, 2001.

147. **Mangold JE, Payne TJ, Ma JZ, Chen G, and Li MD**. Bitter taste receptor gene polymorphisms are an important factor in the development of nicotine dependence in African Americans. *Journal of medical genetics* 45: 578-582, 2008.

148. **Manigrasso M, Buonanno G, Fuoco FC, Stabile L, and Avino P**. Aerosol deposition doses in the human respiratory tree of electronic cigarette smokers. *Environmental Pollution* 196: 257-267, 2015.

149. **Maouche K, Polette M, Jolly T, Medjber K, Cloëz-Tayarani I, Changeux J-P, Burlet H, Terryn C, Coraux C, and Zahm J-M**. α7 nicotinic acetylcholine receptor regulates airway epithelium differentiation by controlling basal cell proliferation. *The American journal of pathology* 175: 1868-1882, 2009.

150. **Marian C, O'Connor RJ, Djordjevic MV, Rees VW, Hatsukami DK, and Shields PG**. Reconciling human smoking behavior and machine smoking patterns: implications for understanding smoking behavior and the impact on laboratory studies. *Cancer Epidemiology Biomarkers & Prevention* 18: 3305-3320, 2009.

151. **Marini S, Buonanno G, Stabile L, and Ficco G**. Short-term effects of electronic and tobacco cigarettes on exhaled nitric oxide. *Toxicology and Applied Pharmacology* 278: 9-15, 2014.

152. **Maruyama T, Kanaji T, Nakade S, Kanno T, and Mikoshiba K**. 2APB, 2-aminoethoxydiphenyl borate, a membrane-penetrable modulator of Ins (1, 4, 5) P3-induced Ca2+ release. *The Journal of Biochemistry* 122: 498-505, 1997.

153. **Mason S, Paradiso A, and Boucher R**. Regulation of transepithelial ion transport and intracellular calcium by extracellular ATP in human normal and cystic fibrosis airway epithelium. *British journal of pharmacology* 103: 1649-1656, 1991.

154. **Matsunaga K, Klein TW, Friedman H, and Yamamoto Y**. Involvement of nicotinic acetylcholine receptors in suppression of antimicrobial activity and cytokine responses of alveolar macrophages to Legionella pneumophila infection by nicotine. *The Journal of Immunology* 167: 6518-6524, 2001.

155. **Maus AD, Pereira EF, Karachunski PI, Horton RM, Navaneetham D, Macklin K, Cortes WS, Albuquerque EX, and Conti-Fine BM**. Human and rodent bronchial epithelial cells express functional nicotinic acetylcholine receptors. *Molecular Pharmacology* 54: 779-788, 1998.

156. **McCarthy M**. “Alarming” rise in popularity of e-cigarettes is seen among US teenagers as use triples in a year. *BMJ* 350: h2083, 2015.

157. **McConnell R, Barrington-Trimis JL, Wang K, Urman R, Hong H, Unger J, Samet J, Leventhal A, and Berhane K**. Electronic cigarette use and respiratory symptoms in adolescents. *American journal of respiratory and critical care medicine* 195: 1043-1049, 2017.

158. **McGrath-Morrow SA, Hayashi M, Aherrera A, Lopez A, Malinina A, Collaco JM, Neptune E, Klein JD, Winickoff JP, and Breysse P**. The effects of electronic cigarette emissions on systemic cotinine levels, weight and postnatal lung growth in neonatal mice. *PloS one* 10: e0118344, 2015.

159. **McHale CM, Zhang L, and Smith MT**. Current understanding of the mechanism of benzene-induced leukemia in humans: implications for risk assessment. *Carcinogenesis* 33: 240-252, 2012.

160. **McKemy DD, Neuhausser WM, and Julius D**. Identification of a cold receptor reveals a general role for TRP channels in thermosensation. *Nature* 416: 52, 2002.

161. **Meisenhelder J, Suh P-G, Rhee SG, and Hunter T**. Phospholipase C-γ is a substrate for the PDGF and EGF receptor protein-tyrosine kinases in vivo and in vitro. *Cell* 57: 1109-1122, 1989.

162. **Merigo F, Benati D, Di Chio M, Osculati F, and Sbarbati A**. Secretory cells of the airway express molecules of the chemoreceptive cascade. *Cell and tissue research* 327: 231-247, 2007.

163. **Merigo F, Benati D, Tizzano M, Osculati F, and Sbarbati A**. α-Gustducin immunoreactivity in the airways. *Cell and tissue research* 319: 211-219, 2005.

164. **Mikheev VB, Brinkman MC, Granville CA, Gordon SM, and Clark PI**. Real-time measurement of electronic cigarette aerosol size distribution and metals content analysis. *Nicotine & Tobacco Research* 18: 1895-1902, 2016.

165. **Milara J, and Cortijo J**. Tobacco, inflammation, and respiratory tract cancer. *Current pharmaceutical design* 18: 3901-3938, 2012.

166. **Millar N**. Assembly and subunit diversity of nicotinic acetylcholine receptors. *Biochemical Society Transactions* 31: 869-874, 2003.

167. **Moon H, Kim MJ, Son HJ, Kweon H-J, Kim JT, Kim Y, Shim J, Suh B-C, and Rhyu M-R**. Five hTRPA1 Agonists Found in Indigenous Korean Mint, Agastache rugosa. *PloS one* 10: e0127060, 2015.

168. **Nairn AC, and Picciotto MR**. Calcium/calmodulin-dependent protein kinases. In: *Seminars in cancer biology*1994, p. 295-303.

169. **Nakabeppu Y, Sakumi K, Sakamoto K, Tsuchimoto D, Tsuzuki T, and Nakatsu Y**. Mutagenesis and carcinogenesis caused by the oxidation of nucleic acids. *Biological chemistry* 387: 373-379, 2006.

170. **Nakagawa Y, Nagasawa M, Yamada S, Hara A, Mogami H, Nikolaev VO, Lohse MJ, Shigemura N, Ninomiya Y, and Kojima I**. Sweet taste receptor expressed in pancreatic β-cells activates the calcium and cyclic AMP signaling systems and stimulates insulin secretion. *PloS one* 4: e5106, 2009.

171. **Naz H, Tarique M, Khan P, Luqman S, Ahamad S, Islam A, Ahmad F, and Hassan MI**. Evidence of vanillin binding to CAMKIV explains the anti-cancer mechanism in human hepatic carcinoma and neuroblastoma cells. *Molecular and cellular biochemistry* 438: 35-45, 2018.

172. **Neilson L, Mankus C, Thorne D, Jackson G, DeBay J, and Meredith C**. Development of an in vitro cytotoxicity model for aerosol exposure using 3D reconstructed human airway tissue; application for assessment of e-cigarette aerosol. *Toxicology in Vitro* 29: 1952-1962, 2015.

173. **Ng SW, Di Capite J, Singaravelu K, and Parekh AB**. Sustained activation of the tyrosine kinase Syk by antigen in mast cells requires local Ca2+ influx through Ca2+ release-activated Ca2+ channels. *Journal of Biological Chemistry* 283: 31348-31355, 2008.

174. **Nguyen H, Finkelstein E, Reznick A, Cross C, and van der Vliet A**. Cigarette smoke impairs neutrophil respiratory burst activation by aldehyde-induced thiol modifications. *Toxicology* 160: 207-217, 2001.

175. **Noah TL, Zhou H, and Jaspers I**. Alteration of the nasal responses to influenza virus by tobacco smoke. *Current opinion in allergy and clinical immunology* 12: 24, 2012.

176. **Noya Y, Seki K-i, Asano H, Mai Y, Horinouchi T, Higashi T, Terada K, Hatate C, Hoshi A, and Nepal P**. Identification of stable cytotoxic factors in the gas phase extract of cigarette smoke and pharmacological characterization of their cytotoxicity. *Toxicology* 314: 1-10, 2013.

177. **Ochs M, Nyengaard JR, Jung A, Knudsen L, Voigt M, Wahlers T, Richter J, and Gundersen HJG**. The number of alveoli in the human lung. *American journal of respiratory and critical care medicine* 169: 120-124, 2004.

178. **Orellana-Barrios MA, Payne D, Mulkey Z, and Nugent K**. Electronic Cigarettes—A Narrative Review for Clinicians. *The American journal of medicine* 128: 674-681, 2015.

179. **Organization WH**. Projections of mortality and causes of death, 2015 and 2030. *Geneva: World Health Organization Available from: URL: http://www who int/healthinfo/global_burden_disease/projections/en/index html Accessed on August* 13: 2013.

180. **Paleari L, Catassi A, Ciarlo M, Cavalieri Z, Bruzzo C, and Servent D**. Role of alpha7-nicotinic acetylcholine receptor in human non-small cell lung cancer proliferation (vol 41, pg 936, 2008). *Cell Proliferation* 42: 568-568, 2009.

181. **Park CY, Hoover PJ, Mullins FM, Bachhawat P, Covington ED, Raunser S, Walz T, Garcia KC, Dolmetsch RE, and Lewis RS**. STIM1 clusters and activates CRAC channels via direct binding of a cytosolic domain to Orai1. *Cell* 136: 876-890, 2009.

182. **Paschke M, Tkachenko A, Ackermann K, Hutzler C, Henkler F, and Luch A**. Activation of the cold-receptor TRPM8 by low levels of menthol in tobacco products. *Toxicology letters* 271: 50-57, 2017.

183. **Phillips DH, and Venitt S**. DNA and protein adducts in human tissues resulting from exposure to tobacco smoke. *International Journal of Cancer* 131: 2733-2753, 2012.

184. **Pickett G, Seagrave J, Boggs S, Polzin G, Richter P, and Tesfaigzi Y**. Effects of 10 cigarette smoke condensates on primary human airway epithelial cells by comparative gene and cytokine expression studies. *Toxicological sciences* kfp298, 2009.

185. **Pinheiro J, Bates D, DebRoy S, and Sarkar D**. R-CORE-TEAM: nlme: Linear and nonlinear mixed effects models 2014. *R package version 3* 1-120, 2016.

186. **Pisinger C, and Døssing M**. A systematic review of health effects of electronic cigarettes. *Preventive medicine* 69: 248-260, 2014.

187. **Pollay RW, and Dewhirst T**. The dark side of marketing seemingly "Light" cigarettes: successful images and failed fact. *Tobacco control* 11: i18-i31, 2002.

188. **Ponzoni L, Moretti M, Sala M, Fasoli F, Mucchietto V, Lucini V, Cannazza G, Gallesi G, Castellana C, and Clementi F**. Different physiological and behavioural effects of e-cigarette vapour and cigarette smoke in mice. *European Neuropsychopharmacology* 25: 1775-1786, 2015.

189. **Prakriya M, Feske S, Gwack Y, Srikanth S, Rao A, and Hogan PG**. Orai1 is an essential pore subunit of the CRAC channel. *Nature* 443: 230, 2006.

190. **Premkumar LS**. Transient receptor potential channels as targets for phytochemicals. *ACS chemical neuroscience* 5: 1117-1130, 2014.

191. **Proctor RN**. The history of the discovery of the cigarette–lung cancer link: evidentiary traditions, corporate denial, global toll. *Tobacco control* 21: 87-91, 2012.

192. **Pulvers K, Hayes RB, Scheuermann TS, Romero DR, Emami AS, Resnicow K, Olendzki E, Person SD, and Ahluwalia JS**. Tobacco use, quitting behavior, and health characteristics among current electronic cigarette users in a national tri-ethnic adult stable smoker sample. *Nicotine & Tobacco Research* 17: 1085-1095, 2015.

193. **Rackley CR, and Stripp BR**. Building and maintaining the epithelium of the lung. *The Journal of clinical investigation* 122: 2724-2730, 2012.

194. **Rager JE, Bauer RN, Müller LL, Smeester L, Carson JL, Brighton LE, Fry RC, and Jaspers I**. DNA methylation in nasal epithelial cells from smokers: identification of ULBP3-related effects. *American Journal of Physiology-Lung Cellular and Molecular Physiology* 305: L432-L438, 2013.

195. **Rajan D, Gaston KA, McCracken CE, Erdman DD, and Anderson LJ**. Response to rhinovirus infection by human airway epithelial cells and peripheral blood mononuclear cells in an in vitro two-chamber tissue culture system. *PLoS one* 8: e66600, 2013.

196. **Randell SH, Fulcher ML, O'Neal W, and Olsen JC**. Primary Epithelial Cell Models for Cystic Fibrosis Research. In: *Cystic Fibrosis: Diagnosis and Protocols, Volume II: Methods and Resources to Understand Cystic Fibrosis*, edited by Amaral MD, and Kunzelmann K. Totowa, NJ: Humana Press, 2011, p. 285-310.

197. **Rangelov K, and Sethi S**. Role of infections. *Clinics in chest medicine* 35: 87-100, 2014.

198. **Rasmussen JE, Sheridan JT, Polk W, Davies CM, and Tarran R**. Cigarette smoke-induced Ca2+ release leads to cystic fibrosis transmembrane conductance regulator (CFTR) dysfunction. *Journal of Biological Chemistry* 289: 7671-7681, 2014.

199. **Reidel B, Radicioni G, Clapp PW, Ford AA, Abdelwahab S, Rebuli ME, Haridass P, Alexis NE, Jaspers I, and Kesimer M**. E-cigarette use causes a unique innate immune response in the lung, involving increased neutrophilic activation and altered mucin secretion. *American journal of respiratory and critical care medicine* 197: 492-501, 2018.

200. **Reinikovaite V, Rodriguez IE, Karoor V, Rau A, Trinh BB, Deleyiannis FW-B, and Taraseviciene-Stewart L**. The effects of electronic cigarette vapour on the lung: direct comparison to tobacco smoke. *European Respiratory Journal* 1701661, 2018.

201. **Ren X, Zhou L, Terwilliger R, Newton S, and De Araujo IE**. Sweet taste signaling functions as a hypothalamic glucose sensor. *Frontiers in integrative neuroscience* 3: 12, 2009.

202. **Research Ma**. "Global E Cigarette & Vaporizer Market - Analysis & Forecast Through 2015 to 2025" 2016, p. 1-236.

203. **Ribeiro CMP, Paradiso AM, Livraghi A, and Boucher RC**. The mitochondrial barriers segregate agonist-induced calcium-dependent functions in human airway epithelia. *The Journal of general physiology* 122: 377-387, 2003.

204. **Ricciardolo FL, Di Stefano A, Sabatini F, and Folkerts G**. Reactive nitrogen species in the respiratory tract. *European journal of pharmacology* 533: 240-252, 2006.

205. **Rickert WS, and Robinson JC**. Estimating the hazards of less hazardous cigarettes. II. Study of cigarette yields of nicotine, carbon monoxide, and hydrogen cyanide in relation to levels of cotinine, carboxyhemoglobin, and thiocyanate in smokers. *Journal of Toxicology and Environmental Health, Part A Current Issues* 7: 391-403, 1981.

206. **Riker CA, Lee K, Darville A, and Hahn EJ**. E-cigarettes: promise or peril? *Nursing Clinics of North America* 47: 159-171, 2012.

207. **Robinson DR, Wu Y-M, and Lin S-F**. The protein tyrosine kinase family of the human genome. *Oncogene* 19: 5548, 2000.

208. **Robinson R, Hensel E, Morabito P, and Roundtree K**. Electronic cigarette topography in the natural environment. *PloS one* 10: e0129296, 2015.

209. **Rom O, Pecorelli A, Valacchi G, and Reznick AZ**. Are E-cigarettes a safe and good alternative to cigarette smoking? *Annals of the New York Academy of Sciences* 1340: 65-74, 2015.

210. **Rose JE**. Multiple brain pathways and receptors underlying tobacco addiction. *Biochemical pharmacology* 74: 1263-1270, 2007.

211. **Rowell TR, Reeber SL, Lee SL, Harris RA, Nethery RC, Herring AH, Glish GL, and Tarran R**. Flavored E-cigarette Liquids Reduce Proliferation and Viability in the CALU3 Airway Epithelial Cell Line. *American Journal of Physiology-Lung Cellular and Molecular Physiology* ajplung. 00392.02016, 2017.

212. **Rowell TR, and Tarran R**. Will chronic e-cigarette use cause lung disease? *American Journal of Physiology-Lung Cellular and Molecular Physiology* 309: L1398-L1409, 2015.

213. **Ryter SW, and Choi AM**. Autophagy in lung disease pathogenesis and therapeutics. *Redox biology* 4: 215-225, 2015.

214. **Saccone NL, Wang JC, Breslau N, Johnson EO, Hatsukami D, Saccone SF, Grucza RA, Sun L, Duan W, and Budde J**. The CHRNA5-CHRNA3-CHRNB4 nicotinic receptor subunit gene cluster affects risk for nicotine dependence in African-Americans and in European-Americans. *Cancer research* 69: 6848-6856, 2009.

215. **Samanta K, Bakowski D, and Parekh AB**. Key Role for Store-Operated Ca2+ Channels in Activating Gene Expression in Human Airway Bronchial Epithelial Cells. *PloS one* 9: e105586, 2014.

216. **Sassano MF, Davis ES, Keating JE, Zorn B, Kochar T, Wolfgang M, Glish GL, and Tarran R**. Evaluation of e-liquid toxicity using an open-source high-throughput screening assay. *PLoS Biology* in press: 2018.

217. **Scheffler S, Dieken H, Krischenowski O, and Aufderheide M**. Cytotoxic evaluation of e-liquid aerosol using different lung-derived cell models. *International Journal of Environmental Research and Public Health* 12: 12466-12474, 2015.

218. **Scheffler S, Dieken H, Krischenowski O, Förster C, Branscheid D, and Aufderheide M**. Evaluation of e-cigarette liquid vapor and mainstream cigarette smoke after direct exposure of primary human bronchial epithelial cells. *International Journal of Environmental Research and Public Health* 12: 3915-3925, 2015.

219. **Schneider D, Ganesan S, Comstock AT, Meldrum CA, Mahidhara R, Goldsmith AM, Curtis JL, Martinez FJ, Hershenson MB, and Sajjan U**. Increased cytokine response of rhinovirus-infected airway epithelial cells in chronic obstructive pulmonary disease. *American journal of respiratory and critical care medicine* 182: 332-340, 2010.

220. **Schroeder MJ, and Hoffman AC**. Electronic cigarettes and nicotine clinical pharmacology. *Tobacco Control* 23: ii30-ii35, 2014.

221. **Schwartz AG, Prysak GM, Bock CH, and Cote ML**. The molecular epidemiology of lung cancer. *Carcinogenesis* 28: 507-518, 2006.

222. **Schweitzer KS, Chen SX, Law S, Van Demark M, Poirier C, Justice MJ, Hubbard WC, Kim ES, Lai X, and Wang M**. Endothelial disruptive proinflammatory effects of nicotine and e-cigarette vapor exposures. *American Journal of Physiology-Lung Cellular and Molecular Physiology* 309: L175-L187, 2015.

223. **Shah AS, Ben-Shahar Y, Moninger TO, Kline JN, and Welsh MJ**. Motile cilia of human airway epithelia are chemosensory. *Science* 325: 1131-1134, 2009.

224. **Shalala DE, Broome CV, and Satcher D**. Tobacco Use Among US Racial/Ethnic Minority Groups African Americans American Indians and Alaska Natives Asian Americans and Pacific Islanders Hispanics: A Report of the Surgeon General: Executive Summary. *Morbidity and Mortality Weekly Report: Recommendations and Reports* 47: i-16, 1998.

225. **Shears SB**. Measurement of inositol phosphate turnover in intact cells and cell-free systems. *Signalling by Inositides* 33, 1997.

226. **Sherwood CL, and Boitano S**. Airway epithelial cell exposure to distinct e-cigarette liquid flavorings reveals toxicity thresholds and activation of CFTR by the chocolate flavoring 2, 5-dimethypyrazine. *Respiratory Research* 17: L175-L187, 2016.

227. **Shibamoto T**. Diacetyl: occurrence, analysis, and toxicity. *Journal of agricultural and food chemistry* 62: 4048-4053, 2014.

228. **Shibukawa Y, and Suzuki T**. Ca2+ Signaling Mediated by IP3-Dependent Ca2+ Releasing and Store-Operated Ca2+ Channels in Rat Odontoblasts. *Journal of Bone and Mineral Research* 18: 30-38, 2003.

229. **Slade J, Bero LA, Hanauer P, Barnes DE, and Glantz SA**. Nicotine and addiction: the Brown and Williamson documents. *Jama* 274: 225-233, 1995.

230. **Sloane PA, Shastry S, Wilhelm A, Courville C, Tang LP, Backer K, Levin E, Raju SV, Li Y, and Mazur M**. A pharmacologic approach to acquired cystic fibrosis transmembrane conductance regulator dysfunction in smoking related lung disease. *PloS one* 7: e39809, 2012.

231. **Smith MR, Court DW, Kim H, Park JB, Rhee SG, Rhim JS, and Kung H**. Overexpression of phosphoinositide-specific phospholipase Cgamma in NIH 3T3 cells promotes transformation and tumorigenicity. *Carcinogenesis* 19: 177-185, 1998.

232. **Sosnowski TR, and Kramek-Romanowska K**. Predicted Deposition of E-Cigarette Aerosol in the Human Lungs. *Journal of Aerosol Medicine and Pulmonary Drug Delivery* 29: 299-309, 2016.

233. **Spielman AI, Huque T, Nagai H, Whitney G, and Brand JG**. Generation of inositol phosphates in bitter taste transduction. *Physiology & behavior* 56: 1149-1155, 1994.

234. **Spindle TR, Breland AB, Karaoghlanian NV, Shihadeh AL, and Eissenberg T**. Preliminary results of an examination of electronic cigarette user puff topography: the effect of a mouthpiece-based topography measurement device on plasma nicotine and subjective effects. *Nicotine & Tobacco Research* 17: 142-149, 2015.

235. **Spitz MR, Amos CI, Dong Q, Lin J, and Wu X**. The CHRNA5-A3 region on chromosome 15q24-25.1 is a risk factor both for nicotine dependence and for lung cancer. *Journal of the National Cancer Institute* 100: 1552-1556, 2008.

236. **Srivats S, Balasuriya D, Pasche M, Vistal G, Edwardson JM, Taylor CW, and Murrell-Lagnado RD**. Sigma1 receptors inhibit store-operated Ca2+ entry by attenuating coupling of STIM1 to Orai1. *J Cell Biol* 213: 65-79, 2016.

237. **Stepanov I, Muzic J, Le CT, Sebero E, Villalta P, Ma B, Jensen J, Hatsukami D, and Hecht SS**. Analysis of 4-hydroxy-1-(3-pyridyl)-1-butanone (HPB)-releasing DNA adducts in human exfoliated oral mucosa cells by liquid chromatography–electrospray ionization–tandem mass spectrometry. *Chemical research in toxicology* 26: 37-45, 2013.

238. **Stratton K, Shetty P, Wallace R, and Bondurant S**. Clearing the smoke: the science base for tobacco harm reduction—executive summary. *Tobacco Control* 10: 189-195, 2001.

239. **Su T-P, Hayashi T, Maurice T, Buch S, and Ruoho AE**. The sigma-1 receptor chaperone as an inter-organelle signaling modulator. *Trends in pharmacological sciences* 31: 557-566, 2010.

240. **Sussan TE, Gajghate S, Thimmulappa RK, Ma J, Kim J-H, Sudini K, Consolini N, Cormier SA, Lomnicki S, and Hasan F**. Exposure to electronic cigarettes impairs pulmonary anti-bacterial and anti-viral defenses in a mouse model. *PloS one* 10: e0116861, 2015.

241. **Takai Y, Kishimoto A, Iwasa Y, Kawahara Y, Mori T, and Nishizuka Y**. Calcium-dependent activation of a multifunctional protein kinase by membrane phospholipids. *Journal of Biological Chemistry* 254: 3692-3695, 1979.

242. **Takemura H, and Putney Jr J**. Capacitative calcium entry in parotid acinar cells. *Biochemical Journal* 258: 409, 1989.

243. **Takiguchi Y, Sekine I, Iwasawa S, Kurimoto R, and Tatsumi K**. Chronic obstructive pulmonary disease as a risk factor for lung cancer. *World J Clin Oncol* 5: 660-666, 2014.

244. **Talhout R, Opperhuizen A, and Van Amsterdam JG**. Sugars as tobacco ingredient: Effects on mainstream smoke composition. *Food and Chemical Toxicology* 44: 1789-1798, 2006.

245. **Talhout R, Schulz T, Florek E, Van Benthem J, Wester P, and Opperhuizen A**. Hazardous compounds in tobacco smoke. *International journal of environmental research and public health* 8: 613-628, 2011.

246. **Talih S, Balhas Z, Salman R, Karaoghlanian N, and Shihadeh A**. "Direct Dripping": A High-Temperature, High-Formaldehyde Emission Electronic Cigarette Use Method. *Nicotine & Tobacco Research* ntv080, 2015.

247. **Tapper AR, McKinney SL, Nashmi R, Schwarz J, Deshpande P, Labarca C, Whiteaker P, Marks MJ, Collins AC, and Lester HA**. Nicotine activation of α4* receptors: sufficient for reward, tolerance, and sensitization. *Science* 306: 1029-1032, 2004.

248. **Tarran R, and Redinbo MR**. Mammalian short palate lung and nasal epithelial clone 1 (SPLUNC1) in pH-dependent airway hydration. *The international journal of biochemistry & cell biology* 52: 130-135, 2014.

249. **Team RC**. R: A language and environment for statistical computing. R Foundation for Statistical Computing, Vienna, Austria. 2016. 2017.

250. **Team RC**. R: A language and environment for statistical computing. Vienna: R Foundation for Statistical Computing 2014. 2016.

251. **Tice RR, Hook GG, Donner M, McRee DI, and Guy AW**. Genotoxicity of radiofrequency signals. I. Investigation of DNA damage and micronuclei induction in cultured human blood cells. *Bioelectromagnetics* 23: 113-126, 2002.

252. **Tierney PA, Karpinski CD, Brown JE, Luo W, and Pankow JF**. Flavour chemicals in electronic cigarette fluids. *Tobacco Control* 25: e10-e15, 2015.

253. **Tizzano M, Gulbransen BD, Vandenbeuch A, Clapp TR, Herman JP, Sibhatu HM, Churchill ME, Silver WL, Kinnamon SC, and Finger TE**. Nasal chemosensory cells use bitter taste signaling to detect irritants and bacterial signals. *Proceedings of the National Academy of Sciences* 107: 3210-3215, 2010.

254. **U.S. DoHaHS**. E-Cigarette Use Among Youth and Young Adults; A Report of the Surgeon General. *Atlanta, GA: US Department of Health and Human Services, Centers for Disease Control and Prevention, National Center for Chronic Disease Prevention and Health Promotion, Office on Smoking and Health* 1-275, 2016.

255. **Vansickel AR, and Eissenberg T**. Electronic cigarettes: effective nicotine delivery after acute administration. *Nicotine & Tobacco Research* 15: 267-270, 2013.

256. **Vardavas CI, Anagnostopoulos N, Kougias M, Evangelopoulou V, Connolly GN, and Behrakis PK**. Short-term pulmonary effects of using an electronic cigarette: impact on respiratory flow resistance, impedance, and exhaled nitric oxide. *Chest Journal* 141: 1400-1406, 2012.

257. **Vucic EA, Chari R, Thu KL, Wilson IM, Cotton AM, Kennett JY, Zhang M, Lonergan KM, Steiling K, and Brown CJ**. DNA methylation is globally disrupted and associated with expression changes in chronic obstructive pulmonary disease small airways. *American journal of respiratory cell and molecular biology* 50: 912-922, 2014.

258. **Walle T, Walle UK, Sedmera D, and Klausner M**. Benzo [A] pyrene-induced oral carcinogenesis and chemoprevention: studies in bioengineered human tissue. *Drug metabolism and disposition* 34: 346-350, 2006.

259. **Wang MP, Ho SY, Leung LT, and Lam TH**. Electronic cigarette use and respiratory symptoms in Chinese adolescents in Hong Kong. *JAMA pediatrics* 170: 89-91, 2016.

260. **Warren GW, and Singh AK**. Nicotine and lung cancer. *Journal of carcinogenesis* 12: 1, 2013.

261. **Ways DK, Kukoly CA, Hooker JL, Bryant WO, Posekany KJ, Fletcher DJ, Cook PP, and Parker PJ**. MCF-7 breast cancer cells transfected with protein kinase C-alpha exhibit altered expression of other protein kinase C isoforms and display a more aggressive neoplastic phenotype. *The Journal of clinical investigation* 95: 1906-1915, 1995.

262. **West JB**. *Pulmonary physiology and pathophysiology: an integrated, case-based approach*. Lippincott Williams & Wilkins, 2007.

263. **West KA, Brognard J, Clark AS, Linnoila IR, Yang X, Swain SM, Harris C, Belinsky S, and Dennis PA**. Rapid Akt activation by nicotine and a tobacco carcinogen modulates the phenotype of normal human airway epithelial cells. *The Journal of clinical investigation* 111: 81-90, 2003.

264. **Whitsett JA, and Alenghat T**. Respiratory epithelial cells orchestrate pulmonary innate immunity. *Nature immunology* 16: 27-35, 2015.

265. **Wieslander G, Norbäck D, and Lindgren T**. Experimental exposure to propylene glycol mist in aviation emergency training: acute ocular and respiratory effects. *Occupational and environmental medicine* 58: 649-655, 2001.

266. **Williams CL, Phelps SH, and Porter RA**. Expression of Ca2+/calmodulin-dependent protein kinase types II and IV, and reduced DNA synthesis due to the Ca2+/calmodulin-dependent protein kinase inhibitor KN-62 (1-[N, O-Bis (5-isoquinolinesulfonyl)-N-methyl-L-tyrosyl]-4-phenylpiperazine) in small cell lung carcinoma. *Biochemical pharmacology* 51: 707-715, 1996.

267. **Wu Q, Jiang D, Minor M, and Chu HW**. Electronic cigarette liquid increases inflammation and virus infection in primary human airway epithelial cells. *PloS one* 9: e108342, 2014.

268. **Wu S-w, Fowler DK, Shaffer FJ, Lindberg JE, and Peters JH**. Ethyl vanillin activates TRPA1. *Journal of Pharmacology and Experimental Therapeutics* 362: 368-377, 2017.

269. **Xu H, Delling M, Jun JC, and Clapham DE**. Oregano, thyme and clove-derived flavors and skin sensitizers activate specific TRP channels. *Nature neuroscience* 9: 628, 2006.

270. **Yang H, Shen F, Herenyiova M, and Weber G**. Phospholipase C (EC 3.1. 4.11): a malignancy linked signal transduction enzyme. *Anticancer research* 18: 1399-1404, 1998.

271. **Yoshida M, Takahashi Y, and Inoue S**. Histamine induces melanogenesis and morphologic changes by protein kinase A activation via H2 receptors in human normal melanocytes. *Journal of investigative dermatology* 114: 334-342, 2000.

272. **Yoshikawa H, Kurokawa M, Ozaki N, Nara K, Atou K, Takada E, Kamochi H, and Suzuki N**. Nicotine inhibits the production of proinflammatory mediators in human monocytes by suppression of I-κB phosphorylation and nuclear factor-κB transcriptional activity through nicotinic acetylcholine receptor α7. *Clinical & Experimental Immunology* 146: 116-123, 2006.

273. **Zhang S, Day I, and Ye S**. Nicotine induced changes in gene expression by human coronary artery endothelial cells. *Atherosclerosis* 154: 277-283, 2001.

274. **Zhou C-HC, Beltramini JN, Fan Y-X, and Lu GM**. Chemoselective catalytic conversion of glycerol as a biorenewable source to valuable commodity chemicals. *Chemical Society Reviews* 37: 527-549, 2008.

275. **Zhou M, Liu Y, and Duan Y**. Breath biomarkers in diagnosis of pulmonary diseases. *Clinica Chimica Acta* 413: 1770-1780, 2012.

276. **Zhu S-H, Sun JY, Bonnevie E, Cummins SE, Gamst A, Yin L, and Lee M**. Four hundred and sixty brands of e-cigarettes and counting: implications for product regulation. *Tobacco control* 23: iii3-iii9, 2014.

277. **Zia S, Ndoye A, Nguyen VT, and Grando SA**. Nicotine enhances expression of the alpha 3, alpha 4, alpha 5, and alpha 7 nicotinic receptors modulating calcium metabolism and regulating adhesion and motility of respiratory epithelial cells. *Research communications in molecular pathology and pharmacology* 97: 243-262, 1997.